Mathematical Theory of Laminated Transmission Lines—Part II

By SAMUEL P. MORGAN, JR.

This part of the paper continues the analysis of the low-loss, broad-band, laminated transmission lines proposed by A. M. Clogston, and deals particularly with "Clogston 2" lines, in which the entire propagation space is filled with laminated material.

TABLE OF CONTENTS

VIII. PRINCIPAL MODE IN CLOGSTON 2 LINES WITH INFINITESIMALLY THIN LAMINAE

In Part I* of this paper we have set up a general mathematical framework for the analysis of Clogston-type laminated transmission lines and have applied it to Clogston 1 lines having laminated conductors, but with the total thickness of the laminations small compared to the overall dimensions of the line, so that most of the forward power flow takes place in the main dielectric. In Part II we shall consider Clogston 2 lines, which instead of containing a main dielectric have the propagation space entirely filled with laminations; and we shall also derive results, in Sections IX and X, for the general laminated transmission

* S. P. Morgan, Jr., *Bell System Tech. J.*, **31,** 883 (1952). Since the two parts of the paper are very closely related, the sections, equations, figures, and footnotes have been numbered consecutively throughout the whole paper. A table of symbols appears at the end of Part I.

line in which the relative fractions of space occupied by the main dielectric and the laminations are arbitrary.

A parallel-plane Clogston 2 line is shown schematically in Fig. 10. It consists of a stack of alternate layers of conducting and insulating material, whose total thickness is a. As before, the electrical constants of the conducting and insulating layers are denoted by μ_1, g_1 and ϵ_2, μ_2 respectively; and the fraction of conducting material in the stack is called θ. The stack is bounded at $y = \pm\frac{1}{2}a$ by sheaths whose normal surface impedance is $Z_n(\gamma)$, where γ is the longitudinal propagation constant of the mode under consideration.

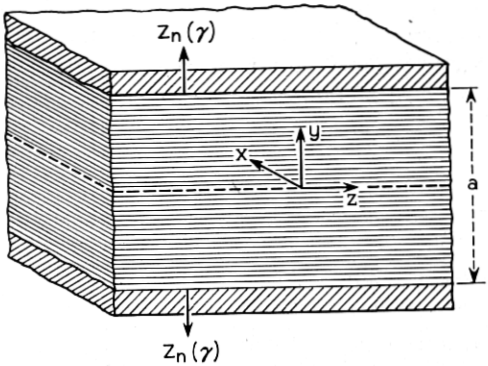

Fig. 10—Parallel-plane Clogston 2 transmission line.

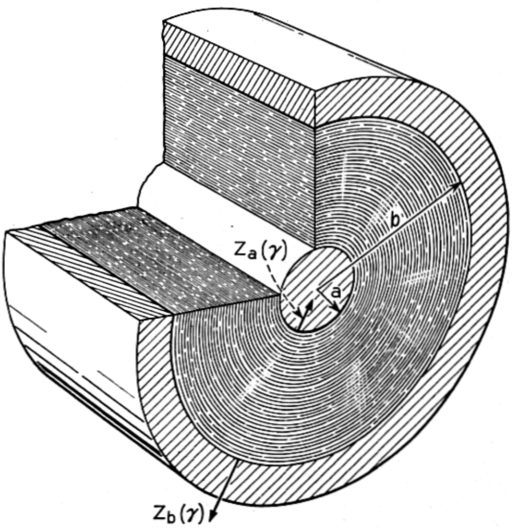

Fig. 11—Coaxial Clogston 2 transmission line.

The cross section of a coaxial Clogston 2 cable is shown schematically in Fig. 11. It consists of a laminated coaxial stack bounded internally by a cylindrical core of radius a, which may be equal to zero so far as the theoretical analysis is concerned, and externally by a cylindrical sheath of radius b. We denote the radial impedance looking into the core at $\rho = a$ by $Z_a(\gamma)$, and the radial impedance looking into the sheath at $\rho = b$ by $Z_b(\gamma)$.

In this section we shall assume the laminae to be infinitesimally thin, so that the stack may be regarded as a homogeneous, anisotropic medium, completely characterized by its average electrical constants. The case of finite lamina thickness will be treated in Section XI. We shall neglect dielectric and magnetic dissipation throughout, except in Section XIII.

For modes of the type which we consider, whose only field components are H_x, E_y, E_z in the plane line or H_ϕ, E_ρ, E_z in the coaxial line, the average electrical constants of the stack are given by equations (90) of Section III, namely,

$$\begin{aligned} \bar{\epsilon} &= \epsilon_2/(1 - \theta), \\ \bar{\mu} &= \theta\mu_1 + (1 - \theta)\mu_2 , \\ \bar{g} &= \theta g_1 . \end{aligned} \tag{268}$$

As observed in Section III, Maxwell's equations for the average fields in such an artificial anisotropic medium take the form, for a plane stack,

$$\begin{aligned} \partial\bar{H}_x/\partial z &= i\omega\bar{\epsilon}\bar{E}_y , \\ \partial\bar{H}_x/\partial y &= -\bar{g}\bar{E}_z , \\ \partial\bar{E}_y/\partial z - \partial\bar{E}_z/\partial y &= i\omega\bar{\mu}\bar{H}_x ; \end{aligned} \tag{269}$$

while for a cylindrical stack,

$$\begin{aligned} \partial\bar{H}_\phi/\partial z &= -i\omega\bar{\epsilon}\bar{E}_\rho , \\ \partial(\rho\bar{H}_\phi)/\partial\rho &= \bar{g}\rho\bar{E}_z , \\ \partial\bar{E}_z/\partial\rho - \partial\bar{E}_\rho/\partial z &= i\omega\bar{\mu}\bar{H}_\phi . \end{aligned} \tag{270}$$

We wish to determine the modes which can propagate in the laminated medium when guided by plane or cylindrical impedance sheets. This problem was solved for a homogeneous, isotropic dielectric in Section II of Part I; and the method of solution is so similar for the anisotropic medium that we shall omit details of the analysis and pass at once to the results.

In the parallel-plane line, the modes for which $\bar{H}_x$ is an even function of y about the center plane $y = 0$ have field components given by

$$\begin{aligned} \bar{H}_z &= \text{ch}\, \Gamma_\ell y\, e^{-\gamma z}, \\ \bar{E}_y &= -\frac{\gamma}{i\omega\bar{\epsilon}}\, \text{ch}\, \Gamma_\ell y\, e^{-\gamma z}, \\ \bar{E}_z &= -K\, \text{sh}\, \Gamma_\ell y\, e^{-\gamma z}, \end{aligned} \tag{271}$$

up to an arbitrary amplitude factor, where Γ_ℓ and K are defined, as in Section III, by

$$\Gamma_\ell = \left[\frac{i\bar{g}}{\omega\bar{\epsilon}}\,(\omega^2\bar{\mu}\bar{\epsilon} + \gamma^2)\right]^{\frac{1}{2}}, \tag{272}$$

$$K = \Gamma_\ell/\bar{g} = \left[\frac{i}{\omega\bar{\epsilon}\bar{g}}\,(\omega^2\bar{\mu}\bar{\epsilon} + \gamma^2)\right]^{\frac{1}{2}}. \tag{273}$$

Matching impedances at the boundaries $y = \pm\frac{1}{2}a$ leads to the condition

$$K \tanh \tfrac{1}{2}\Gamma_\ell a = -Z_n(\gamma). \tag{274}$$

In the odd case, the fields are given by

$$\begin{aligned} \bar{H}_z &= \text{sh}\, \Gamma_\ell y\, e^{-\gamma z}, \\ \bar{E}_y &= -\frac{\gamma}{i\omega\bar{\epsilon}}\, \text{sh}\, \Gamma_\ell y\, e^{-\gamma z}, \\ \bar{E}_z &= -K\, \text{ch}\, \Gamma_\ell y\, e^{-\gamma z}, \end{aligned} \tag{275}$$

up to an arbitrary amplitude factor, and the boundary condition becomes

$$K \coth \tfrac{1}{2}\Gamma_\ell a = -Z_n(\gamma). \tag{276}$$

General expressions for the field components in the coaxial line are

$$\begin{aligned} \bar{H}_\phi &= [AI_1(\Gamma_\ell\rho) + BK_1(\Gamma_\ell\rho)]e^{-\gamma z}, \\ \bar{E}_\rho &= \frac{\gamma}{i\omega\bar{\epsilon}}\,[AI_1(\Gamma_\ell\rho) + BK_1(\Gamma_\ell\rho)]e^{-\gamma z}, \\ \bar{E}_z &= K[AI_0(\Gamma_\ell\rho) - BK_0(\Gamma_\ell\rho)]e^{-\gamma z}, \end{aligned} \tag{277}$$

where A and B are arbitrary constants and Γ_ℓ and K are defined as before. The boundary conditions at $\rho = a$ and $\rho = b$ take the form

$$K \frac{AI_0(\Gamma_\ell a) - BK_0(\Gamma_\ell a)}{AI_1(\Gamma_\ell a) + BK_1(\Gamma_\ell a)} = Z_a(\gamma),$$
$$K \frac{AI_0(\Gamma_\ell b) - BK_0(\Gamma_\ell b)}{AI_1(\Gamma_\ell b) + BK_1(\Gamma_\ell b)} = -Z_b(\gamma), \tag{278}$$

and these equations can be satisfied by values of A and B that are not both zero if and only if

$$\frac{KK_0(\Gamma_\ell a) + Z_a(\gamma)K_1(\Gamma_\ell a)}{KI_0(\Gamma_\ell a) - Z_a(\gamma)I_1(\Gamma_\ell a)} = \frac{KK_0(\Gamma_\ell b) - Z_b(\gamma)K_1(\Gamma_\ell b)}{KI_0(\Gamma_\ell b) + Z_b(\gamma)I_1(\Gamma_\ell b)}. \tag{279}$$

Now K is given in terms of Γ_ℓ by equation (273), while from equation (272) we have

$$\gamma^2 = -\omega^2\bar{\mu}\bar{\epsilon} - (i\omega\bar{\epsilon}/\bar{g})\Gamma_\ell^2. \tag{280}$$

Hence if the dependence of the boundary impedances on γ is known, equations (274) and (276) for the plane line and equation (279) for the coaxial line are transcendental relations from which in principle we may determine Γ_ℓ, and therefore γ, for each mode of the type that we are considering. If the value of Γ_ℓ for a particular mode satisfies the inequality

$$\frac{1}{8}\left|\frac{\Gamma_\ell^2}{\omega\bar{\mu}\bar{g}}\right|^2 \ll 1, \tag{281}$$

then on taking the square root of the right side of equation (280) by the binomial theorem, we find that the attenuation and phase constants of the given mode are approximately

$$\alpha = \operatorname{Re}\gamma = -\operatorname{Re}\frac{\Gamma_\ell^2}{2\bar{g}\sqrt{\bar{\mu}/\bar{\epsilon}}}, \tag{282}$$

$$\beta = \operatorname{Im}\gamma = \omega\sqrt{\bar{\mu}\bar{\epsilon}} - \operatorname{Im}\frac{\Gamma_\ell^2}{2\bar{g}\sqrt{\bar{\mu}/\bar{\epsilon}}}. \tag{283}$$

Throughout the rest of this section we shall consider only the lowest or principal mode. In a parallel-plane line the principal mode corresponds to the lowest root in Γ_ℓ (that is, the root having the smallest modulus) of equation (274), which may be written in the form

$$\tfrac{1}{2}\Gamma_\ell a \tanh \tfrac{1}{2}\Gamma_\ell a = -\tfrac{1}{2}\bar{g}aZ_n(\gamma). \tag{284}$$

We may express γ in terms of Γ_ℓ by equation (280), and so if $Z_n(\gamma)$ varies with γ in any reasonably simple way, or better yet if $Z_n(\gamma)$ is essentially independent of γ in the range of interest, equation (284) may be solved numerically for Γ_ℓ by successive approximations.

A numerical solution of equation (284) is, however, rarely necessary, since the right-hand side of the equation is just the ratio of the sheath impedance $Z_n(\gamma)$ to the resistance "per square", namely $1/(\frac{1}{2}\bar{g}a)$, of all the conducting layers in a stack of thickness $\frac{1}{2}a$ in parallel, and this ratio will almost always be large compared to unity. This is another way of saying that the total one-way conduction current in the stack is large compared to the sum of the conduction and displacement currents in either sheath. Even if the sheaths are infinitely thick metal plates of conductivity g_1, we have from equation (79) of Section III, since $\gamma \approx i\omega\sqrt{\bar{\mu}\bar{\epsilon}}$,

$$\tfrac{1}{2}\bar{g}aZ_n(\gamma) = \tfrac{1}{2}\theta g_1 a\eta_1 = (1 + i)\theta a/2\delta_1 , \tag{285}$$

and for most frequencies of interest the thickness $\frac{1}{2}\theta a$ of conducting material in half the stack will be several times the skin thickness δ_1 in the metal. If the medium outside the stack is free space, then $Z_n(\gamma)$ will be a few hundred ohms and a fortiori the right side of (284) will be large compared to unity. So long as the inequality

$$\left| \tfrac{1}{2}\bar{g}aZ_n(\gamma) \right| \gg 1 \tag{286}$$

is satisfied, the lowest root of (284) will be approximately

$$\Gamma_\ell = i\pi/a; \tag{287}$$

and so from (282) and (283) the attenuation and phase constants of a plane Clogston 2 line with infinitesimally thin laminae and high-impedance walls are

$$\alpha = \frac{\pi^2}{2\sqrt{\bar{\mu}/\bar{\epsilon}}\,\bar{g}a^2}, \tag{288}$$

$$\beta = \omega\sqrt{\bar{\mu}\bar{\epsilon}}. \tag{289}$$

To this approximation, there is neither amplitude nor phase distortion.

The principal mode in a coaxial Clogston 2 corresponds to the lowest root in Γ_ℓ of equation (279). To solve this equation numerically with finite boundary impedances $Z_a(\gamma)$ and $Z_b(\gamma)$, while possible in principle, would evidently be a major undertaking. We shall therefore assume throughout the present paper that the total conduction and displacement currents flowing in the core and the sheath are negligible compared to the conduction currents in the laminated medium. This is equivalent to assuming that the boundary impedances $Z_a(\gamma)$ and $Z_b(\gamma)$ are effectively infinite, so that equation (279) reduces to the simple form

$$\frac{K_1(\Gamma_\ell a)}{I_1(\Gamma_\ell a)} = \frac{K_1(\Gamma_\ell b)}{I_1(\Gamma_\ell b)} . \tag{290}$$

Equation (290) may be converted to one involving ordinary Bessel and Neumann functions by the substitution

$$\Gamma_\ell^2 = -\chi^2, \qquad \Gamma_\ell = i\chi . \tag{291}$$

Then since

$$\begin{aligned} I_n(\Gamma_\ell \rho) &= i^n J_n(\chi\rho), \\ K_n(\Gamma_\ell \rho) &= \tfrac{1}{2}\pi i^{-(n+1)} [J_n(\chi\rho) - iN_n(\chi\rho)], \end{aligned} \tag{292}$$

the equation may easily be transformed into

$$J_1(\chi a)N_1(\chi b) - J_1(\chi b)N_1(\chi a) = 0. \tag{293}$$

For any given value of the ratio a/b, equation (293) has an infinite number of real roots in χ. The lowest root χ_1 has been tabulated[18] as a function of b/a, and may be written in the form

$$\chi_1 = \frac{\pi f_1(a/b)}{b - a}, \tag{294}$$

where $f_1(a/b)$ is a monotone decreasing function of a/b which is equal to 1.2197 when $a/b = 0$ and to 1 when $a/b = 1$. Hence the attenuation and phase constants of the principal mode in a coaxial Clogston 2 with infinitesimally thin laminae and high-impedance walls are

$$\alpha = \frac{\pi^2 f_1^2(a/b)}{2\sqrt{\bar{\mu}/\bar{\epsilon}}\ \bar{g}(b - a)^2}, \tag{295}$$

$$\beta = \omega\sqrt{\bar{\mu}\bar{\epsilon}} , \tag{296}$$

and again to this approximation there is neither amplitude nor phase distortion.

Comparing equations (288) and (295), we see that the attenuation constant of the principal mode in a coaxial Clogston 2 with infinitesimally thin laminae (that is, the low-frequency attenuation constant if the laminae are of finite thickness) is equal to the attenuation constant of

---

18 E. Jahnke and F. Emde, *Tables of Functions*, fourth ed., Dover, New York, 1945, pp. 204–207. What we call $\pi f_1(a/b)$ is tabulated by Jahnke and Emde, p. 205, as $(k - 1)x_1^{(1)}$, where $k = b/a$, while our $f_1(a/b)$ is plotted as $1 + \alpha$ on p. 207.

the principal mode in a plane Clogston 2 times the factor $f_1^2(a/b)$, provided that the thickness of the plane stack is equal to the thickness $b - a$ of the coaxial stack. The functions $f_1^2(a/b)$ and $f_1^2(a/b)/(1 - a/b)^2$ are plotted against a/b in Fig. 12. From the plots it is apparent that $f_1^2(a/b)$ decreases steadily from a value of 1.488 at $a/b = 0$ to 1 at $a/b = 1$, while $f_1^2(a/b)/(1 - a/b)^2$ increases steadily from 1.488 at $a/b = 0$ to infinity at $a/b = 1$. Therefore if the stack thickness $b - a$ is fixed, the attenuation constant will be smaller the greater is the mean radius of the stack; while if the outer radius b is fixed, the attenuation constant will be reduced by reducing the radius a of the inner core, and the lowest attenuation will be achieved when $a = 0$.

It should be noted that our expressions for the attenuation and phase constants of Clogston 2 lines cannot be valid down to the mathematical limit of zero frequency, since the inequality (281), on which we based the approximations (282) and (283) for α and β, will ultimately break down as the frequency approaches zero. A similar failure of the approximate expressions which we used for the attenuation and phase constants of Clogston 1 lines was pointed out in Section II of Part I. Here, as before, we shall limit the use of the term "low frequency" to frequencies still high enough so that the attenuation per radian is small and the approximate formulas (282) and (283) for α and β are valid.

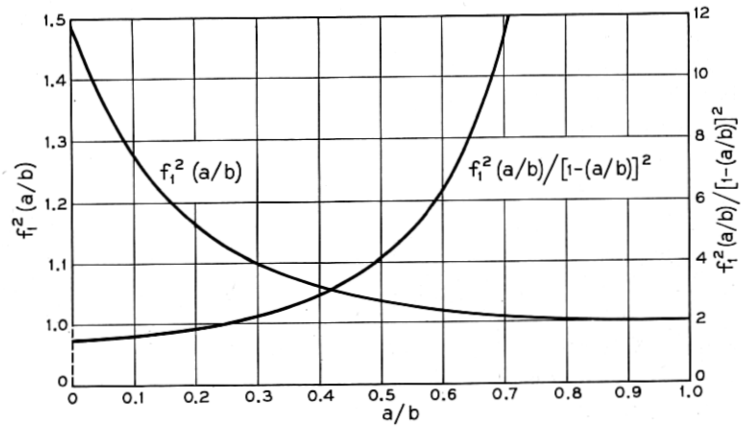

Fig. 12—Curves related to the function

$$f_1^2(a/b) = (b - a)^2\chi_1^2/\pi^2,$$

where

$$J_1(\chi_1 a)N_1(\chi_1 b) - J_1(\chi_1 b)N_1(\chi_1 a) = 0.$$

Usually we shall be able to apply these formulas down to frequencies of a few kc·sec^{-1}.

The field components of the principal mode in a plane Clogston 2 with infinitesimally thin laminae and high-impedance boundaries at $y = \pm\frac{1}{2}a$ are given by equations (271), on substituting for Γ_t from (287). We have, approximately,

$$H_x = H_0 \cos \frac{\pi y}{a} e^{-\gamma z},$$

$$\bar{E}_y = -\sqrt{\frac{\bar{\mu}}{\bar{\epsilon}}} H_0 \cos \frac{\pi y}{a} e^{-\gamma z}, \tag{297}$$

$$E_z = \frac{\pi}{\bar{g}a} H_0 \sin \frac{\pi y}{a} e^{-\gamma z},$$

where H_0 is an arbitrary amplitude factor, and in the coefficient of the expression for $\bar{E}_y$ we have replaced γ by its approximate value $i\omega\sqrt{\bar{\mu}\bar{\epsilon}}$. The bars have been omitted from H_x and E_z since these field components are continuous at the boundaries of the laminae.

The potential difference between any two points in the same transverse plane is the integral of $-\bar{E}_y$ between the points. In particular, the total potential difference between the upper and lower sheaths is

$$V = -\int_{-\frac{1}{2}a}^{\frac{1}{2}a} \bar{E}_y \, dy = \frac{2a}{\pi}\sqrt{\frac{\bar{\mu}}{\bar{\epsilon}}} H_0 e^{-\gamma z}. \tag{298}$$

The average value of the conduction current density $\bar{J}_z$ is

$$\bar{J}_z = \bar{g}E_z = \frac{\pi}{a} H_0 \sin \frac{\pi y}{a} e^{-\gamma z}, \tag{299}$$

and the current per unit width flowing in the positive z-direction in the upper half of the stack is

$$I = \int_0^{\frac{1}{2}a} \bar{J}_z \, dy = H_0 e^{-\gamma z}, \tag{300}$$

so that the ratio of voltage between the sheaths to total one-way current per unit width is

$$\frac{V}{I} = \frac{2a}{\pi}\sqrt{\frac{\bar{\mu}}{\bar{\epsilon}}}. \tag{301}$$

The fields of the principal mode in a coaxial Clogston 2 with infinitesimally thin laminae and high-impedance boundaries are given by equations (277), which simplify somewhat if we write $i\chi_1$ for Γ_ℓ, replace the modified Bessel functions with ordinary Bessel functions according to (292), and remember that H_ϕ must vanish at the high-impedance boundaries. We then get, approximately,

$$\begin{aligned} H_\phi &= H_0[\quad {}_1(\chi_1 b)J_1(\chi_1\rho) - J_1(\chi_1 b)N_1(\chi_1\rho)]e^{-\gamma z}, \\ \bar{E}_\rho &= \sqrt{\frac{\bar{\mu}}{\bar{\epsilon}}}\, H_0[N_1(\chi_1 b)J_1(\chi_1\rho) - J_1(\chi_1 b)N_1(\chi_1\rho)]e^{-\gamma z}, \qquad (302) \\ E_z &= \frac{\chi_1}{\bar{g}}\, H_0[N_1(\chi_1 b)J_0(\chi_1\rho) - J_1(\chi_1 b)N_0(\chi_1\rho)]e^{-\gamma z}, \end{aligned}$$

where H_0 is an arbitrary amplitude factor.

The potential difference between any two points in the same transverse plane is the integral of $-\bar{E}_\rho$ between the points. Thus the total potential difference between the core and the outer sheath is

$$\begin{aligned} V &= -\int_a^b \bar{E}_\rho \, d\rho \\ &= \sqrt{\frac{\bar{\mu}}{\bar{\epsilon}}}\, \frac{H_0}{\chi_1} [N_1(\chi_1 b)J_0(\chi_1\rho) - J_1(\chi_1 b)N_0(\chi_1\rho]_a^b e^{-\gamma z} \qquad (303) \\ &= \sqrt{\frac{\bar{\mu}}{\bar{\epsilon}}}\, \frac{2H_0}{\pi\chi_1}\left[\frac{J_1(\chi_1 b)}{\chi_1 a J_1(\chi_1 a)} - \frac{1}{\chi_1 b}\right]e^{-\gamma z}, \end{aligned}$$

after some transformations using equation (293) and the well-known identity

$$N_0(x)J_1(x) - N_1(x)J_0(x) = 2/\pi x. \qquad (304)$$

The average value of the conduction current density $\bar{J}_z$ is

$$\bar{J}_z = \bar{g}E_z = H_0\chi_1[N_1(\chi_1 b)J_0(\chi_1\rho) - J_1(\chi_1 b)N_0(\chi_1\rho)]e^{-\gamma z}. \qquad (305)$$

The current reverses at $\rho = c$, where $a < c < b$ and c satisfies

$$N_1(\chi_1 b)J_0(\chi_1 c) - J_1(\chi_1 b)N_0(\chi_1 c) = 0; \qquad (306)$$

hence the value of c may be found with the aid of a table of Bessel functions or from plotted curves.[19] The total one-way current in the outer part of the stack is

$$\begin{aligned} I &= 2\pi \int_c^b \bar{J}_z \rho \, d\rho \\ &= 2\pi c H_0[J_1(\chi_1 b)N_1(\chi_1 c) - N_1(\chi_1 b)J_1(\chi_1 c)]e^{-\gamma z} \qquad (307) \\ &= -\frac{4H_0 J_1(\chi_1 b)}{\chi_1 J_0(\chi_1 c)}\, e^{-\gamma z}, \end{aligned}$$

[19] Reference 18, p. 208.

where in the last step we have made use of (304) and (306). The ratio of voltage across the stack to total one-way current is, from (303) and (307),

$$\frac{V}{I} = \sqrt{\frac{\bar{\mu}}{\bar{\epsilon}}} \frac{J_0(\chi_1 c)}{2\pi} \left[\frac{1}{\chi_1 b J_1(\chi_1 b)} - \frac{1}{\chi_1 a J_1(\chi_1 a)} \right]. \tag{308}$$

If there is no inner core, so that $a = 0$, the expressions which we have just derived become indeterminate forms, and it is simplest to make an independent calculation of the fields for this special case. The Neumann functions are now excluded because of their singularity at $\rho = 0$, and the condition (293) is replaced by

$$J_1(\chi b) = 0, \tag{309}$$

from which

$$\chi_1 = 3.8317/b. \tag{310}$$

The expressions for the fields are

$$\begin{aligned} H_\phi &= H_0 J_1(\chi_1 \rho) e^{-\gamma z}, \\ \bar{E}_\rho &= \sqrt{\frac{\bar{\mu}}{\bar{\epsilon}}} H_0 J_1(\chi_1 \rho) e^{-\gamma z}, \\ E_z &= \frac{\chi_1}{\bar{g}} H_0 J_0(\chi_1 \rho) e^{-\gamma z}, \end{aligned} \tag{311}$$

where H_0 is now a different arbitrary amplitude factor.

The total potential difference across the stack becomes, after putting in numerical values,

$$V = -\int_0^a \bar{E}_\rho \, d\rho = 0.3661\sqrt{\bar{\mu}/\bar{\epsilon}}\, H_0 b e^{-\gamma z}. \tag{312}$$

The conduction current density is

$$\bar{J}_z = \bar{g} E_z = \chi_1 H_0 J_0(\chi_1 \rho) e^{-\gamma z}; \tag{313}$$

and $\bar{J}_z$ changes sign at

$$J_0(\chi_1 c) = 0, \qquad c = 2.4048/\chi_1 = 0.6276b. \tag{314}$$

The total one-way current is

$$I = 2\pi c H_0 J_1(\chi_1 c) e^{-\gamma z} = 2.047 H_0 b e^{-\gamma z}, \tag{315}$$

and the ratio of total voltage to total current is

$$V/I = 0.1788\sqrt{\bar{\mu}/\bar{\epsilon}}\,. \tag{316}$$

The fields of the principal mode in both plane and coaxial Clogston 2 lines will be plotted in the next section, when we shall also be able to show the fields in various transition structures between the extreme Clogston 1 and the complete Clogston 2.

As a numerical example, let us compare the attenuation constant of a conventional coaxial cable with that of a completely filled Clogston 2 cable of the same size. If a and b denote the radii of the inner and outer conductors of a conventional coaxial cable of optimum proportions ($b/a = 3.5911$), then at frequencies high enough to give a well-developed skin effect on both conductors, the attenuation constant is given by equation (151) of Section IV, namely

$$\alpha = \frac{1.796}{\eta_0 g_1 \delta_1 b}, \tag{317}$$

where η_0 is the intrinsic impedance of the main dielectric, which may be air. On the other hand, the attenuation constant of a Clogston 2 cable of outer radius b, with infinitesimally thin laminae and no inner core, is, from equations (282), (291), and (310),

$$\alpha = \frac{7.341}{\sqrt{\bar{\mu}/\bar{\epsilon}}\, \bar{g} b^2}. \tag{318}$$

It will be shown in the next section that for infinitesimally thin laminae whose permeabilities are all equal, the optimum value of θ is 2/3. Assuming no magnetic materials and setting $\theta = 2/3$, we find that the ratio of the attenuation constant α_c of the Clogston cable to the attenuation constant α_s of an *air-filled* standard coaxial cable of the same size, made of the same conducting material, is

$$\alpha_c/\alpha_s = 10.62\sqrt{\epsilon_{2r}}\, \delta_1/b. \tag{319}$$

For copper conductors, δ_1 is given by equation (78) of Section III, and the crossover frequency above which the Clogston cable has a lower attenuation constant than the standard coaxial cable turns out to be

$$f_{\text{Mc}} = 763.5\epsilon_{2r}/b_{\text{mils}}^2, \tag{320}$$

where frequency is measured in Mc·sec^{-1} and the radius of the cable in mils. We also note that at the crossover frequency the electrical radius of the inner conductor of the standard coaxial is $2.96\sqrt{\epsilon_{2r}}\, \delta_1$, so that the use of equation (317) for α_s appears to be (barely) justified. Applying equation (320) to an ideal Clogston 2 cable of outer diameter 0.375 inches, excluding the sheath, with copper conductors, polyethylene insulation, and no inner core, we have

$$b = 187.5 \text{ mils}, \qquad \epsilon_{2r} = 2.26, \tag{321}$$

and the crossover frequency is about 50 $\text{kc}\cdot\text{sec}^{-1}$.

It must be emphasized that several factors which have not yet been taken into account will conspire to reduce the practical improvement in transmission that can be obtained with a Clogston 2 cable. As we have already seen for Clogston 1 lines in Part I, the effect of finite lamina thickness in a Clogston 2 will be to cause the attenuation constant to increase with increasing frequency, and ultimately to become higher than the attenuation constant of a conventional coaxial cable. Dissipation in the insulating layers may also contribute appreciably to the total loss at the upper end of the frequency band. Perhaps most important of all, the average electrical properties of the laminated medium must be held extremely uniform across the stack, or the field pattern of the principal mode will be distorted and its attenuation constant correspondingly increased. In later sections we shall discuss these effects, in order to estimate the stringency of the requirements on a physical Clogston cable if its factor of improvement over a conventional cable is to approximate closely to the theoretical limit given, for example, by equation (319).

IX. PARTIALLY FILLED CLOGSTON LINES. OPTIMUM PROPORTIONS FOR PRINCIPAL MODE

The distinction which has heretofore been made between Clogston 1 and Clogston 2 lines is rather artificial, inasmuch as both structures are limiting cases of the general Clogston-type line in which an arbitrary fraction of the total space is occupied by laminated material and the rest by an isotropic main dielectric. We shall now consider the modes which can propagate in a general partially filled line, restricting ourselves for simplicity to stacks of infinitesimally thin layers backed by high-impedance walls. Under these assumptions we first set up equations which must be satisfied by the propagation constants and the fields of all modes having only H_x, E_y, E_z or H_ϕ, E_ρ, E_z field components in a partially filled Clogston line, and then proceed to a study of the lowest or principal mode. We exhibit field plots for this mode at various stages of the transition between the extreme Clogston 1 and the complete Clogston 2 geometry, and investigate the conditions under which the attenuation constant passes through a minimum as the space occupied by the stacks is increased. This leads to the determination of certain optimum proportions for a line intended to transmit the principal mode.

In Section X we shall give a similar but briefer treatment of the various higher modes which can exist in partially or completely filled Clogston lines.

The notation for the parallel-plane line is established in Fig. 5 of Part I. The stacks are bounded externally by high-impedance sheaths at $y = \pm\frac{1}{2}a$, while the main dielectric is bounded by the planes $y = \pm\frac{1}{2}b = \pm(\frac{1}{2}a - s)$. No restrictions are placed on the relative thicknesses b and s of the main dielectric and the stacks. The average electrical constants of the stacks are $\bar{\epsilon}$, $\bar{\mu}$, and $\bar{g}$, while the electrical constants ϵ_0 and μ_0 of the main dielectric are assumed to satisfy Clogston's condition (102) but are otherwise arbitrary.

As in Section II, the modes may be divided into two classes, according to whether H_x is an even function or an odd function about the center plane $y = 0$. The normal surface impedance $Z(\gamma)$ looking into either stack may be obtained from equation (92) of Section III; if the impedance of the outer sheath is effectively infinite we have

$$Z(\gamma) = K \coth \Gamma_t s = (\Gamma_t/\bar{g}) \coth \Gamma_t s, \tag{322}$$

where

$$\Gamma_t = \left[\frac{i\bar{g}}{\omega\bar{\epsilon}} (\omega^2\bar{\mu}\bar{\epsilon} + \gamma^2)\right]^{\frac{1}{2}}. \tag{323}$$

Substituting for $Z(\gamma)$ into equations (11) and (13) of Section II, we find that the impedance-matching conditions become

$$\tanh \tfrac{1}{2}\kappa_0 b \tanh \Gamma_t s = -\frac{i\omega\epsilon_0}{\bar{g}} \frac{\Gamma_t}{\kappa_0}, \tag{324}$$

$$\coth \tfrac{1}{2}\kappa_0 b \tanh \Gamma_t s = -\frac{i\omega\epsilon_0}{\bar{g}} \frac{\Gamma_t}{\kappa_0}, \tag{325}$$

for the even and odd modes respectively, where

$$\kappa_0 = (\sigma_0^2 - \gamma^2)^{\frac{1}{2}} = (-\omega^2\mu_0\epsilon_0 - \gamma^2)^{\frac{1}{2}}. \tag{326}$$

From (323) we have

$$\gamma^2 = -\omega^2\bar{\mu}\bar{\epsilon} - (i\omega\bar{\epsilon}/\bar{g})\Gamma_t^2, \tag{327}$$

and so from (326),

$$\kappa_0^2 = -\omega^2(\mu_0\epsilon_0 - \bar{\mu}\bar{\epsilon}) + (i\omega\bar{\epsilon}/\bar{g})\Gamma_t^2. \tag{328}$$

If Clogston's condition is satisfied, namely

$$\mu_0\epsilon_0 = \bar{\mu}\bar{\epsilon}, \tag{329}$$

then

$$\kappa_0^2 = (i\omega\bar{\epsilon}/\bar{g})\Gamma_\ell^2, \qquad \kappa_0 = \sqrt{i\omega\bar{\epsilon}/\bar{g}}\,\Gamma_\ell, \tag{330}$$

and the equations for the even and odd modes become, respectively,

$$\tanh \tfrac{1}{2}\sqrt{i\omega\bar{\epsilon}/\bar{g}}\,\Gamma_\ell b \tanh \Gamma_\ell s = -\frac{\epsilon_0}{\bar{\epsilon}}\sqrt{\frac{i\omega\bar{\epsilon}}{\bar{g}}} = -\frac{\bar{\mu}}{\mu_0}\sqrt{\frac{i\omega\bar{\epsilon}}{\bar{g}}}, \tag{331}$$

$$\coth \tfrac{1}{2}\sqrt{i\omega\bar{\epsilon}/\bar{g}}\,\Gamma_\ell b \tanh \Gamma_\ell s = -\frac{\epsilon_0}{\bar{\epsilon}}\sqrt{\frac{i\omega\bar{\epsilon}}{\bar{g}}} = -\frac{\bar{\mu}}{\mu_0}\sqrt{\frac{i\omega\bar{\epsilon}}{\bar{g}}}. \tag{332}$$

For reference we shall now write down the field components of the various modes. The fields in the main dielectric are given by equations (8) and (12) of Section II, while the fields in the stacks may be obtained without difficulty if we recall that the tangential field components must be continuous at the inner boundary of each stack and that the tangential magnetic field must vanish at the high-impedance surface which forms the outer boundary of the stack.

Taking the even modes first, we have for the fields in the main dielectric,

$$\begin{aligned} H_x &= H_0 \operatorname{ch} \kappa_0 y\, e^{-\gamma z}, \\ E_y &= -H_0 \frac{\gamma}{i\omega\epsilon_0} \operatorname{ch} \kappa_0 y\, e^{-\gamma z}, \\ E_z &= -H_0 \frac{\kappa_0}{i\omega\epsilon_0} \operatorname{sh} \kappa_0 y\, e^{-\gamma z}, \end{aligned} \tag{333}$$

for $-\frac{1}{2}b \leqq y \leqq \frac{1}{2}b$, where H_0 is an arbitrary amplitude factor, γ and κ_0 are given in terms of Γ_ℓ by (327) and (330), and Γ_ℓ satisfies (331). The fields in the stacks are

$$\begin{aligned} H_x &= H_0 \frac{\operatorname{ch} \frac{1}{2}\kappa_0 b}{\operatorname{sh} \Gamma_\ell s} \operatorname{sh} \Gamma_\ell(\tfrac{1}{2}a \mp y)\, e^{-\gamma z}, \\ \bar{E}_y &= -H_0 \frac{\gamma}{i\omega\bar{\epsilon}} \frac{\operatorname{ch} \frac{1}{2}\kappa_0 b}{\operatorname{sh} \Gamma_\ell s} \operatorname{sh} \Gamma_\ell(\tfrac{1}{2}a \mp y)\, e^{-\gamma z}, \\ E_z &= \pm H_0 \frac{\Gamma_\ell}{\bar{g}} \frac{\operatorname{ch} \frac{1}{2}\kappa_0 b}{\operatorname{sh} \Gamma_\ell s} \operatorname{ch} \Gamma_\ell(\tfrac{1}{2}a \mp y)\, e^{-\gamma z}, \end{aligned} \tag{334}$$

for $\frac{1}{2}b \leqq |y| \leqq \frac{1}{2}a$, where in case of ambiguous signs the upper sign is to be associated with the upper stack ($y > 0$) and the lower sign with the lower stack ($y < 0$). The continuity of E_z at $y = \pm\frac{1}{2}b$ is a consequence of equation (324) or (331).

For the odd modes, the fields in the main dielectric are

$$
\begin{aligned}
H_x &= H_0 \operatorname{sh} \kappa_0 y \, e^{-\gamma z}, \\
E_y &= -H_0 \frac{\gamma}{i\omega\epsilon_0} \operatorname{sh} \kappa_0 y \, e^{-\gamma z}, \\
E_z &= -H_0 \frac{\kappa_0}{i\omega\epsilon_0} \operatorname{ch} \kappa_0 y \, e^{-\gamma z},
\end{aligned}
\tag{335}
$$

for $-\frac{1}{2}b \leqq y \leqq \frac{1}{2}b$, where H_0 is again an arbitrary amplitude factor and γ and κ_0 are defined as before in terms of Γ_t, which is now a root of (332). The fields in the stacks are

$$
\begin{aligned}
H_x &= \pm H_0 \frac{\operatorname{sh} \frac{1}{2}\kappa_0 b}{\operatorname{sh} \Gamma_t s} \operatorname{sh} \Gamma_t(\tfrac{1}{2}a \mp y) \, e^{-\gamma z}, \\
\bar{E}_y &= \mp H_0 \frac{\gamma}{i\omega\bar{\epsilon}} \frac{\operatorname{sh} \frac{1}{2}\kappa_0 b}{\operatorname{sh} \Gamma_t s} \operatorname{sh} \Gamma_t(\tfrac{1}{2}a \mp y) \, e^{-\gamma z}, \\
E_z &= +H_0 \frac{\Gamma_t}{\bar{g}} \frac{\operatorname{sh} \frac{1}{2}\kappa_0 b}{\operatorname{sh} \Gamma_t s} \operatorname{ch} \Gamma_t(\tfrac{1}{2}a \mp y) \, e^{-\gamma z},
\end{aligned}
\tag{336}
$$

for $\frac{1}{2}b \leqq |y| \leqq \frac{1}{2}a$, where again the upper signs refer to the upper stack and the lower signs to the lower stack. The continuity of E_z at $y = \pm\frac{1}{2}b$ is now a consequence of equation (325) or (332).

The notation for the partially filled coaxial cable is shown in Fig. 6 of Part I, where as before we assume that the laminae are infinitesimally thin, the boundary impedances are effectively infinite, and the main dielectric satisfies Clogston's condition. The radius of the inner core is a and that of the outer sheath is b, while the stack thicknesses are s_1 and s_2 respectively; but no restrictions, other than obvious geometrical limitations, are placed on the relative values of a, b, s_1, and s_2. The inner and outer radii of the main dielectric are denoted by ρ_1 $(= a + s_1)$ and ρ_2 $(= b - s_2)$ respectively.

The boundary conditions at the surfaces of the main dielectric will be satisfied, as in Section II, by matching radial impedances at the stack-dielectric interfaces. If the impedance Z_a looking into the core at $\rho = a$ is effectively infinite, then the impedance looking into the inner stack at ρ_1 is given by equation (98) of Section III to be

$$
Z_1 = \frac{\Gamma_t}{\bar{g}} \frac{K_0(\Gamma_t\rho_1)I_1(\Gamma_t a) + K_1(\Gamma_t a)I_0(\Gamma_t\rho_1)}{K_1(\Gamma_t a)I_1(\Gamma_t\rho_1) - K_1(\Gamma_t\rho_1)I_1(\Gamma_t a)}. \tag{337}
$$

Similarly, if the sheath impedance Z_b is infinite, then looking into the outer stack at ρ_2 we have

$$Z_2 = \frac{\Gamma_\ell}{\bar{g}} \frac{K_0(\Gamma_\ell \rho_2) I_1(\Gamma_\ell b) + K_1(\Gamma_\ell b) I_0(\Gamma_\ell \rho_2)}{K_1(\Gamma_\ell \rho_2) I_1(\Gamma_\ell b) - K_1(\Gamma_\ell b) I_1(\Gamma_\ell \rho_2)}. \tag{338}$$

The condition that the radial impedances shall be matched at the surfaces of the main dielectric is given by equation (38) of Section II, which takes the form

$$\frac{\kappa_0 K_0(\kappa_0\rho_1) + i\omega\epsilon_0 Z_1 K_1(\kappa_0\rho_1)}{\kappa_0 I_0(\kappa_0\rho_1) - i\omega\epsilon_0 Z_1 I_1(\kappa_0\rho_1)} = \frac{\kappa_0 K_0(\kappa_0\rho_2) - i\omega\epsilon_0 Z_2 K_1(\kappa_0\rho_2)}{\kappa_0 I_0(\kappa_0\rho_2) + i\omega\epsilon_0 Z_2 I_1(\kappa_0\rho_2)}, \tag{339}$$

where κ_0 is related to Γ_ℓ by equation (330). If we substitute the expressions (337) and (338) for Z_1 and Z_2 into (339), we have a single equation whose roots in Γ_ℓ correspond to all the circular transverse magnetic modes on the coaxial Clogston line. The propagation constant γ of each mode is given in terms of Γ_ℓ by equation (327).

Once the boundary conditions have been satisfied for a particular mode by a suitable determination of Γ_ℓ, it is a routine matter to obtain the field components for this mode. In the main dielectric the fields are of the form given by equations (33) of Section II. Hence for $\rho_1 \leqq \rho \leqq \rho_2$ we have

$$\begin{aligned} H_\phi &= [AI_1(\kappa_0\rho) + BK_1(\kappa_0\rho)]e^{-\gamma z}, \\ E_\rho &= \frac{\gamma}{i\omega\epsilon_0}[AI_1(\kappa_0\rho) + BK_1(\kappa_0\rho)]e^{-\gamma z}, \\ E_z &= \frac{\kappa_0}{i\omega\epsilon_0}[AI_0(\kappa_0\rho) - BK_0(\kappa_0\rho)]e^{-\gamma z}, \end{aligned} \tag{340}$$

where one of the constants A and B is arbitrary, but the ratio A/B must be taken equal to either side of equation (339). The fields in the stacks are of the form of equations (277) of Section VIII, where the constants are to be determined so that $H_\phi = 0$ at $\rho = a$ and $\rho = b$, and so that the tangential field components are continuous at ρ_1 and ρ_2. Imposing these conditions, we find that in the inner stack, for $a \leqq \rho \leqq \rho_1$,

$$\begin{aligned} H_\phi &= C[K_1(\Gamma_\ell a)I_1(\Gamma_\ell \rho) - I_1(\Gamma_\ell a)K_1(\Gamma_\ell \rho)]e^{-\gamma z}, \\ \bar{E}_\rho &= \frac{\gamma}{i\omega\bar{\epsilon}} C[K_1(\Gamma_\ell a)I_1(\Gamma_\ell \rho) - I_1(\Gamma_\ell a)K_1(\Gamma_\ell \rho)]e^{-\gamma z}, \\ E_z &= \frac{\Gamma_\ell}{\bar{g}} C[K_1(\Gamma_\ell a)I_0(\Gamma_\ell \rho) + I_1(\Gamma_\ell a)K_0(\Gamma_\ell \rho)]e^{-\gamma z}, \end{aligned} \tag{341}$$

where

$$C = \frac{AI_1(\kappa_0\rho_1) + BK_1(\kappa_0\rho_1)}{K_1(\Gamma_\ell a)I_1(\Gamma_\ell\rho_1) - I_1(\Gamma_\ell a)K_1(\Gamma_\ell\rho_1)}. \tag{342}$$

In the outer stack, for $\rho_2 \leqq \rho \leqq b$,

$$\begin{aligned} H_\phi &= D[K_1(\Gamma_\ell b)I_1(\Gamma_\ell\rho) - I_1(\Gamma_\ell b)K_1(\Gamma_\ell\rho)]e^{-\gamma z}, \\ \bar{E}_\rho &= \frac{\gamma}{i\omega\bar{\epsilon}} D[K_1(\Gamma_\ell b)I_1(\Gamma_\ell\rho) - I_1(\Gamma_\ell b)K_1(\Gamma_\ell\rho)]e^{-\gamma z}, \\ E_z &= \frac{\Gamma_\ell}{\bar{g}} D[K_1(\Gamma_\ell b)I_0(\Gamma_\ell\rho) + I_1(\Gamma_\ell b)K_0(\Gamma_\ell\rho)]e^{-\gamma z}, \end{aligned} \tag{343}$$

where

$$D = \frac{AI_1(\kappa_0\rho_2) + BK_1(\kappa_0\rho_2)}{K_1(\Gamma_\ell b)I_1(\Gamma_\ell\rho_2) - I_1(\Gamma_\ell b)K_1(\Gamma_\ell\rho_2)}. \tag{344}$$

For the remainder of the present section we shall confine our attention to the principal mode. In the parallel-plane line this mode corresponds to the lowest root in Γ_ℓ of equation (331), that is,

$$\tanh \tfrac{1}{2}\sqrt{i\omega\bar{\epsilon}/\bar{g}}\ \Gamma_\ell b \tanh \Gamma_\ell s = -\frac{\bar{\mu}}{\mu_0}\sqrt{\frac{i\omega\bar{\epsilon}}{\bar{g}}}. \tag{345}$$

We note that the right side of the equation is very small compared to unity, being of the order of the square root of the ratio of displacement current density in the insulators to conduction current density in the conductors, and also that the coefficient of Γ_ℓ in the first factor on the left will under all ordinary conditions be much smaller than the coefficient of Γ_ℓ in the second factor. Hence in seeking the lowest root we are justified in replacing the first hyperbolic tangent on the left side of (345) by its argument, so that the equation becomes

$$\Gamma_\ell s \tanh \Gamma_\ell s = -\frac{\bar{\mu}}{\mu_0}\frac{2s}{b}. \tag{346}$$

If we now let

$$\Gamma_\ell^2 = -\chi^2, \qquad \Gamma_\ell = i\chi, \tag{347}$$

we obtain

$$\chi s \tan \chi s = \frac{\bar{\mu}}{\mu_0}\frac{2s}{b}. \tag{348}$$

Since the right side of (348) is a positive real constant, the equation has exactly one root in the interval $0 < \chi s \leqq \frac{1}{2}\pi$, which may most easily be found from a table[20] of the function $x \tan x$. If we call this root χ_1, equation (327) for the propagation constant γ becomes

$$\gamma^2 = -\omega^2\bar{\mu}\bar{\epsilon} + (i\omega\bar{\epsilon}/\bar{g})\chi_1^2 ; \tag{349}$$

and on taking the square root by the binomial theorem we find for the attenuation and phase constants of the principal mode,

$$\alpha = \frac{\chi_1^2}{2\sqrt{\bar{\mu}/\bar{\epsilon}}\,\bar{g}}, \tag{350}$$

$$\beta = \omega\sqrt{\bar{\mu}\bar{\epsilon}}. \tag{351}$$

It is easy to verify that (350) reduces to the expressions previously obtained for the attenuation constants of Clogston 1 and Clogston 2 lines in the limiting cases $s \ll \frac{1}{2}a$ and $s = \frac{1}{2}a$ respectively. If $s \ll \frac{1}{2}a$, (348) gives

$$\chi_1^2 = \frac{2(\bar{\mu}/\mu_0)}{bs}, \tag{352}$$

so that from (350), on making use of Clogston's condition,

$$\alpha = \frac{(\bar{\mu}/\mu_0)}{\sqrt{\bar{\mu}/\bar{\epsilon}}\,\bar{g}bs} = \frac{1}{\sqrt{\mu_0/\epsilon_0}\,\bar{g}bs}, \tag{353}$$

which agrees with equation (110) of Section IV. If $s = \frac{1}{2}a$, so that $b = 0$, then from (348),

$$\chi_1 = \tfrac{1}{2}\pi/s = \pi/a, \tag{354}$$

and (350) becomes

$$\alpha = \frac{\pi^2}{2\sqrt{\bar{\mu}/\bar{\epsilon}}\,\bar{g}a^2}, \tag{355}$$

which is the same as equation (288) of the preceding section.

The general expressions (333) and (334) for the fields in a plane Clogston line with infinitesimally thin laminae and high-impedance walls simplify considerably for the principal mode, since κ_0 is so small that to a good approximation for $|y| \leqq \frac{1}{2}b$ we may replace sh $\kappa_0 y$ by $\kappa_0 y$ and ch $\kappa_0 y$ by unity. We then have, in the main dielectric,

---

[20] See for example Reference 18, Addenda, pp. 32–35.

$$
\begin{aligned}
H_x &\approx H_0 e^{-\gamma z}, \\
E_y &\approx -\sqrt{\frac{\mu_0}{\epsilon_0}}\, H_0 e^{-\gamma z}, \\
E_z &\approx \frac{\mu_0 \chi_1^2}{\bar{\mu}\bar{g}}\, H_0 y e^{-\gamma z},
\end{aligned} \tag{356}
$$

for $-\frac{1}{2}b \leqq y \leqq \frac{1}{2}b$, where H_0 is an arbitrary amplitude factor. The fields in the stacks are

$$
\begin{aligned}
H_x &\approx H_0 \frac{\sin \chi_1(\frac{1}{2}a \mp y)}{\sin \chi_1 s}\, e^{-\gamma z}, \\
\bar{E}_y &\approx -\sqrt{\frac{\bar{\mu}}{\bar{\epsilon}}}\, H_0 \frac{\sin \chi_1(\frac{1}{2}a \mp y)}{\sin \chi_1 s}\, e^{-\gamma z}, \\
E_z &\approx \pm \frac{\chi_1}{\bar{g}}\, H_0 \frac{\cos \chi_1(\frac{1}{2}a \mp y)}{\sin \chi_1 s}\, e^{-\gamma z},
\end{aligned} \tag{357}
$$

for $\frac{1}{2}b \leqq |y| \leqq \frac{1}{2}a$, where the upper signs refer to the upper stack and the lower signs to the lower stack. The potential and current distribu-

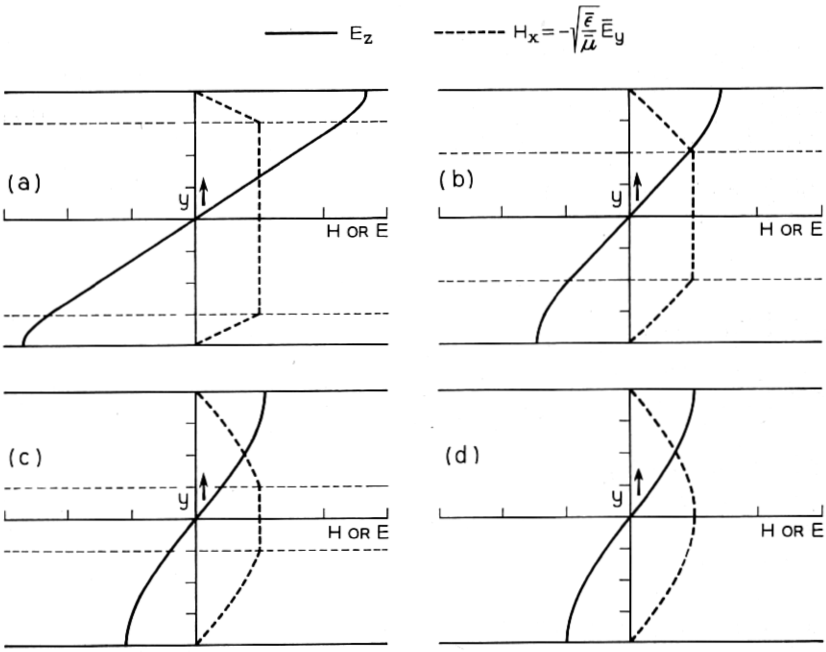

Fig. 13—Fields of principal mode in partially and completely filled plane Clogston lines with $\mu_0 = \bar{\mu}$, $\epsilon_0 = \bar{\epsilon}$.

tions may easily be obtained, if desired, from the expressions for the field components.

As a numerical example we have plotted in Fig. 13 the fields of the principal mode for plane transmission lines in which the stacks fill respectively one-quarter, one-half, three-quarters, and all of the total available space. For simplicity we have taken $\mu_0 = \bar{\mu}$, $\epsilon_0 = \bar{\epsilon}$, and normalized the fields so that the total one-way current is the same in all four cases. The average current density is of course $\bar{g}E_z$ in the stacks and zero in the main dielectric. The first case approximates most nearly to the extreme Clogston 1 line discussed in Part I, while the last case is the complete Clogston 2, and the intermediate cases show the transition between these two structures. The following table gives $\chi_1 s$ as a function of the fraction $s/\frac{1}{2}a$ of the total space filled by the stacks, and also the quantity $(\chi_1 a/\pi)^2$, which is equal to the ratio of the attenuation constant of the line to the attenuation constant of the complete Clogston 2.

$s/\frac{1}{2}a$	$\chi_1 s \tan \chi_1 s$	$\chi_1 s$	$(\chi_1 a/\pi)^2$
1/4	1/3	0.5471	1.941
1/2	1	0.8603	1.200
3/4	3	1.1924	1.024
1	∞	1.5708	1.000

The principal mode in a coaxial Clogston cable corresponds to the lowest root in Γ_ℓ of equation (339). For the principal mode we are justified in assuming that in the main dielectric

$$|\kappa_0 \rho| \ll 1, \tag{358}$$

so that the Bessel functions occurring in equation (339) may be replaced by their approximate values for small argument. We thus find that, to a very good approximation, equation (339) reduces to the same form as equation (41) of Section II, namely

$$\frac{\kappa_0^2}{i\omega\epsilon_0} \log \frac{\rho_2}{\rho_1} = -\left(\frac{Z_1}{\rho_1} + \frac{Z_2}{\rho_2}\right), \tag{359}$$

where the stack impedances Z_1 and Z_2 are given by (337) and (338). If as before we let

$$\Gamma_\ell^2 = -\chi^2, \qquad \Gamma_\ell = i\chi, \tag{360}$$

then from (330) κ_0^2 becomes

$$\kappa_0^2 = -(i\omega\bar{\epsilon}/\bar{g})\chi^2; \tag{361}$$

and replacing the modified Bessel functions in (337) and (338) with ordinary Bessel functions according to equations (292) of Section VIII, we obtain

$$Z_1 = \frac{\chi}{\bar{g}} \frac{J_1(\chi a)N_0(\chi\rho_1) - N_1(\chi a)J_0(\chi\rho_1)}{J_1(\chi a)N_1(\chi\rho_1) - N_1(\chi a)J_1(\chi\rho_1)}, \tag{362}$$

$$Z_2 = \frac{\chi}{\bar{g}} \frac{J_1(\chi b)N_0(\chi\rho_2) - N_1(\chi b)J_0(\chi\rho_2)}{J_1(\chi\rho_2)N_1(\chi b) - N_1(\chi\rho_2)J_1(\chi b)}. \tag{363}$$

Substituting (361), (362), and (363) into (359) and setting $\bar{\epsilon}/\epsilon_0 = \mu_0/\bar{\mu}$, we get after a little rearrangement,

$$\begin{aligned} &\frac{1}{\chi\rho_1} \frac{J_1(\chi a)N_0(\chi\rho_1) - N_1(\chi a)J_0(\chi\rho_1)}{J_1(\chi a)N_1(\chi\rho_1) - N_1(\chi a)J_1(\chi\rho_1)} \\ &\qquad + \frac{1}{\chi\rho_2} \frac{J_1(\chi b)N_0(\chi\rho_2) - N_1(\chi b)J_0(\chi\rho_2)}{J_1(\chi\rho_2)N_1(\chi b) - N_1(\chi\rho_2)J_1(\chi b)} = \frac{\mu_0}{\bar{\mu}} \log \frac{\rho_2}{\rho_1}. \end{aligned} \tag{364}$$

If χ_1 is the smallest positive root of equation (364), then the attenuation and phase constants of the principal mode are

$$\alpha = \frac{\chi_1^2}{2\sqrt{\bar{\mu}/\bar{\epsilon}}\,\bar{g}}, \tag{365}$$

$$\beta = \omega\sqrt{\bar{\mu}\bar{\epsilon}}. \tag{366}$$

These expressions for α and β are of exactly the same form as equations (295) and (296) for a complete Clogston 2, except that χ_1 is now determined from equation (364) instead of equation (293). It is easy to show that (364) reduces to (293) if there is no main dielectric, that is, if $\rho_1 = \rho_2$.

For any given values of the four ratios a/b, ρ_1/b, ρ_2/b, and $\mu_0/\bar{\mu}$, equation (364) may be solved for $\chi_1 b$ by numerical or graphical methods. However if we wish to examine many cases, so as to investigate the effects of varying some or all of the parameters, a more efficient procedure for finding χ_1 is needed. Such a method is provided by the observation that in spite of the complicated appearance of equation (364), it is really just the equation which determines the eigenvalues in a rather simple two-point boundary-value problem, which is well adapted to solution on a differential analyzer. We digress briefly to formulate this problem.

The differential equations for the fields in the main dielectric can be put in the form of equations (67) of Section III, namely

$$\begin{aligned} d(-\rho H_\phi)/d\rho &= -i\omega\epsilon_0\rho E_z , \\ dE_z/d\rho &= -(\kappa_0^2/i\omega\epsilon_0\rho)(-\rho H_\phi), \end{aligned} \tag{367}$$

where the propagation factor $e^{-\gamma z+i\omega t}$ has been suppressed. On the other hand, equations (270) for the fields in a stack of infinitesimally thin laminae yield

$$\begin{aligned} d(-\rho H_\phi)/d\rho &= -\bar{g}\rho E_z , \\ dE_z/d\rho &= -(\Gamma_\iota^2/\bar{g}\rho)(-\rho H_\phi), \end{aligned} \tag{368}$$

where Γ_ι is given by (323). If we neglect the displacement current in the main dielectric compared with the conduction current in the stacks, replace Γ_ι by $i\chi$, express κ_0 in terms of χ by (361), and write $\mu_0/\bar{\mu}$ for $\bar{\epsilon}/\epsilon_0$, we obtain the following equations for the fields in the coaxial Clogston line:

For $a \leqq \rho \leqq \rho_1$,

$$\begin{aligned} d(-\rho H_\phi)/d\rho &= -\rho(\bar{g}E_z), \\ d(\bar{g}E_z)/d\rho &= (\chi^2/\rho)(-\rho H_\phi); \end{aligned} \tag{369i}$$

while for $\rho_1 \leqq \rho \leqq \rho_2$,

$$\begin{aligned} d(-\rho H_\phi)/d\rho &= 0, \\ d(\bar{g}E_z)/d\rho &= (\mu_0\chi^2/\bar{\mu}\rho)(-\rho H_\phi); \end{aligned} \tag{369ii}$$

and for $\rho_2 \leqq \rho \leqq b$,

$$\begin{aligned} d(-\rho H_\phi)/d\rho &= -\rho(\bar{g}E_z), \\ d(\bar{g}E_z)/d\rho &= (\chi^2/\rho)(-\rho H_\phi). \end{aligned} \tag{369iii}$$

The quantities $-\rho H_\phi$ and $\bar{g}E_z$ must be continuous at ρ_1 amd ρ_2; and the two-point boundary condition at the infinite-impedance surfaces $\rho = a$ and $\rho = b$, namely

$$-aH_\phi(a) = -bH_\phi(b) = 0, \tag{370}$$

determines a sequence of eigenvalues $\chi_1^2, \chi_2^2, \chi_3^2, \cdots$, of which the lowest corresponds to the principal mode. It is a routine matter to integrate equations (369) in terms of Bessel functions and logarithms, and to show that the continuity and boundary conditions lead exactly to equation (364).

If equations (369) are set up on a differential analyzer with adjustable values of χ^2, a/b, ρ_1/b, ρ_2/b, and $\mu_0/\bar{\mu}$, it is a simple procedure to make a few runs with different choices of χ^2, and so to locate the approximate value of χ_1^2 which satisfies the boundary conditions for the given values of the other parameters. If additional accuracy is wanted, it is then not too difficult to refine this approximate value by desk computation. The results of quite a number of exploratory calculations which were made on the Laboratories' general purpose analog computer will be shown later in this section.

The fields of the principal mode in the main dielectric of a Clogston cable are given approximately by equations (46) of Section II, namely

$$
\begin{aligned}
H_\phi &\approx \frac{I}{2\pi\rho}\, e^{-\gamma z},\\
E_\rho &\approx \sqrt{\frac{\mu_0}{\epsilon_0}}\, \frac{I}{2\pi\rho}\, e^{-\gamma z},\\
E_z &\approx \frac{I}{2\pi \log\,(\rho_2/\rho_1)} \left[\frac{Z_1}{\rho_1} \log \frac{\rho_2}{\rho} + \frac{Z_2}{\rho_2} \log \frac{\rho_1}{\rho}\right] e^{-\gamma z},
\end{aligned}
\tag{371}
$$

for $\rho_1 \leqq \rho \leqq \rho_2$, where I is an amplitude factor equal to the total current flowing in the positive z-direction in the inner stack, and Z_1 and Z_2 are given by writing χ_1 for χ in (362) and (363) respectively. The fields in the inner stack are

$$
\begin{aligned}
H_\phi &\approx \frac{I}{2\pi\rho_1}\, \frac{N_1(\chi_1 a)J_1(\chi_1\rho) - J_1(\chi_1 a)N_1(\chi_1\rho)}{N_1(\chi_1 a)J_1(\chi_1\rho_1) - J_1(\chi_1 a)N_1(\chi_1\rho_1)}\, e^{-\gamma z},\\
\bar{E}_\rho &\approx \sqrt{\frac{\bar{\mu}}{\bar{\epsilon}}}\, \frac{I}{2\pi\rho_1}\, \frac{N_1(\chi_1 a)J_1(\chi_1\rho) - J_1(\chi_1 a)N_1(\chi_1\rho)}{N_1(\chi_1 a)J_1(\chi_1\rho_1) - J_1(\chi_1 a)N_1(\chi_1\rho_1)}\, e^{-\gamma z},\\
E_z &\approx \frac{\chi_1}{\bar{g}}\, \frac{I}{2\pi\rho_1}\, \frac{N_1(\chi_1 a)J_0(\chi_1\rho) - J_1(\chi_1 a)N_0(\chi_1\rho)}{N_1(\chi_1 a)J_1(\chi_1\rho_1) - J_1(\chi_1 a)N_1(\chi_1\rho_1)}\, e^{-\gamma z},
\end{aligned}
\tag{372}
$$

for $a \leqq \rho \leqq \rho_1$; while in the outer stack we have

$$
\begin{aligned}
H_\phi &\approx \frac{I}{2\pi\rho_2}\, \frac{N_1(\chi_1 b)J_1(\chi_1\rho) - J_1(\chi_1 b)N_1(\chi_1\rho)}{N_1(\chi_1 b)J_1(\chi_1\rho_2) - J_1(\chi_1 b)N_1(\chi_1\rho_2)}\, e^{-\gamma z},\\
\bar{E}_\rho &\approx \sqrt{\frac{\bar{\mu}}{\bar{\epsilon}}}\, \frac{I}{2\pi\rho_2}\, \frac{N_1(\chi_1 b)J_1(\chi_1\rho) - J_1(\chi_1 b)N_1(\chi_1\rho)}{N_1(\chi_1 b)J_1(\chi_1\rho_2) - J_1(\chi_1 b)N_1(\chi_1\rho_2)}\, e^{-\gamma z},\\
E_z &\approx \frac{\chi_1}{\bar{g}}\, \frac{I}{2\pi\rho_2}\, \frac{N_1(\chi_1 b)J_0(\chi_1\rho) - J_1(\chi_1 b)N_0(\chi_1\rho)}{N_1(\chi_1 b)J_1(\chi_1\rho_2) - J_1(\chi_1 b)N_1(\chi_1\rho_2)}\, e^{-\gamma z},
\end{aligned}
\tag{373}
$$

for $\rho_2 \leqq \rho \leqq b$. The potential and current distributions may be calculated in the usual way from the fields.

As numerical examples we have plotted in Fig. 14 the fields of the principal mode in two Clogston coaxial cables. Fig. 14(a) shows a cable in which $\mu_0 = \bar{\mu}$, $\epsilon_0 = \bar{\epsilon}$, and with the dimensions $a = 0.084b$, $\rho_1 = 0.415b$, and $\rho_2 = 0.831b$, these proportions having been found optimum, as discussed below, for a cable without magnetic loading in which the total thickness of both stacks is arbitrarily chosen equal to $\frac{1}{2}b$. Fig. 14(b) shows the fields of a complete Clogston 2 with no inner core, the scale being chosen so that the total one-way current is the same in both cases. The attenuation constant of the first cable is 1.234 times that of the second one. Fig. 14 may be compared with Fig. 13 for the plane geometry, whence it should be possible to visualize approximately the fields of the principal mode in other coaxial structures representing various stages of the transition between the extreme Clogston 1 and the complete Clogston 2 cable.

Now let us consider a Clogston line with infinitesimally thin laminae, having fixed external dimensions and containing only materials with given electrical constants. We may pose two questions: (1) Supposing that for some practical reason the total available thickness of laminated material is also fixed, how should this material be divided between the two stacks to minimize the attenuation constant of the line? (2) Assuming that the total thickness of laminations in the line is at our disposal, what is the optimum amount of laminated material from the standpoint of minimizing the attenuation, and how should this material be distributed in the optimum case?

For plane transmission lines the first question is trivial; the stacks should always be of equal thickness. In a coaxial cable, if the filling ratio $(s_1 + s_2)/b$ is given, the proportions of the cable are completely determined when we specify, for example, the relative radius a/b of the core and the relative thickness $s_1/(s_1 + s_2)$ of the inner stack. The opti-

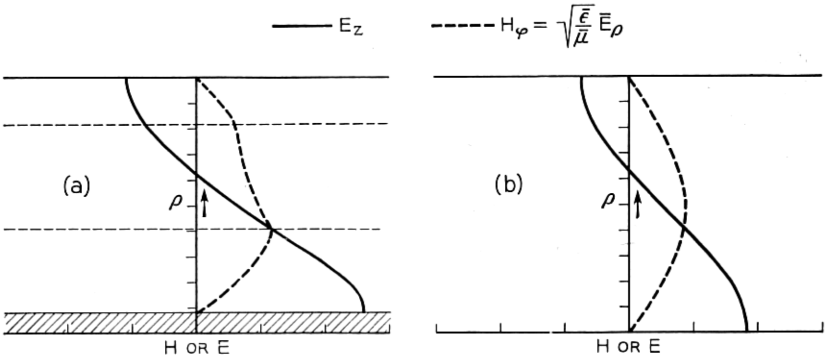

Fig. 14—Fields of principal mode in partially and completely filled coaxial Clogston lines with $\mu_0 = \bar{\mu}$, $\epsilon_0 = \bar{\epsilon}$.

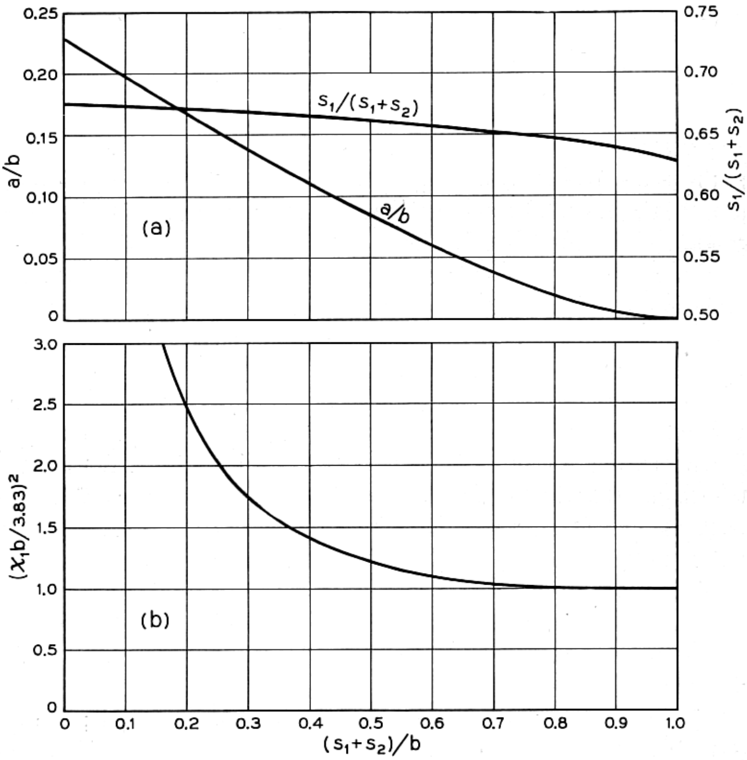

Fig. 15—Relative proportions and relative attenuation constants of optimum Clogston cables with different filling ratios and $\mu_0 = \bar{\mu}$, $\epsilon_0 = \bar{\epsilon}$.

mum values of these two ratios in the extreme Clogston 1 case, where $(s_1 + s_2) \ll b$, have already been given in equations (138) and (139) of Section IV, while in a complete Clogston 2 with $s_1 + s_2 = b$, the stacks should be divided at the radius $0.6276b$, where according to equation (314) the current density is zero. For intermediate filling ratios, with any fixed magnetic loading ratio $\mu_0/\bar{\mu}$, the optimum distribution of laminated material can most easily be found numerically by calculating χ_1^2 or $(\chi_1 b)^2$ for a number of different choices of the ratios a/b and $s_1/(s_1 + s_2)$, and then locating the minimum by double interpolation.

The results of applying this numerical procedure to Clogston cables with various filling ratios and no magnetic loading are plotted in Fig. 15, the necessary values of $\chi_1 b$ having been found on the analog computer and then refined by desk computation. Fig. 15(a) shows the optimum values of a/b and $s_1/(s_1 + s_2)$ as functions of the filling ratio $(s_1 + s_2)/b$, while Fig. 15(b) shows the corresponding value of $(\chi_1 b/3.83)^2$, which by equation (365) is proportional to the attenuation constant. We note that the Clogston 2 line with filling ratio unity has the lowest attenuation constant of any cable of the same size without magnetic loading, but that the attenuation constant increases only slowly as the filling ratio decreases, so long as the ratio is greater than about one-half. It also appears that the minimum in $\chi_1 b$, considered as a function of a/b and $s_1/(s_1 + s_2)$ for a fixed filling ratio, is quite broad, which means that in practice one can attain very nearly optimum performance even while deviating somewhat from the optimum proportions.

If the filling ratio is at our disposal, then the solution of the optimum problem is as follows: When there is no magnetic loading of the main dielectric relative to the stacks, that is, when $\mu_0 \leqq \bar{\mu}$, then minimum attenuation is obtained with a complete Clogston 2. If on the other hand there is magnetic loading of the main dielectric, so that $\mu_0 > \bar{\mu}$, then minimum attenuation is obtained with a filling ratio less than unity, whose value is a function of the ratio $\mu_0/\bar{\mu}$.

According to equation (350), the attenuation constant of a plane Clogston line is

$$\alpha = \frac{\chi_1^2}{2\sqrt{\bar{\mu}/\bar{\epsilon}}\,\bar{g}}, \tag{374}$$

where χ_1 is given by equation (348),

$$\chi_1 \tan \chi_1 s = \frac{2\bar{\mu}}{\mu_0 b} = \frac{\bar{\mu}}{\mu_0(\frac{1}{2}a - s)}. \tag{375}$$

To find the minimum value of χ_1 when a and $\mu_0/\bar{\mu}$ are given, we differentiate (375) with respect to s and set $d\chi_1/ds$ equal to zero. This gives

$$\chi_1^2 \sec^2 \chi_1 s = \frac{\bar{\mu}}{\mu_0(\frac{1}{2}a - s)^2}, \tag{375.5}$$

which when solved simultaneously with equation (375) leads to

$$\sin \chi_1 s = \sqrt{\bar{\mu}/\mu_0}, \qquad \chi_1 = \frac{1}{s} \sin^{-1} \sqrt{\bar{\mu}/\mu_0}. \tag{376}$$

Substituting this value of χ_1 into (375) and solving for s in terms of a, we get

$$s = \tfrac{1}{2}a \frac{\mu_0 \sin^{-1} \sqrt{\bar{\mu}/\mu_0}}{\mu_0 \sin^{-1} \sqrt{\bar{\mu}/\mu_0} + \sqrt{\bar{\mu}(\mu_0 - \bar{\mu})}}, \tag{377}$$

and from (374) the corresponding attenuation constant is

$$\alpha = \frac{2}{\sqrt{\bar{\mu}/\bar{\epsilon}}\,\bar{g}a^2} \left[\sin^{-1} \sqrt{\bar{\mu}/\mu_0} + \sqrt{\bar{\mu}(\mu_0 - \bar{\mu})/\mu_0^2}\right]^2. \tag{378}$$

As $\mu_0/\bar{\mu}$ increases from unity to very large values, the optimum value of s decreases from $\frac{1}{2}a$ toward $\frac{1}{4}a$, so that the filling ratio decreases from unity toward one-half. If $\mu_0/\bar{\mu} < 1$, equation (376) does not yield a real solution, but the complete Clogston 2 is still the physical structure having the lowest attenuation.

For a coaxial Clogston line without magnetic loading the optimum filling ratio is unity, as we have seen above, while in the presence of magnetic loading a smaller filling ratio is optimum. This filling ratio and the optimum distribution of the laminated material in the cable can be determined by numerical analysis for any given value of $\mu_0/\bar{\mu}$. It is reasonably evident on physical grounds, and can be proved mathematically by a variational argument applied to the lowest eigenvalue of equations (369), that whatever may be the radii ρ_1 and ρ_2 of the main dielectric, the lowest attenuation constant is achieved when $a = 0$, that is, when there is no core inside the inner stack. (This is only a mathematical limit; from a practical standpoint, the use of a small core in the manufacturing process is not likely to make any significant increase in the attenuation of the cable.) For each value of the loading ratio $\mu_0/\bar{\mu}$, therefore, we have merely to minimize the value of $(\chi_1 b)^2$ as a function of the two ratios ρ_1/b and ρ_2/b, which can be done by the double interpolation procedure mentioned earlier. We find that as $\mu_0/\bar{\mu}$ increases from unity to very large values, the optimum value of ρ_1 decreases from $0.6276b$ toward $0.3930b$, while ρ_2 increases from $0.6276b$ toward $0.8226b$, so that the filling ratio decreases from unity toward 0.5704. The limiting values of ρ_1 and ρ_2 when $\mu_0/\bar{\mu} \gg 1$ are derived from equation (364) by the method shown in Appendix II.

As a numerical example we have considered a Clogston cable with $\mu_0 = 3\bar{\mu}$. The optimum proportions of this cable and the corresponding value of χ_1 are approximately

$$\rho_1 = 0.426b, \qquad \rho_2 = 0.796b, \qquad \chi_1 = 2.720/b; \tag{379}$$

and the minimum attenuation constant is

$$\alpha = \frac{3.699}{\sqrt{\bar{\mu}/\bar{\epsilon}}\,\bar{g}b^2}. \tag{380}$$

The attenuation constant of a complete Clogston 2 with the same stack parameters $\bar{\mu}$ and $\bar{\epsilon}$ is, from (318),

$$\alpha = \frac{7.341}{\sqrt{\bar{\mu}/\bar{\epsilon}}\,\bar{g}b^2}, \tag{381}$$

so that the attenuation constant of the optimum loaded cable is only about 0.504 times that of the optimum unloaded one. In this example, of course, we have said nothing about the effects of magnetic dissipation.

In the above work we have assumed that the electrical constants $\bar{\mu}$, $\bar{\epsilon}$, $\bar{g}$ of the stacks and μ_0, ϵ_0 of the main dielectric were all fixed quantities. We now consider the case in which the electrical constants of the conducting and insulating layers are given, but the fraction θ of conducting material in the stacks may be varied. We also suppose that the constants of the main dielectric are at our disposal, so that Clogston's condition may always be satisfied. When then is the optimum value of θ?

If we express $\bar{\epsilon}$, $\bar{\mu}$, and $\bar{g}$ in terms of the constants of the individual layers by equations (268) of Section VIII, we find that the expression for the attenuation constant of the principal mode in a Clogston line becomes

$$\alpha = \frac{\chi_1^2}{2\sqrt{\bar{\mu}/\bar{\epsilon}}\,\bar{g}} = \frac{\sqrt{\epsilon_2}\,\chi_1^2}{2\theta(1-\theta)^{\frac{1}{2}}[\theta\mu_1 + (1-\theta)\mu_2]^{\frac{1}{2}}g_1}, \tag{382}$$

where χ_1 is the lowest root of equation (348) for a plane line or equation (364) for a coaxial cable. We wish to minimize α as a function of θ.

If the conducting and insulating layers have different permeabilities ($\mu_1 \neq \mu_2$), then in the general partially filled line χ_1 depends on θ, through the factor $\bar{\mu}$ in equation (348) or (364), as well as on the geometric proportions of the line. In the limiting case of an extreme Clogston 1 line we found in Section IV, equation (145), that the optimum value of θ is

$$\theta = \frac{\mu_1 + (\mu_1^2 + 8\mu_1\mu_2)^{\frac{1}{2}}}{3\mu_1 + (\mu_1^2 + 8\mu_1\mu_2)^{\frac{1}{2}}}; \tag{383}$$

while in a Clogston 2 with no main dielectric, it turns out from (348) or (364) that χ_1 is independent of θ, and an elementary calculation shows that the value of θ which minimizes α is

$$\theta = \frac{3(\mu_1 - 2\mu_2) + (9\mu_1^2 - 4\mu_1\mu_2 + 4\mu_2^2)^{\frac{1}{2}}}{8(\mu_1 - \mu_2)}. \tag{384}$$

For the general partially filled line, however, there seems to be no simple expression for the optimum value of θ.

If the conducting and insulating layers have equal permeabilities, then the average permeability $\bar{\mu}$ ($= \mu_1 = \mu_2$) is independent of θ, and matters are much simpler. Since χ_1 is also independent of θ, the minimum value of α in equation (382) is achieved when

$$\theta = 2/3, \tag{385}$$

that is, when *the thickness of the conducting layers is twice the thickness of the insulating layers*. Thus the result obtained in Section IV for extreme Clogston 1 lines is shown to hold for Clogston lines with an arbitrary degree of filling, provided only that the permeabilities of the conducting and insulating layers are equal.

We emphasize that the preceding results apply only when the layers are infinitesimally thin. If the layers are of finite thickness, then the optimum value of θ will be less than that calculated for infinitesimally thin layers. The case of finite layers will be discussed in Section XI.

X. HIGHER MODES IN CLOGSTON LINES

We shall now investigate certain of the higher modes which are possible in Clogston-type transmission lines. As elsewhere in this paper, we shall restrict ourselves to modes having H_x, E_y, E_z or H_ϕ, E_ρ, E_z field components only, and for simplicity we shall assume stacks of infinitesimally thin laminae backed by high-impedance boundaries; but we shall place no restrictions on the relative thicknesses of the stacks and the main dielectric. We shall suppose, however, that the main dielectric always satisfies Clogston's condition. From physical considerations we anticipate the existence of higher modes of two types:

(1) In a partially filled Clogston line containing a finite thickness of main dielectric, there will be a group of modes very similar to the modes which can propagate between perfect conductors when the frequency is high enough to allow one or more field reversals in the space between the conductors. In a Clogston line these modes will have most of their field energy in the main dielectric, and for lack of a better term may be called "dielectric modes". They will all be cut off at sufficiently low frequencies, and for this reason are not likely to be of much engineering importance. The cutoff frequency of any particular dielectric mode is approximately inversely proportional to the thickness of the main dielectric, so that these modes cannot exist in a completely filled Clogston 2.

(2) There will also be a group of modes which are closely bound up with the laminated stacks, and which correspond to one or more current reversals in the stacks themselves; we shall call these the "stack modes".[21] The stack modes will propagate down to zero frequency on either a partially or a completely filled Clogston line. They will have higher attenuation constants than the principal mode, but occasions may arise in which they are of considerable practical importance. We shall therefore consider these modes in some detail in what follows.

[21] The stack modes in plane lines were discussed by Clogston in Reference 1, Sections IV–VI.

As we have seen in the preceding section, the even and odd modes in a plane Clogston line with infinitesimally thin laminae and high-impedance boundaries correspond respectively to the roots of equations (331) and (332), namely

$$\tanh \tfrac{1}{2}\sqrt{i\omega\bar{\epsilon}/\bar{g}}\;\Gamma_\ell b \tanh \Gamma_\ell s = -\frac{\bar{\mu}}{\mu_0}\sqrt{\frac{i\omega\bar{\epsilon}}{\bar{g}}}, \tag{386}$$

$$\coth \tfrac{1}{2}\sqrt{i\omega\bar{\epsilon}/\bar{g}}\;\Gamma_\ell b \tanh \Gamma_\ell s = -\frac{\bar{\mu}}{\mu_0}\sqrt{\frac{i\omega\bar{\epsilon}}{\bar{g}}}. \tag{387}$$

In either case the propagation constant γ is related to Γ_ℓ by

$$\gamma^2 = -\omega^2\bar{\mu}\bar{\epsilon} - (i\omega\bar{\epsilon}/\bar{g})\Gamma_\ell^2, \tag{388}$$

and the field components are given by (333) and (334) for the even modes, or by (335) and (336) for the odd modes.

Our first observation relative to equations (386) and (387) is that the right-hand sides of these equations are extremely small compared to unity. Since the right-hand members are of the order of magnitude of $(\omega\bar{\epsilon}/\bar{g})^{\frac{1}{2}}$, at least one of the two factors on the left side of each equation must be of the order of $(\omega\bar{\epsilon}/\bar{g})^{\frac{1}{4}}$, which is still small compared to unity. If we consider the factors separately, there will be an infinite number of values of Γ_ℓ for which each vanishes, since the hyperbolic tangent vanishes whenever its argument is equal to $m\pi i$, where m is any integer, and the hyperbolic cotangent vanishes whenever its argument equals $(m + \frac{1}{2})\pi i$. Since the coefficients of Γ_ℓ in the two factors on the left side of either equation have different phase angles, we see that both factors cannot vanish simultaneously for any non-zero value of Γ_ℓ. However as we have noted earlier the coefficient of Γ_ℓ in the first factor is very much smaller than the coefficient of Γ_ℓ in the second factor, and so in equation (386) both hyperbolic tangents may be small in the neighborhood of the first few non-zero roots of the second one. On the other hand the second hyperbolic tangent will not be small in the neighborhood of the non-zero roots of the first one; and in equation (387) the hyperbolic tangent and cotangent will never be small simultaneously. With these remarks in mind we shall proceed to a more detailed study of the various higher modes.

One group of modes is given to a good approximation by the condition that the first factor on the left side of equation (386) or (387) vanishes, that is,

$$\sqrt{i\omega\bar{\epsilon}/\bar{g}}\;\Gamma_\ell b \approx m\pi i, \tag{389}$$

where $m = 1, 2, 3, \cdots$, and the even values of m correspond to the even modes while the odd values correspond to the odd modes. In this section we shall exclude the case $m = 0$, which corresponds to the principal mode discussed in the preceding section. From (389) and equation (330) of Section IX, we get

$$\Gamma_\ell \approx \frac{m\pi}{b} \sqrt{\frac{i\bar{g}}{\omega\bar{\epsilon}}} = \frac{(1 + i)m\pi}{\sqrt{2}b} \sqrt{\frac{\bar{g}}{\omega\bar{\epsilon}}}, \tag{390}$$

$$\kappa_0 \approx \frac{m\pi i}{b}. \tag{391}$$

The fields of the mth mode are given by substituting these quantities into (333) and (334) if m is even, or (335) and (336) if m is odd.

From equation (388), making use of Clogston's condition, the propagation constant of the mth mode of this family is given by

$$\gamma^2 \approx -\omega^2\mu_0\epsilon_0 + m^2\pi^2/b^2 = -4\pi^2/\lambda_0^2 + m^2\pi^2/b^2, \tag{392}$$

where λ_0 is the wavelength of a free wave in the main dielectric at the operating frequency. To this approximation the values of γ are the same as the propagation constants of the family of modes (with H_x, E_y, and E_z field components only) which are possible in a dielectric slab of thickness b between perfectly conducting planes. The cutoff wavelength of the mth mode is

$$\lambda_c = 2b/m, \tag{393}$$

the propagation constant being real, to the present approximation, if $\lambda_0 > \lambda_c$ and pure imaginary if $\lambda_0 < \lambda_c$. We see that the cutoff frequency is inversely proportional to the width of the main dielectric, so that this family of modes is not possible in a completely filled Clogston 2.

It is worth noting that the effective skin depth of the stacks for the mth mode is, from (390),

$$\Delta = \frac{1}{\text{Re}\,\Gamma_\ell} = \frac{b}{m\pi} \sqrt{\frac{2\omega\bar{\epsilon}}{\bar{g}}} = \frac{\lambda_c}{\lambda_0} \sqrt{\frac{2}{\omega\bar{\mu}\bar{g}}}. \tag{394}$$

If the mode is just above cutoff, then Δ is of the order of magnitude of δ_1 $(= \sqrt{2/\omega\mu_1 g_1})$, but as ω increases indefinitely Δ also increases indefinitely, for the ideal stack of infinitesimally thin laminae. The physical explanation is simple: When the mode is near cutoff the phase velocity is very high, but as the frequency is increased the phase velocity approaches the velocity of a free wave in the main dielectric, for which the effective skin depth of the stacks was designed by Clogston's condition to be infinite. By increasing the $\mu_0\epsilon_0$ product of the main dielectric, it would be possible to make the effective skin thickness of a stack of infinitesimally thin layers infinite for any given mode at any single specified frequency, but at the moment this possibility appears of scarcely more than academic interest. Of course the practical limitation on effective skin depth at high frequencies is the finite thickness of the layers, a consideration which we do not take into account in the present section.

The attenuation constants of the dielectric modes, when these modes are above cutoff, may be calculated either by obtaining the small corrections to the values of Γ_ℓ due to the fact that the right side of equation (386) or (387) is not rigorously zero, or by taking one-half the ratio of dissipated power per unit length to transmitted power. Either method gives for the mth mode, assuming the stack thickness s to be large compared to Δ,

$$\alpha = \frac{m\pi}{b^2} \frac{\bar{\mu}}{\mu_0} \frac{\sqrt{2/\omega\bar{\mu}\bar{g}}}{\sqrt{1 - (\lambda_0/\lambda_c)^2}} . \tag{395}$$

Equation (395) assumes conducting layers very thin compared to the skin depth, a situation which may be difficult to achieve at frequencies high enough to permit the modes of this family to propagate.

Another family of modes which can exist on a parallel-plane Clogston line is given by the condition that the second factor on the left side of equation (386) or (387) shall be nearly equal to zero. As pointed out above the even modes present a slight complication; since the coefficient of Γ_ℓ in the first hyperbolic tangent on the left side of (386) is very small, this factor may be comparable to or smaller than the term on the right side in the neighborhood of the first few roots of the equation, in which case the second hyperbolic tangent will not be small compared to unity at these roots. For all the modes in which we can conceivably be interested, however, $|\Gamma_\ell b|$ will be a small fraction of the very large number $2\sqrt{\bar{g}/\omega\bar{\epsilon}}$, and we may therefore replace the first hyperbolic tangent on the left side of (386) by its argument. Thus on making the usual substitution,

$$\Gamma_\ell^2 = -\chi^2, \qquad \Gamma_\ell = i\chi, \tag{396}$$

we get for the even modes,

$$\chi s \tan \chi s = \frac{\bar{\mu}}{\mu_0} \frac{2s}{b} , \tag{397}$$

which is the same as equation (348) of the preceding section. On the other hand, the odd modes of this family are all given approximately by

$$\tan \chi s = 0, \tag{398}$$

since the hyperbolic cotangent on the left side of (387) will never be small for the same value of Γ_t (or χ) as the hyperbolic tangent.

Equation (397) has an infinite number of positive real roots, which may be denoted by

$$\chi_1, \chi_3, \chi_5, \cdots, \chi_{2p+1}, \cdots, \tag{399}$$

and it is clear that

$$p\pi/s < \chi_{2p+1} \leqq (p + \tfrac{1}{2})\pi/s. \tag{400}$$

If the thickness b of the main dielectric is not zero, so that the right side of equation (397) is finite, the higher roots χ_{2p+1} approach nearer and nearer to $p\pi/s$ as p increases; but if $b = 0$, then

$$\chi_{2p+1} = (p + \tfrac{1}{2})\pi/s = (2p + 1)\pi/a \tag{401}$$

for all p. The positive roots of equation (398) may be called

$$\chi_2, \chi_4, \chi_6, \cdots, \chi_{2p}, \cdots, \tag{402}$$

where

$$\chi_{2p} = p\pi/s \tag{403}$$

for all p; and both sets of roots may be combined in the single sequence

$$\chi_1, \chi_2, \chi_3, \cdots, \chi_p, \cdots. \tag{404}$$

The advantages of designating the principal mode as the first rather than the zero-th mode seem to outweigh the minor disadvantage that in the sequence (404) the odd subscripts correspond to what we have been calling the even modes, and vice versa.

The attenuation and phase constants of the pth mode are obtained in terms of χ_p from (388) and (396). Under the usual assumption that the attenuation per radian is small, we have

$$\alpha = \frac{\chi_p^2}{2\sqrt{\bar{\mu}/\bar{\epsilon}}\,\bar{g}}, \tag{405}$$

$$\beta = \omega\sqrt{\bar{\mu}\bar{\epsilon}}, \tag{406}$$

which become, for the completely filled Clogston 2,

$$\alpha = \frac{p^2\pi^2}{2\sqrt{\bar{\mu}/\bar{\epsilon}}\,\bar{g}a^2}, \tag{407}$$

$$\beta = \omega\sqrt{\bar{\mu}\bar{\epsilon}}. \tag{408}$$

From (330) and (396) we have for the pth mode,

$$\Gamma_\ell = i\chi_p , \tag{409}$$

$$\kappa_0 = (-1 + i)\sqrt{\omega\bar{\epsilon}/2\bar{g}}\ \chi_p . \tag{410}$$

The fields may be obtained by substituting Γ_ℓ and κ_0 into equations (333) and (334) when p is odd, or (335) and (336) when p is even. For the modes in which we are interested, that is, for sufficiently small values of p, we may replace sh $\kappa_0 y$ by $\kappa_0 y$ and ch $\kappa_0 y$ by unity when $| y | \leqq \frac{1}{2}b$. Then for the modes with odd subscripts $2p + 1$ we have, in the main dielectric,

$$\begin{aligned} H_x &\approx H_0 e^{-\gamma_{2p+1} z}, \\ E_y &\approx -\sqrt{\frac{\mu_0}{\epsilon_0}}\, H_0 e^{-\gamma_{2p+1} z}, \\ E_z &\approx \frac{\mu_0 \chi_{2p+1}^2}{\bar{\mu}\bar{g}}\, H_0 e^{-\gamma_{2p+1} z}, \end{aligned} \tag{411}$$

for $-\frac{1}{2}b \leqq y \leqq \frac{1}{2}b$, while in the stacks,

$$\begin{aligned} H_x &\approx H_0 \frac{\sin \chi_{2p+1}(\frac{1}{2}a \mp y)}{\sin \chi_{2p+1} s}\, e^{-\gamma_{2p+1} z}, \\ \bar{E}_y &\approx -\sqrt{\frac{\bar{\mu}}{\bar{\epsilon}}}\, H_0 \frac{\sin \chi_{2p+1}(\frac{1}{2}a \mp y)}{\sin \chi_{2p+1} s}\, e^{-\gamma_{2p+1} z}, \\ E_z &\approx \pm\frac{\chi_{2p+1}}{\bar{g}}\, H_0 \frac{\cos \chi_{2p+1}(\frac{1}{2}a \mp y)}{\sin \chi_{2p+1} s}\, e^{-\gamma_{2p+1} z}, \end{aligned} \tag{412}$$

for $\frac{1}{2}b \leqq | y | \leqq \frac{1}{2}a$, where the upper signs refer to the upper stack and the lower signs to the lower stack. Of course the arbitrary amplitude factor H_0 need not be the same for different values of p. Similarly for the modes with even subscripts $2p$ the fields in the main dielectric are

$$\begin{aligned} H_x &\approx 0, \\ E_y &\approx 0, \\ E_z &\approx (-)^p \frac{p\pi}{\bar{g}s}\, H_0 e^{-\gamma_{2p} z}, \end{aligned} \tag{413}$$

for $-\frac{1}{2}b \leqq y \leqq \frac{1}{2}b$, while in the stacks,

$$
\begin{aligned}
H_x &\approx \pm H_0 \sin \frac{p\pi(\frac{1}{2}a \mp y)}{s} e^{-\gamma_{2p}z}, \\
\bar{E}_y &\approx \mp \sqrt{\frac{\bar{\mu}}{\bar{\epsilon}}} H_0 \sin \frac{p\pi(\frac{1}{2}a \mp y)}{s} e^{-\gamma_{2p}z}, \\
E_z &\approx \frac{p\pi}{\bar{g}s} H_0 \cos \frac{p\pi(\frac{1}{2}a \mp y)}{s} e^{-\gamma_{2p}z},
\end{aligned} \tag{414}
$$

for $\frac{1}{2}b \leqq |y| \leqq \frac{1}{2}a$, and again the upper signs refer to the upper stack and the lower signs to the lower stack.

In a complete Clogston 2 the expressions for the fields simplify a good deal. For the modes with odd subscripts $2p + 1$ the fields are, for $-\frac{1}{2}a \leqq y \leqq \frac{1}{2}a$,

$$
\begin{aligned}
H_x &\approx H_0 \cos \frac{(2p+1)\pi y}{a} e^{-\gamma_{2p+1}z}, \\
\bar{E}_y &\approx -\sqrt{\frac{\bar{\mu}}{\bar{\epsilon}}} H_0 \cos \frac{(2p+1)\pi y}{a} e^{-\gamma_{2p+1}z}, \\
E_z &\approx \frac{(2p+1)\pi}{\bar{g}a} H_0 \sin \frac{(2p+1)\pi y}{a} e^{-\gamma_{2p+1}z},
\end{aligned} \tag{415}
$$

while for the modes with even subscripts $2p$,

$$
\begin{aligned}
H_x &\approx H_0 \sin \frac{2p\pi y}{a} e^{-\gamma_{2p}z}, \\
\bar{E}_y &\approx -\sqrt{\frac{\bar{\mu}}{\bar{\epsilon}}} H_0 \sin \frac{2p\pi y}{a} e^{-\gamma_{2p}z}, \\
E_z &\approx -\frac{2p\pi}{\bar{g}a} H_0 \cos \frac{2p\pi y}{a} e^{-\gamma_{2p}z}.
\end{aligned} \tag{416}
$$

The fields of the higher modes in a plane Clogston 2 are simply related to the fields of the principal mode shown in Fig. 13(d). The fields of the pth mode may be obtained conceptually by stacking up p "layers", each of thickness a/p, the fields in each layer being identical with the fields of the principal mode except for the scale reduction and a phase difference of 180° between adjacent layers. Equation (407) shows that the attenuation constant of the pth mode in a plane Clogston 2 with infinitesimally thin laminae and high-impedance walls is just p^2 times the attenuation constant of the principal mode.

It may be observed that if we are considering a partially filled plane Clogston line with $b > 0$, then the propagation constants of the $2p$th and the $(2p + 1)$st stack modes will be nearly the same for sufficiently large values of p (how large depends on the ratio of stack thickness to main dielectric thickness). Except for differences in sign, the fields in the stacks will also be the same up to second order differences which our approximations do not show. The physical interpretation is that for a thick enough main dielectric and/or sufficiently large values of p, the fields are confined almost entirely to the two stacks, being relatively small in the main dielectric, while the stacks act like a pair of almost independent Clogston 2 lines each of thickness s and carrying a particular Clogston 2 higher mode.

Figs. 16 and 17 show field plots for the second and third stack modes (i.e., the first and second higher modes) in the same four plane Clogston lines that were used to exhibit the behavior of the principal mode in Fig. 13. Note however that these plots are not normalized and that the horizontal scales on the figures are not all the same. The following table gives $\chi_2 s$ and $\chi_3 s$ as functions of the fraction $s/\frac{1}{2}a$ of the total space filled by the stacks, and also the quantities $(\chi_2 a/\pi)^2$ and $(\chi_3 a/\pi)^2$, which are just the ratios of the attenuation constants of

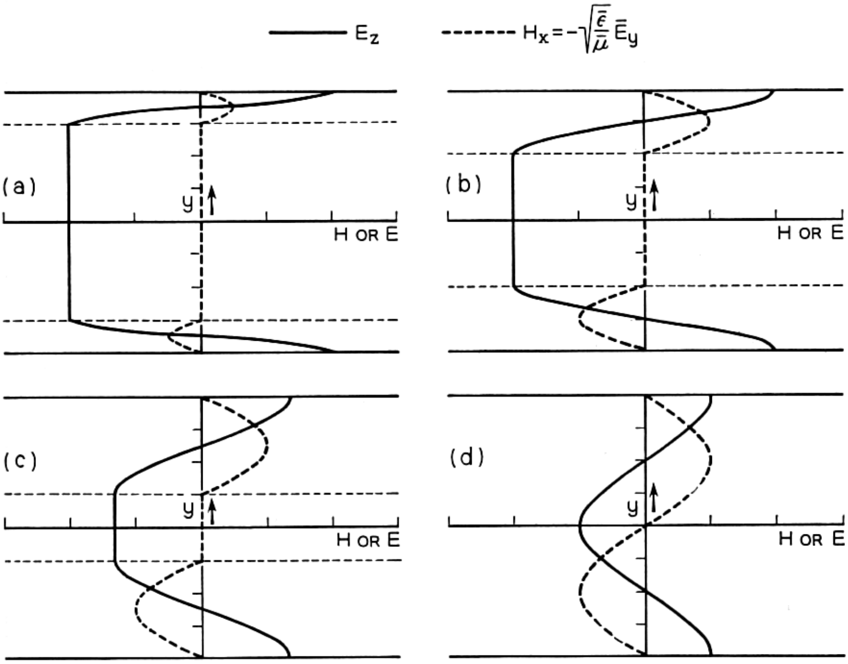

Fig. 16—Fields of second stack mode in partially and completely filled plane Clogston lines with $\mu_0 = \bar{\mu}$, $\epsilon_0 = \bar{\epsilon}$.

these modes to the attenuation constant of the principal mode in a completely filled Clogston 2.

$s/\frac{1}{2}a$	$\chi_2 s$	$\chi_3 s$	$(\chi_2 a/\pi)^2$	$(\chi_3 a/\pi)^2$
$\frac{1}{4}$	π	3.244	64.0	68.2
$\frac{1}{2}$	π	3.426	16.0	19.0
$\frac{3}{4}$	π	3.809	7.1	10.5
1	π	4.712	4.0	9.0

These results may be compared with those given in Section IX for the principal mode in plane Clogston lines having the same proportions.

Turning now to the cylindrical geometry, we remember that all the circular transverse magnetic modes in a coaxial Clogston line with infinitesimally thin laminae and high-impedance boundaries are given by the roots of equation (339) of Section IX, namely

$$\frac{\kappa_0 K_0(\kappa_0\rho_1) + i\omega\epsilon_0 Z_1 K_1(\kappa_0\rho_1)}{\kappa_0 I_0(\kappa_0\rho_1) - i\omega\epsilon_0 Z_1 I_1(\kappa_0\rho_1)} = \frac{\kappa_0 K_0(\kappa_0\rho_2) - i\omega\epsilon_0 Z_2 K_1(\kappa_0\rho_2)}{\kappa_0 I_0(\kappa_0\rho_2) + i\omega\epsilon_0 Z_2 I_1(\kappa_0\rho_2)}, \quad (417)$$

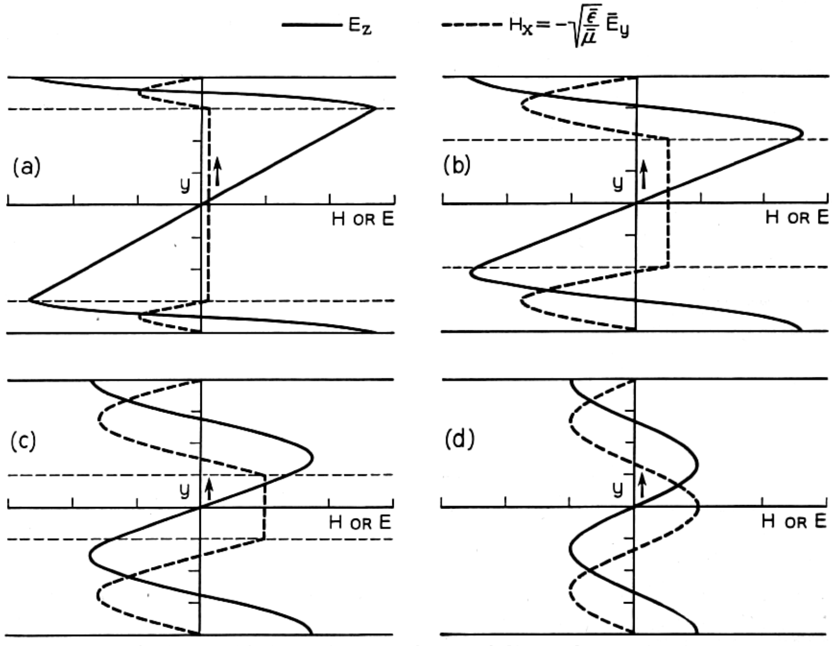

Fig. 17—Fields of third stack mode in partially and completely filled plane Clogston lines with $\mu_0 = \bar{\mu}$, $\epsilon_0 = \bar{\epsilon}$.

where

$$Z_1 = \frac{\Gamma_\ell}{\bar{g}} \frac{K_0(\Gamma_\ell \rho_1)I_1(\Gamma_\ell a) + K_1(\Gamma_\ell a)I_0(\Gamma_\ell \rho_1)}{K_1(\Gamma_\ell a)I_1(\Gamma_\ell \rho_1) - K_1(\Gamma_\ell \rho_1)I_1(\Gamma_\ell a)}, \tag{418}$$

$$Z_2 = \frac{\Gamma_\ell}{\bar{g}} \frac{K_0(\Gamma_\ell \rho_2)I_1(\Gamma_\ell b) + K_1(\Gamma_\ell b)I_0(\Gamma_\ell \rho_2)}{K_1(\Gamma_\ell \rho_2)I_1(\Gamma_\ell b) - K_1(\Gamma_\ell b)I_1(\Gamma_\ell \rho_2)}. \tag{419}$$

Physically it is clear that the modes of the coaxial cable must be of the same general types as the modes of the parallel-plane line, and so in seeking the roots of equation (417) we shall be guided by the results which we have already found for the plane structure.

The dielectric modes in the cable may be located, to a first approximation, by setting Z_1 and Z_2 equal to zero, whence (417) becomes

$$\frac{K_0(\kappa_0 \rho_1)}{I_0(\kappa_0 \rho_1)} = \frac{K_0(\kappa_0 \rho_2)}{I_0(\kappa_0 \rho_2)}. \tag{420}$$

The substitution

$$\kappa_0^2 = -h^2, \qquad \kappa_0 = ih, \tag{421}$$

transforms (420) into

$$J_0(h\rho_1)N_0(h\rho_2) - J_0(h\rho_2)N_0(h\rho_1) = 0. \tag{422}$$

Equation (422) has an infinite number of real roots $h_1, h_2, h_3, \cdots, h_m, \cdots$, of which the mth one may be written in the form[22]

$$h_m = \frac{m\pi F_m(\rho_1/\rho_2)}{\rho_2 - \rho_1}, \tag{423}$$

where $F_m(\rho_1/\rho_2)$ is a function which increases from slightly less than unity at $\rho_1/\rho_2 = 0$ to unity at $\rho_1/\rho_2 = 1$. From equations (330) and (423) we have, approximately,

$$\Gamma_\ell = h_m \sqrt{\frac{i\bar{g}}{\omega\bar{\epsilon}}} = \frac{(1 + i)m\pi F_m(\rho_1/\rho_2)}{\sqrt{2}\,(\rho_2 - \rho_1)} \sqrt{\frac{\bar{g}}{\omega\bar{\epsilon}}}, \tag{424}$$

$$\kappa_0 = ih_m = \frac{im\pi F_m(\rho_1/\rho_2)}{\rho_2 - \rho_1}, \tag{425}$$

and the fields of the mth mode are given by substituting these expressions into equations (340) to (344) of the preceding section.

From equation (388) the propagation constant of the mth dielectric

[22] Reference 18, pp. 204–206. What we call $m\pi F_m(\rho_1/\rho_2)$ is tabulated by Jahnke and Emde, pp. 205–206, as $(k - 1)x_0^{(m)}$, where $k = \rho_2/\rho_1$.

mode is defined by

$$\gamma^2 = -\omega^2\mu_0\epsilon_0 + h_m^2 = -4\pi^2/\lambda_0^2 + h_m^2 \tag{426}$$

to the present approximation, and the cutoff wavelength is

$$\lambda_c = \frac{2\pi}{h_m} = \frac{2(\rho_2 - \rho_1)}{mF_m(\rho_1/\rho_2)}, \tag{427}$$

which tends to zero with the thickness $\rho_2 - \rho_1$ of the main dielectric.

As in the parallel-plane case, when the mth dielectric mode is just able to propagate the effective skin depth in the stacks is of the order of δ_1, and the stack impedances are approximately

$$Z_1 = Z_2 = K = \Gamma_\ell/\bar{g}, \tag{428}$$

under the present assumption of infinitesimally thin laminae. The power dissipated in the stacks and the corresponding attenuation constant may be calculated by a straightforward procedure if desired.

Before leaving the subject of higher dielectric modes in a Clogston cable, we should point out that although we have mentioned only the transverse magnetic modes with circular symmetry, in reality there exist a double infinity of both transverse magnetic and transverse electric higher modes. These modes are discussed in textbooks[23] for coaxial lines bounded by perfect conductors, and they will propagate, with minor changes due to wall losses, in either ordinary or Clogston-type coaxial cables if the frequency is high enough. At ordinary engineering frequencies, however, the higher modes contribute only to the local fields excited at discontinuities, and are therefore not of any great practical importance.

To find the stack modes in a Clogston cable we assume, subject to a posteriori verification, that in the main dielectric we shall have $|\kappa_0\rho| \ll 1$ for all the modes of interest. Then if we set $\Gamma_\ell = i\chi$, equation (417) reduces, as in Section IX, to

$$\begin{aligned}\frac{1}{\chi\rho_1}\,&\frac{J_1(\chi a)N_0(\chi\rho_1) - N_1(\chi a)J_0(\chi\rho_1)}{J_1(\chi a)N_1(\chi\rho_1) - N_1(\chi a)J_1(\chi\rho_1)}\\ &+ \frac{1}{\chi\rho_2}\,\frac{J_1(\chi b)N_0(\chi\rho_2) - N_1(\chi b)J_0(\chi\rho_2)}{J_1(\chi\rho_2)N_1(\chi b) - N_1(\chi\rho_2)J_1(\chi b)} = \frac{\mu_0}{\bar{\mu}}\log\frac{\rho_2}{\rho_1},\end{aligned} \tag{429}$$

which is the same as equation (364). Equation (429) has an infinite

[23] A good account is given by N. Marcuvitz, *Waveguide Handbook*, M. I. T. Rad. Lab. Series, **10**, McGraw-Hill, New York, 1951, pp. 72–80.

number of real roots,

$$\chi_1, \chi_2, \chi_3, \cdots, \chi_p, \cdots, \tag{430}$$

of which χ_1 corresponds to the principal mode and $\chi_2, \chi_3, \cdots$, to the higher stack modes. The χ's are the eigenvalues of the system of equations (369), and as such may be located approximately with a differential analyzer, or as accurately as desired by numerical solution of equation (429). The attenuation and phase constants of the pth mode are

$$\alpha = \frac{\chi_p^2}{2\sqrt{\bar{\mu}/\bar{\epsilon}}\,\bar{g}}, \tag{431}$$

$$\beta = \omega\sqrt{\bar{\mu}\bar{\epsilon}}, \tag{432}$$

provided that the attenuation per radian is small, i.e., that p is not too large. The fields are given by writing χ_p for χ_1 and γ_p for γ in equations (371) to (373) of Section IX.

For a Clogston 2 with no main dielectric we can set $\rho_1 = \rho_2$ in equation (429) and obtain the much simpler form

$$J_1(\chi a)N_1(\chi b) - J_1(\chi b)N_1(\chi a) = 0. \tag{433}$$

The pth root of (433) may be written[24]

$$\chi_p = \frac{p\pi f_p(a/b)}{b - a}, \tag{434}$$

where the functions $f_p(a/b)$ have values slightly greater than unity when $a/b = 0$, and decrease monotonically toward 1 as a/b approaches unity. The attenuation and phase constants of the pth mode in a Clogston 2 are given by

$$\alpha = \frac{p^2\pi^2 f_p^2(a/b)}{2\sqrt{\bar{\mu}/\bar{\epsilon}}\,\bar{g}(b - a)^2}, \tag{435}$$

$$\beta = \omega\sqrt{\bar{\mu}\bar{\epsilon}}, \tag{436}$$

provided that p is not too large. The attenuation constant of the pth mode is thus approximately p^2 times the attenuation constant of the principal mode, the approximation being better the closer the ratio a/b is to unity. The fields of the pth mode may be obtained by writing χ_p for χ_1 and γ_p for γ in equations (302) of Section VIII, or equations (311) if $a = 0$. Qualitatively these fields are very similar to the fields of

[24] Reference 18, pp. 204–206. What we call $p\pi f_p(a/b)$ is tabulated by Jahnke and Emde as $(k - 1)x_1^{(p)}$, where $k = b/a$.

the pth mode in a parallel-plane Clogston 2, with the same number of field maxima and field reversals for a given value of p, though of course the spacings and amplitudes of the field maxima are not all equal in the coaxial cable.

As numerical examples we have plotted in Figs. 18 and 19 the fields of the second and third stack modes (i.e., the first and second higher modes) in the same two Clogston cables which were used to show the principal mode in Fig. 14. The horizontal scales on these figures are arbitrary and have no relation to one another. Figs. 18(a) and 19(a) represent a partially filled cable with the same dimensions, namely $a = 0.084b$, $\rho_1 = 0.415b$, and $\rho_2 = 0.831b$, as in Fig. 14(a), while Figs. 18(b) and 19(b) represent a completely filled cable, as in Fig. 14(b). The following table shows, as a function of the filling ratio $(s_1 + s_2)/b$, the quantity $(\chi_p b/3.83)^2$ for $p = 1, 2, 3$; this quantity is just the ratio of the attenuation constant of the given mode to the attenuation constant of the principal mode in a completely filled Clogston 2.

$(s_1 + s_2)/b$	$(\chi_1 b/3.83)^2$	$(\chi_2 b/3.83)^2$	$(\chi_3 b/3.83)^2$
0.5	1.234	8.369	24.273
1.0	1.000	3.352	7.050

We note that although the proportions of the partially filled cable were found in Section IX to be optimum, in the sense of minimizing the attenuation constant, for the principal mode in a cable with filling ratio 0.5, there is no reason to believe that the same proportions will be optimum for the second and third modes with the same filling ratio.

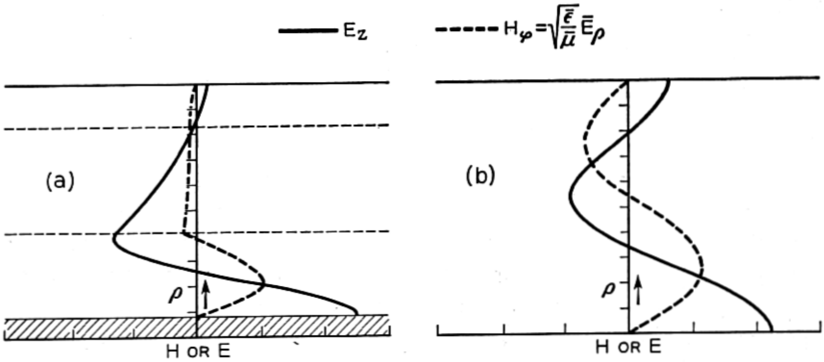

Fig. 18—Fields of second stack mode in partially and completely filled coaxial Clogston lines with $\mu_0 = \bar{\mu}$, $\epsilon_0 = \bar{\epsilon}$.

XI. EFFECT OF FINITE LAMINA THICKNESS. FREQUENCY DEPENDENCE OF ATTENUATION IN CLOGSTON 2 LINES

We shall now study Clogston 2 lines with laminae of finite thickness, and shall investigate the important practical question of how the propagation constant varies with frequency in such lines. Much of the analysis of the present section will deal with parallel-plane structures, but we may be confident that the results will also give at least a good qualitative estimate of the behavior of coaxial cables.

The notation for the plane Clogston 2, shown in Fig. 10, is the same as before, except that we now assume the thicknesses of the individual conducting and insulating layers to be t_1 and t_2 respectively. For definiteness we shall suppose that there are $2n$ conducting layers and $2n$ insulating layers in the whole stack, with a conducting layer next to the lower sheath and an insulating layer next to the upper sheath, though the precise arrangement is of no real importance if the number of layers is large. The total thickness a of the stack is $2n(t_1 + t_2)$, and the fraction of conducting material will as usual be called θ.

The boundary conditions for any mode (having H_x, E_y, and E_z field components only) require that the sum of the impedances looking in opposite directions normal to any plane y = constant be zero. If we match impedances at the lower sheath $y = -\frac{1}{2}a$ and use equation (65) of Section III for the impedance looking into the stack, we have

$$\frac{\frac{1}{2}Z_n(\gamma)(K_1e^{2n\Gamma} + K_2e^{-2n\Gamma}) + K_1K_2 \operatorname{sh} 2n\Gamma}{Z_n(\gamma) \operatorname{sh} 2n\Gamma + \frac{1}{2}(K_1e^{-2n\Gamma} + K_2e^{2n\Gamma})} + Z_n(\gamma) = 0, \quad (437)$$

where Γ, K_1, and K_2 are given by equations (61) and (63). If equation

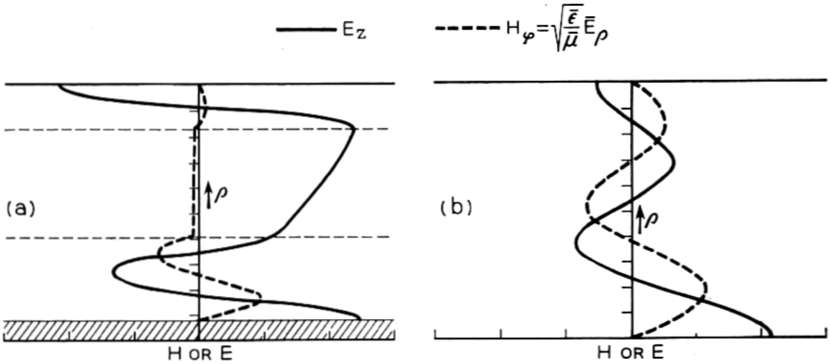

Fig. 19—Fields of third stack mode in partially and completely filled coaxial Clogston lines with $\mu_0 = \bar{\mu}$, $\epsilon_0 = \bar{\epsilon}$.

(437) is solved for $e^{4n\Gamma}$, it takes the form

$$e^{4n\Gamma} = \frac{[Z_n(\gamma) - K_1][Z_n(\gamma) - K_2]}{[Z_n(\gamma) + K_1][Z_n(\gamma) + K_2]}. \tag{438}$$

In order to simplify the general expressions for Γ, K_1, and K_2, we make the following approximations:

(i) We neglect $\omega\epsilon/g_1$ compared to unity, where ϵ represents the dielectric constant of either the conducting or the insulating layers. As we have said before, this is an exceedingly good approximation at all engineering frequencies.

(ii) We neglect γ^2/σ_1^2 $(= \gamma^2/i\omega\mu_1 g_1)$ compared to unity. It turns out that not only is this approximation valid in the frequency range of greatest interest, where γ is approximately equal to $i\omega\sqrt{\bar{\mu}\bar{\epsilon}}$, but also it is valid all the way down to zero frequency, so that in the present section we can easily derive results for the complete frequency range down to dc. So long as $\gamma^2/\sigma_1^2 \ll 1$, we have from equations (56) of Section III,

$$\kappa_1 \approx \sigma_1, \qquad \eta_{1y} \approx \eta_1. \tag{439}$$

(iii) We suppose that the thickness t_2 of the layers of insulation is so small that we may replace sh $\kappa_2 t_2$ by $\kappa_2 t_2$ and ch $\kappa_2 t_2$ by unity. These approximations will be amply justified if t_2 is not greater than a few times the skin depth in the conducting layers at the highest operating frequency.

The foregoing approximations lead to results identical with equations (86) and (87) of Section III, namely

$$\text{ch}\,\Gamma = \frac{\eta_{2y}\kappa_2 t_2}{2\eta_{1y}}\,\text{sh}\,\kappa_1 t_1 + \text{ch}\,\kappa_1 t_1, \tag{440}$$

and

$$\begin{aligned} K_1 &= -\tfrac{1}{2}\eta_{2y}\kappa_2 t_2 + \sqrt{(\tfrac{1}{2}\eta_{2y}\kappa_2 t_2)^2 + \eta_{1y}\eta_{2y}\kappa_2 t_2 \coth \kappa_1 t_1 + \eta_{1y}^2}, \\ K_2 &= +\tfrac{1}{2}\eta_{2y}\kappa_2 t_2 + \sqrt{(\tfrac{1}{2}\eta_{2y}\kappa_2 t_2)^2 + \eta_{1y}\eta_{2y}\kappa_2 t_2 \coth \kappa_1 t_1 + \eta_{1y}^2}. \end{aligned} \tag{441}$$

To simplify the notation, we introduce the symbol q defined by

$$\begin{aligned} q &= -\frac{\eta_{2y}\kappa_2 t_2}{\eta_1\sigma_1 t_1} \\ &= -\frac{(1-\theta)\mu_2}{\theta\mu_1}\left[1 + \frac{\gamma^2}{\omega^2\mu_2\epsilon_2}\right] \\ &= 1 - \frac{\bar{\mu}}{\theta\mu_1}\left[1 + \frac{\gamma^2}{\omega^2\bar{\mu}\bar{\epsilon}}\right], \end{aligned} \tag{442}$$

where $\bar{\epsilon}$ and $\bar{\mu}$ are given by equations (268) of Section VIII. The propagation constant γ is thus related to q by

$$\begin{aligned} \gamma &= i\omega\sqrt{\mu_2\epsilon_2}\left[1 + \frac{\theta\mu_1 q}{(1-\theta)\mu_2}\right]^{\frac{1}{2}} \\ &= i\omega\sqrt{\bar{\mu}\bar{\epsilon}}\left[1 + \frac{\theta\mu_1(q-1)}{\bar{\mu}}\right]^{\frac{1}{2}}. \end{aligned} \tag{443}$$

In terms of q and the electrical thickness parameter Θ used in Part I, namely

$$\Theta = \sigma_1 t_1 = (1+i)t_1/\delta_1 \approx \kappa_1 t_1 , \tag{444}$$

equations (440) and (441) become, approximately,

$$\text{ch } \Gamma = \text{ch } \Theta - \tfrac{1}{2}q\Theta \text{ sh } \Theta, \tag{445}$$

and

$$\begin{aligned} K_1 &= \frac{\Theta}{g_1 t_1}\left[\tfrac{1}{2}q\Theta + \sqrt{\tfrac{1}{4}q^2\Theta^2 - q\Theta \coth \Theta + 1}\,\right], \\ K_2 &= \frac{\Theta}{g_1 t_1}\left[-\tfrac{1}{2}q\Theta + \sqrt{\tfrac{1}{4}q^2\Theta^2 - q\Theta \coth \Theta + 1}\,\right]. \end{aligned} \tag{446}$$

In the general case when the sheath impedance $Z_n(\gamma)$ is a given function of γ, we substitute the expressions for K_1 and K_2 into equation (438), namely

$$e^{4n\Gamma} = \frac{Z_n^2(\gamma) - (K_1 + K_2)Z_n(\gamma) + K_1K_2}{Z_n^2(\gamma) + (K_1 + K_2)Z_n(\gamma) + K_1K_2}, \tag{447}$$

and then determine γ for each mode by simultaneous numerical solution of equations (443), (445), and (447). At least as a first approximation we may neglect the total current in either sheath compared to the one-way current in the stack; to this approximation $Z_n(\gamma)$ is effectively infinite and (447) becomes

$$e^{4n\Gamma} = 1. \tag{448}$$

The non-zero roots of this equation are

$$\Gamma = ip\pi/2n, \qquad p = 1, 2, 3, \cdots , \tag{449}$$

where $p = 1$ corresponds to the principal mode and the higher values of p to the higher modes discussed in Section X. (We would get nothing new by including negative values of p.) The quantities q and γ for each mode are then given by equations (445) and (443) respectively. If we wish to take the finite value of $Z_n(\gamma)$ into account, we may calculate K_1 and K_2 from (446) and then obtain a second approximation to Γ from (447); and this process may be repeated as often as desired. From the experience gained in treating a particular example we feel that the method of successive approximations is entirely feasible, but it does involve a considerable amount of numerical work.

In the calculation just described we have to choose the correct sign of the complex square root occurring in the expressions for K_1 and K_2. Without attempting to give a complete discussion of this point here, we observe that it may be shown that

$$\text{sh } \Gamma = \text{sh } \Theta \sqrt{\tfrac{1}{4}q^2\Theta^2 - q\Theta \coth \Theta + 1}. \tag{450}$$

Under ordinary circumstances Γ will be a small complex number with a phase angle of about 90°, and Θ will be a small complex number with a phase angle of 45°. Hence the phase angle of the square root may be expected to be in the neighborhood of 45° rather than 225°.

In the remainder of this section we shall restrict ourselves to the case of high-impedance sheaths, so that the values of Γ are given to a sufficiently good approximation by equation (449). We shall discuss the principal mode and the higher modes concurrently, but shall assume throughout that the mode number p is small compared to n. From (445) and (449), the value of q for the pth mode is

$$q = \frac{2\left(\text{ch } \Theta - \cos \dfrac{p\pi}{2n}\right)}{\Theta \text{ sh } \Theta}, \tag{451}$$

and the propagation constant γ is obtained by substituting this value of q into equation (443).

We shall now discuss the variation of the propagation constant of a plane Clogston 2 line with frequency over the full frequency range from zero to very high frequencies.[25] To do this we shall derive approximate expressions for the propagation constant at what may be called, roughly, very low frequencies, low frequencies, high frequencies, and very high frequencies. It will appear presently that the limits of these various frequency ranges depend among other things on the dimensions of the laminated transmission line and the thicknesses of the individual layers, and that the frequency range of greatest engineering importance is what we have called simply "low frequencies".

From equation (444) we have

[25] In this connection see also Reference 1, Appendices A and B, pp. 525–529.

$$\Theta = (1 + i)t_1\sqrt{\omega\mu_1 g_1/2} = (1 + i)t_1\sqrt{\pi\mu_1 g_1 f}, \tag{452}$$

which is proportional to the square root of frequency. For small Θ equation (451) may be written

$$\begin{aligned} q &= \left[2(\text{ch }\Theta - 1) + 4\sin^2\frac{p\pi}{4n}\right]\frac{\text{csch }\Theta}{\Theta} \\ &= \left[4\sin^2\frac{p\pi}{4n}\right]\frac{1}{\Theta^2} + \left[1 - \frac{2}{3}\sin^2\frac{p\pi}{4n}\right] \\ &\qquad - \frac{1}{12}\left[1 - \frac{14}{15}\sin^2\frac{p\pi}{4n}\right]\Theta^2 + \cdots, \end{aligned} \tag{453}$$

on expanding the right side in powers of Θ by Dwight 657.2 and 657.8. If we replace $\sin p\pi/4n$ by $p\pi/4n$ and neglect the square of this quantity in comparison with unity, (453) becomes

$$q \approx \frac{p^2\pi^2}{4n^2}\frac{1}{\Theta^2} + 1 - \frac{\Theta^2}{12} + \cdots. \tag{454}$$

Introducing this expression for q into equation (443) and substituting for Θ from (452), we get for the propagation constant,

$$\gamma = i\omega\sqrt{\bar{\mu}\bar{\epsilon}}\left[1 - \frac{i\theta\mu_1}{\bar{\mu}}\left(\frac{p^2\pi^2}{4n^2\omega\mu_1 g_1 t_1^2} + \frac{\omega\mu_1 g_1 t_1^2}{12}\right)\right]^{\frac{1}{2}}. \tag{455}$$

As the frequency approaches zero in a Clogston 2 line of finite thickness, the term in $1/\omega$ dominates the other terms in square brackets in equation (455). Thus at very low frequencies the attenuation and phase constants of the pth mode are given approximately by

$$\alpha = \frac{p\pi\theta}{2T_1}\sqrt{\frac{\omega\bar{\epsilon}}{2\bar{g}}} = \frac{p\pi}{a}\sqrt{\frac{\pi\bar{\epsilon}f}{\bar{g}}}, \tag{456}$$

$$\beta = \frac{p\pi\theta}{2T_1}\sqrt{\frac{\omega\bar{\epsilon}}{2\bar{g}}} = \frac{p\pi}{a}\sqrt{\frac{\pi\bar{\epsilon}f}{\bar{g}}}, \tag{457}$$

where $2T_1$ ($= 2nt_1$) is the total thickness of conducting material in the stack of thickness a. To this approximation the attenuation and phase constants are equal, and are proportional to the square root of frequency. We note that at very low frequencies,

$$\frac{\gamma^2}{\sigma_1^2} = \frac{2ip^2\pi^2\theta^2\omega\bar{\epsilon}}{8T_1^2\bar{g}}\cdot\frac{1}{i\omega\mu_1 g_1} = \frac{\theta p^2\pi^2\bar{\epsilon}/\mu_1}{a^2\bar{g}^2}, \tag{458}$$

which will be very small compared to unity for lines of all reasonable dimensions, in agreement with our assumption (ii) above.

As the frequency is increased there will be a range in which the terms in parentheses in equation (455) are small compared to unity, so that the square root may be expanded by the binomial theorem. This gives

$$\alpha = \frac{p^2\pi^2}{2\sqrt{\bar{\mu}/\bar{\epsilon}}\,\bar{g}a^2} + \frac{\omega^2\mu_1^2\bar{g}t_1^2}{24\sqrt{\bar{\mu}/\bar{\epsilon}}}, \tag{459}$$

$$\beta = i\omega\sqrt{\bar{\mu}\bar{\epsilon}}. \tag{460}$$

If the line is of finite total thickness a and the frequency is so low or the laminae are so thin that the first term on the right side of (459) is large compared to the second, we have approximately

$$\alpha = \frac{p^2\pi^2}{2\sqrt{\bar{\mu}/\bar{\epsilon}}\,\bar{g}a^2}. \tag{461}$$

This is the frequency-independent attenuation constant that we found in Section X, equation (407), for the pth mode in a plane Clogston 2 with infinitesimally thin laminae. We shall call the range over which the attenuation is essentially flat the "low-frequency" range. On the other hand, if the laminae are of finite thickness the second term on the right side of (459) ultimately becomes dominant, and the attenuation constant is then given approximately by

$$\alpha = \frac{\omega^2\mu_1^2\bar{g}t_1^2}{24\sqrt{\bar{\mu}/\bar{\epsilon}}} = \frac{\pi^2\mu_1^2\bar{g}t_1^2f^2}{6\sqrt{\bar{\mu}/\bar{\epsilon}}}. \tag{462}$$

This is also the attenuation constant of a plane wave in an unbounded laminated medium (except at very high frequencies), as may be seen by letting the stack thickness a tend to infinity in equation (459). By "high frequencies" we shall mean the frequency range in which the attenuation constant is approximately proportional to f^2.

Finally at very high frequencies when $|\Theta| \gg 1$, we have from (451),

$$q \approx 2/\Theta, \tag{463}$$

and so from (443),

$$\gamma = i\omega\sqrt{\mu_2\epsilon_2}\left[1 + \frac{2\theta\mu_1}{(1-\theta)\mu_2\Theta}\right]^{\frac{1}{2}}. \tag{464}$$

Expanding by the binomial theorem and substituting for Θ from (452), we get after a little rearrangement,

$$\alpha = \frac{1}{\sqrt{\mu_2/\epsilon_2}\, t_2 g_1 \delta_1} = \frac{1}{\sqrt{\mu_2/\epsilon_2}\, t_2} \sqrt{\frac{\pi\mu_1 f}{g_1}}, \tag{465}$$

$$\beta = \omega\sqrt{\mu_2\epsilon_2} + \frac{1}{\sqrt{\mu_2/\epsilon_2}\, t_2 g_1 \delta_1}. \tag{466}$$

Comparing these expressions with equations (25) and (26) of Section II, we see that they correspond to waves in parallel-plane transmission lines of width t_2, bounded by electrically thick solid conductors. We shall call this range, in which α is proportional to the square root of frequency, the "very high frequency" range. At these frequencies the propagation constant is the same in a Clogston 2 line of finite thickness as in an infinite laminated medium.

In order to describe the various frequency ranges more precisely, we shall define the three critical frequencies f_1', f_2', and f_3' to be the frequencies at which the approximate expressions for the attenuation constants in two adjacent frequency ranges are equal. These frequencies are closely related to the critical frequencies which we defined in equations (178) of Section V, when we were discussing the surface impedance of a plane stack of finite layers. For a stack containing a total thickness T_1 of conducting material, we recall that the critical frequencies were f_1, where $T_1 = \delta_1$; f_2, where $T_1 = T_\Delta$; and f_3, where $t_1 = \sqrt{3}\,\delta_1$. For the pth mode in a Clogston 2 containing a total thickness $2T_1$ of conducting material, the frequencies turn out to be

$$\begin{aligned} f_1' &= \frac{p^2\pi\theta}{16\bar{\mu} g_1 T_1^2} = \frac{p^2\pi^2\theta\mu_1}{16\bar{\mu}} f_1, \\ f_2' &= \frac{\sqrt{3}\,p}{2\mu_1 g_1 t_1 T_1} = \frac{p\pi}{2} f_2, \\ f_3' &= \left[\frac{36\bar{\mu}}{(1-\theta)\mu_2}\right]^{\frac{1}{3}} \frac{1}{\pi\mu_1 g_1 t_1^2} = \left[\frac{4\bar{\mu}\bar{\epsilon}}{3\mu_2\epsilon_2}\right]^{\frac{1}{3}} f_3, \end{aligned} \tag{467}$$

where of course $p = 1$ for the principal mode. Thus the attenuation constant is given approximately by (456) for $0 \leqq f \leqq f_1'$, by (461) for $f_1' \leqq f \leqq f_2'$, by (462) for $f_2' \leqq f \leqq f_3'$, and by (465) for $f \geqq f_3'$.

If we plot the foregoing approximate expressions for the attenuation constant against frequency on log-log paper, we can get a good idea of the variation of the attenuation of a Clogston 2 over the entire frequency range. Both the approximate expressions and the exact results for a particular numerical case are plotted in Fig. 20, for a Clogston 2 of finite thickness and also for an infinite laminated medium. The actual

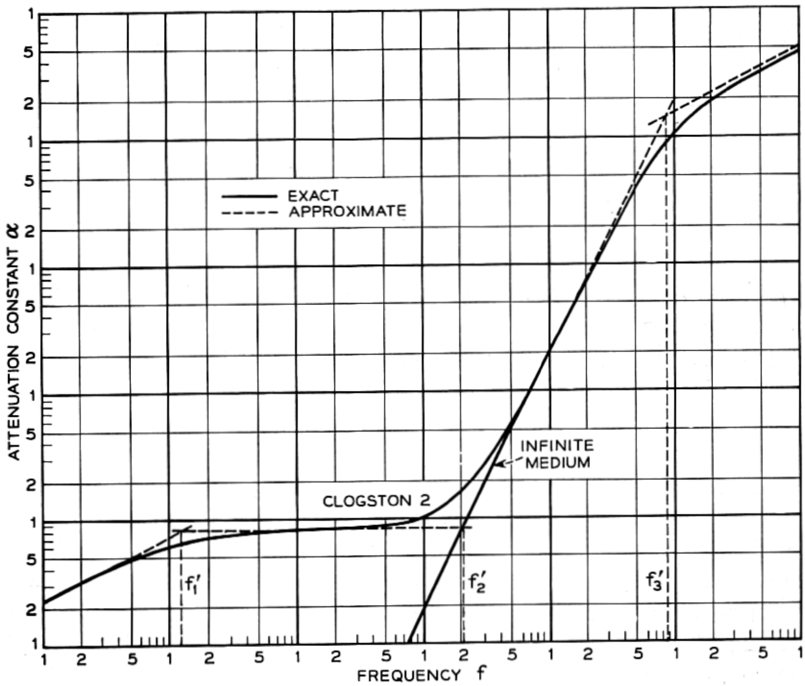

Fig. 20—Attenuation constants of a plane Clogston 2 line and an infinite laminated medium versus frequency on log-log scale.

numerical values are of no special significance, having been chosen solely for convenience in plotting.

So far as the practical applications of Clogston lines are concerned, we are primarily interested in the frequency range $f_1' \leqq f \leqq f_2'$, where the attenuation constant is essentially independent of frequency. To determine the rate at which the attenuation constant of the pth mode begins to deviate from its "flat" value as the frequency is increased, we write equation (459) in the form

$$\begin{aligned} \alpha &= \frac{p^2\pi^2}{2\sqrt{\bar{\mu}/\bar{\epsilon}}\,\bar{g}a^2}\left[1 + \frac{4t_1^2T_1^2}{3p^2\pi^2\delta_1^4}\right] \\ &= \frac{p^2\pi^2}{2\sqrt{\bar{\mu}/\bar{\epsilon}}\,\bar{g}a^2}\left[1 + \frac{4t_1^2T_1^2\mu_1^2g_1^2f^2}{3p^2}\right]. \end{aligned} \tag{468}$$

The two terms in the square brackets are equal, and the attenuation constant is double its "flat" value, when $f = f_2'$, a result which is in very good agreement with the calculated values shown in Fig. 20.

The maximum permissible thickness of the conducting layers in a plane Clogston 2 with high-impedance walls, if the attenuation constant of the pth mode is not to exceed its "flat" value α_0 by more than a specified small fraction $\Delta\alpha/\alpha_0$ at a top frequency f_m, is easily shown from (468) to be

$$t_1 = \frac{\sqrt{3}\,p}{2T_1\mu_1 g_1 f_m}\sqrt{\frac{\Delta\alpha}{\alpha_0}}. \tag{469}$$

Measuring f_m in $\text{Mc}\cdot\text{sec}^{-1}$ and thicknesses in mils, and putting in numerical values for copper, we obtain

$$(t_1)_{\text{mils}} = \frac{36.84p}{(2T_1)_{\text{mils}}(f_m)_{\text{Mc}}}\sqrt{\frac{\Delta\alpha}{\alpha_0}}. \tag{470}$$

We see from (461) that for fixed θ, α_0 is inversely proportional to $(a/p)^2$, where a is the total thickness of the stack and p is the mode number, while from (469) the permissible value of t_1 for a certain fractional change in attenuation is inversely proportional to (a/p), and also inversely proportional to the top frequency f_m.

It is interesting to compare equation (470) for the principal mode ($p = 1$) with equation (199) of Section V for the principal mode in an extreme Clogston 1 line with copper conducting layers. Since in a plane line $\Delta R/R_0 = \Delta\alpha/\alpha_0$, equation (199) may be written

$$(t_1)_{\text{mils}} = \frac{40.62}{(2T_1)_{\text{mils}}(f_m)_{\text{Mc}}}\sqrt{\frac{\Delta\alpha}{\alpha_0}}, \tag{471}$$

where $2T_1$ represents the total thickness of copper in both stacks. We expect that for partially filled plane Clogston lines with different proportions of the available space occupied by stacks, the maximum permissible layer thickness will be given by equations similar to (470) and (471), with values of the numerical coefficient intermediate between 36.84 and 40.62.

We turn next to a discussion of coaxial Clogston cables with finite laminae. A coaxial Clogston 2 is shown schematically in Fig. 11, and an enlarged view of part of the laminated stack in Fig. 4. The boundary conditions which apply to circular transverse magnetic waves on this structure are satisfied if at every point the sum of the radial impedances looking in opposite directions is zero. If we knew the explicit relation between the impedances at the two surfaces of the stack in terms of the stack parameters and the propagation constant γ, the impedance-matching conditions at the inner core and the outer sheath would yield a transcendental equation for the propagation constants of the various possible modes. If the coaxial layers are of finite thickness, however, the relation between the surface impedances of the stack involves the product of as many different matrices as there are layers in the whole stack, and this matrix product is not suited to analytic treatment. We shall therefore approach the problem from another point of view.

We have seen that if the conducting layers in a laminated transmission line are sufficiently thin compared to the skin depth, the attenuation constant is essentially independent of frequency. In practice it is important to know how rapidly the attenuation constant of a Clogston cable with finite laminae begins to deviate from its low-frequency value as the frequency is increased. In accordance with the results for the parallel-plane line, we expect the initial increase to be proportional to the square of the frequency. We shall derive the term proportional to f^2 in the attenuation constant of the coaxial line on the basis of the following assumptions:

We assume that the macroscopic current distribution in a coaxial Clogston 2 is independent of frequency, and hence is given by the expressions which have already been derived for the case of infinitesimally thin laminae. (It is easy to show that this assumption is valid for a *plane* Clogston 2.) If the conducting layers are of finite thickness, then each carries a definite finite fraction of the total current in the line. At low frequencies the current density in any given layer is approximately uniform, but as the frequency is increased it becomes nonuniform because of the development of skin effect, and the power dissipated in the layer is increased. We shall calculate the total power dissipated in the stack, and the corresponding attenuation constant, up to terms in f^2.

Let the jth conducting layer in the stack be a hollow cylinder of conductivity g_1, inner radius ρ_{j-1}, and thickness t_1. Thus if there are $2n$ double layers we have $\rho_0 = a$ and $\rho_{2n} = b$, where as usual a and b denote the inner and outer radii of the whole stack. Let the total current flowing in the positive z-direction inside $\rho = \rho_{j-1}$ be I_{j-1}, and let the current flowing in the jth conducting layer be ΔI_j. It is shown in Appendix III that the average power dissipated per unit length in the jth conductor is approximately

$$\Delta P_j = \frac{1}{4\pi g_1 t_1 \rho_{j-1}} \left[|\Delta I_j|^2 + \frac{t_1^4}{3\delta_1^4} |I_{j-1}|^2 \right], \tag{472}$$

up to terms in $(t_1/\delta_1)^4$, where curvature corrections of the order of t_1/ρ_{j-1} have been neglected in comparison with unity. Presumably the only layers for which it may not be justifiable to neglect curvature corrections will be the extreme inner layers, which occupy at most a small fraction of the total volume of the stack.

The average current density $\bar{J}_z$ in a Clogston 2 with infinitesimally thin laminae is given by equation (305) of Section VIII; namely, writing χ_p for the pth mode and dropping $e^{-\gamma z}$,

$$\bar{J}_z = H_0 \chi_p C_0(\chi_p \rho), \tag{473}$$

where H_0 is an arbitrary amplitude constant. For $n = 0$ and 1, $C_n(\chi_p \rho)$ denotes the combination of Bessel functions

$$C_n(\chi_p \rho) = N_1(\chi_p b) J_n(\chi_p \rho) - J_1(\chi_p b) N_n(\chi_p p); \tag{474}$$

and χ_p is the pth positive root of

$$C_1(\chi a) = N_1(\chi b) J_1(\chi a) - J_1(\chi b) N_1(\chi a) = 0. \tag{475}$$

According to equation (434) of Section X, we may write

$$\chi_p = \frac{p\pi f_p(a/b)}{b - a}, \tag{476}$$

where the functions $f_p(a/b)$ are of the order of unity. The total current $I(\rho)$ flowing in the positive z-direction between the inner core and a cylinder of arbitrary radius ρ is just

$$I(\rho) = 2\pi \int_a^\rho \rho \bar{J}_z \, d\rho = 2\pi H_0 \rho C_1(\chi_p \rho). \tag{477}$$

The thickness of the jth conducting layer in a stack of finite layers may be written

$$t_1 = \theta(t_1 + t_2) = \theta(\rho_j - \rho_{j-1}) = \theta \Delta\rho_j, \tag{478}$$

where $\Delta\rho_j$ represents the thickness $t_1 + t_2$ of the jth double layer. Hence approximately

$$\Delta I_j = 2\pi \rho_{j-1} \bar{J}_z \Delta\rho_j = 2\pi H_0 \chi_p \rho_{j-1} C_0(\chi_p \rho_{j-1}) \Delta\rho_j, \tag{479}$$

it being remembered that the conduction current in the conducting layer is essentially equal to the total current in the double layer, since the displacement currents are negligible. The current flowing inside the radius ρ_{j-1} is, from (477),

$$I_{j-1} = 2\pi H_0 \rho_{j-1} C_1(\chi_p \rho_{j-1}), \tag{480}$$

and so the power dissipated per unit length in the jth conductor is given by (472) as

$$\Delta P_j = \frac{\pi H_0 H_0^* \rho_{j-1}}{\theta g_1}\left[\chi_p^2 C_0^2(\chi_p \rho_{j-1}) + \frac{\theta^2 t_1^2}{3\delta_1^4} C_1^2(\chi_p \rho_{j-1})\right]\Delta \rho_j . \quad (481)$$

The total power ΔP dissipated per unit length in the whole stack is obtained by summing ΔP_j over j. Approximately the sum by an integral, we have

$$\begin{aligned}\Delta P &= \frac{\pi H_0 H_0^*}{\bar{g}}\int_a^b \rho[\chi_p^2 C_0^2(\chi_p\rho) + \frac{\theta^2 t_1^2}{3\delta_1^4} C_1^2(\chi_p\rho)]\, d\rho \\ &= \frac{\pi H_0 H_0^* \chi_p^2}{2\bar{g}}\left[1 + \frac{\theta^2 t_1^2}{3\chi_p^2\delta_1^4}\right][b^2 C_0^2(\chi_p b) - a^2 C_0^2(\chi_p a)].\end{aligned} \quad (482)$$

The average transmitted power P when the laminae are infinitesimally thin is

$$\begin{aligned}P &= \text{Re}\ \tfrac{1}{2}\int_0^{2\pi}\int_a^b \bar{E}_\rho H_\phi^* \rho\, d\rho\, d\phi \\ &= \pi\sqrt{\frac{\bar{\mu}}{\bar{\epsilon}}}\, H_0 H_0^* \int_a^b \rho C_1^2(\chi_p\rho)\, d\rho \\ &= \tfrac{1}{2}\pi\sqrt{\frac{\bar{\mu}}{\bar{\epsilon}}}\, H_0 H_0^*[b^2 C_0^2(\chi_p b) - a^2 C_0^2(\chi_p a)].\end{aligned} \quad (483)$$

If we assume the same value for P when the laminae are of finite thickness, then from (482) and (483) the attenuation constant of the line is

$$\alpha = \frac{\Delta P}{2P} = \frac{\chi_p^2}{2\sqrt{\bar{\mu}/\bar{\epsilon}}\ \bar{g}}\left[1 + \frac{\theta^2 t_1^2}{3\chi_p^2 \delta_1^4}\right]. \quad (484)$$

The similarity of equation (484) to equation (468) for the parallel-plane line becomes obvious if we write χ_p in the form (476) and denote the total thickness $\theta(b - a)$ of conducting material in the coaxial stack by $2T_1$. We then have

$$\begin{aligned}\alpha &= \frac{p^2\pi^2 f_p^2(a/b)}{2\sqrt{\bar{\mu}/\bar{\epsilon}}\ \bar{g}(b-a)^2}\left[1 + \frac{4t_1^2 T_1^2}{3p^2\pi^2 f_p^2(a/b)\delta_1^4}\right] \\ &= \frac{p^2\pi^2 f_p^2(a/b)}{2\sqrt{\bar{\mu}/\bar{\epsilon}}\ \bar{g}(b-a)^2}\left[1 + \frac{4t_1^2 T_1^2 \mu_1^2 g_1^2 f^2}{3p^2 f_p^2(a/b)}\right],\end{aligned} \quad (485)$$

and as the ratio a/b approaches unity the function $f_p^2(a/b)$ approaches unity and (485) becomes identical with (468). We recall that $f_1^2(a/b)$ was plotted against a/b in Fig. 12. For the principal mode in a cable with no inner core ($a = 0$), equation (485) takes the form

$$\alpha = \frac{7.341}{\sqrt{\bar{\mu}/\bar{\epsilon}}\,\bar{g}b^2}[1 + 0.8963t_1^2T_1^2\mu_1^2g_1^2f^2]. \tag{486}$$

It should be emphasized that whereas equation (468) was obtained from a rigorous solution of the boundary-value problem for the plane line, equation (485) for the coaxial cable has been derived on the basis of certain physical assumptions and approximations whose effect on the accuracy of the final result is not very easy to estimate. Presumably one might check the accuracy of (485) for a particular Clogston cable by setting up the matrix relation between the known surface impedances of the core and the outer sheath and solving numerically for the propagation constant. It should not be too difficult to solve the matrix equation by cut-and-try methods for a cable having, say, two hundred double layers, if the matrix of each double layer were assumed to be given by equations (88) of Section III, and high-speed computing machinery were used to perform the matrix multiplications. In the absence of any such numerical results, however, we shall merely assume that equation (485) furnishes a reasonable approximation to the attenuation constant of a coaxial Clogston 2 in the frequency range $f_1' \leqq f \leqq f_3'$, where f_1' and f_3' are the critical frequencies defined by (467).

The first conclusion which we can draw from (485) is that the maximum permissible thickness of the conducting layers in a coaxial Clogston 2 with high-impedance boundaries, if the attenuation constant of the pth mode is not to exceed its "flat" value α_0 by more than a specified small fraction $\Delta\alpha/\alpha_0$ at a top frequency f_m, is

$$t_1 = \frac{\sqrt{3}\,pf_p(a/b)}{2T_1\mu_1g_1f_m}\sqrt{\frac{\Delta\alpha}{\alpha_0}}; \tag{487}$$

or, putting in numerical values for copper,

$$(t_1)_{\text{mils}} = \frac{36.84pf_p(a/b)}{(2T_1)_{\text{mils}}(f_m)_{\text{Mc}}}\sqrt{\frac{\Delta\alpha}{\alpha_0}}. \tag{488}$$

For the principal mode in a Clogston cable with no inner core, this becomes

$$(t_1)_{\text{mils}} = \frac{44.93}{(2T_1)_{\text{mils}}(f_m)_{\text{Mc}}}\sqrt{\frac{\Delta\alpha}{\alpha_0}}. \tag{489}$$

As a second application of equation (485), we shall determine the upper crossover frequency at which the attenuation constant of a Clogston 2 is equal to the attenuation constant of a conventional coaxial cable of the same size. Since the lower crossover frequency was found at the end of Section VIII, we shall then know the theoretical limits of the frequency range over which a given Clogston cable can have lower loss than the corresponding standard coaxial.

According to equation (317) of Section VIII, a conventional coaxial cable of radius b and optimum proportions has an attenuation constant

$$\alpha = \frac{1.796}{\sqrt{\mu_0/\epsilon_0}\, g_1 \delta_1 b} = \frac{1.796\sqrt{\pi \mu_1 g_1 f}}{\sqrt{\mu_0/\epsilon_0}\, g_1 b}. \tag{490}$$

We shall assume that the upper crossover occurs in the high-frequency range where the attenuation constant of a Clogston 2 is approximately proportional to f^2. Then for the pth mode in a cable with no inner core ($a = 0$), equation (485) gives

$$\alpha = \frac{2\pi^2 t_1^2 T_1^2 \mu_1^2 g_1^2 f^2}{3\sqrt{\bar{\mu}/\bar{\epsilon}}\, \bar{g} b^2} = \frac{\pi^2 t_1^2 \mu_1^2 \bar{g} f^2}{6\sqrt{\bar{\mu}/\bar{\epsilon}}}. \tag{491}$$

A little algebra shows that the two attenuation constants are equal when

$$f = \frac{1}{\pi \mu_1 g_1}\left[\frac{10.77}{2T_1 t_1^2}\sqrt{\frac{\bar{\mu}\epsilon_0}{\mu_0 \bar{\epsilon}}}\right]^{\frac{2}{3}}. \tag{492}$$

If the conventional cable is air-filled, then assuming copper conductors and no magnetic materials, we find that equation (492) becomes, numerically,

$$f_{\text{Mc}} = 33.02\left[\frac{1}{(2T_1)_{\text{mils}}(t_1^2)_{\text{mils}}}\sqrt{\frac{1-\theta}{\epsilon_{2r}}}\right]^{\frac{2}{3}}. \tag{493}$$

If we consider a 3/8-inch Clogston cable with 0.1-mil copper conductors, 0.05-mil polyethylene insulators, and no inner core, then

$$\begin{aligned} b &= 187.5 \text{ mils} & \theta &= 2/3 \\ 2T_1 &= 125 \quad \text{mils} & \epsilon_{2r} &= 2.26 \\ t_1 &= 0.1 \quad \text{mils} & & \end{aligned} \tag{494}$$

We found in Section VIII that the lower crossover frequency for this cable is about 50 $\text{kc}\cdot\text{sec}^{-1}$, while from equation (493) the upper crossover frequency turns out to be 15 $\text{Mc}\cdot\text{sec}^{-1}$.

We next discuss the problem of maximizing the frequency band over which the attenuation constant of a Clogston cable of given diameter does not exceed a specified value.[26] We suppose that the thickness t_1 of the conductors is fixed, but that the proportion of conducting material in the cable may be adjusted by changing the thickness of the insulators. Let α_m be the value of the attenuation constant which is not to be exceeded in the operating frequency range, and let f_m be the frequency at which this maximum attenuation is reached. What should be the fraction θ of conducting material in the cable in order to maximize f_m? It is tacitly assumed that α_m is at least slightly greater than the minimum "flat" attenuation constant which is possible with a cable of the given diameter, since obviously we do not wish to work entirely in the very-low-frequency range.

In the frequency range of interest the attenuation constant of the pth mode is given by equation (484), which may be written

$$\alpha = \frac{\chi_p^2}{2\sqrt{\bar{\mu}/\bar{\epsilon}}\,\bar{g}} + \frac{\theta^2 t_1^2 \pi^2 \mu_1^2 g_1^2 f^2}{6\sqrt{\bar{\mu}/\bar{\epsilon}}\,\bar{g}}, \tag{495}$$

where χ_p is a root of (475) and independent of θ. Solving (495) for the frequency f_m at which α is equal to α_m, and substituting for $\bar{\epsilon}$, $\bar{\mu}$, and $\bar{g}$ from (268), we obtain

$$f_m = \frac{\sqrt{3}}{\pi \mu_1 g_1 t_1}\left[\frac{2[\theta\mu_1 + (1-\theta)\mu_2]^{\frac{1}{2}}[(1-\theta)/\epsilon_2]^{\frac{1}{2}} g_1 \alpha_m}{\theta} - \frac{\chi_p^2}{\theta^2}\right]^{\frac{1}{2}}. \tag{496}$$

A routine calculation shows that f_m is a maximum, considered as a function of θ, when θ satisfies

$$\frac{\alpha_m g_1 \theta[\theta\mu_1 + 2(1-\theta)\mu_2]}{[\theta\mu_1 + (1-\theta)\mu_2]^{\frac{1}{2}}(1-\theta)^{\frac{1}{2}}\epsilon_2^{\frac{1}{2}}} = 2\chi_p^2 . \tag{497}$$

Equation (497) is easily reduced to a quartic equation in θ, which may be solved without difficulty when the other parameters are given. The maximum value of f_m is then obtained by substituting θ back into (496).

We shall now investigate in more detail the case in which

$$\mu_1 = \mu_2 , \tag{498}$$

that is, the permeabilities of the conducting and insulating layers are equal. In this case the low-frequency attenuation constant α_0, which is just the first term on the right side of equation (495), is given by

$$\alpha_0 = \frac{\chi_p^2}{2\theta\sqrt{1-\theta}\,\sqrt{\mu_2/\epsilon_2}\,g_1}, \tag{499}$$

[26] A similar problem was first investigated in an unpublished memorandum by H. S. Black.

and α_0 has a minimum when

$$\theta = 2/3. \tag{500}$$

The minimum value of the low-frequency attenuation constant, which we may call α_{00}, is just

$$\alpha_{00} = \frac{3\sqrt{3}\,\chi_p^2}{4\sqrt{\mu_2/\epsilon_2}\,g_1}. \tag{501}$$

Writing

$$\chi_p^2 = \frac{4\sqrt{\mu_2/\epsilon_2}\,g_1\alpha_{00}}{3\sqrt{3}}, \tag{502}$$

we find that equation (496) takes the form

$$f_m = \frac{\sqrt{3}\,\chi_p}{\pi\mu_1 g_1 t_1}\left[\frac{3\sqrt{3}\,(1-\theta)^{\frac{1}{2}}}{2\theta}\frac{\alpha_m}{\alpha_{00}} - \frac{1}{\theta^2}\right]^{\frac{1}{2}}, \tag{503}$$

for any value of θ. From equation (497), f_m is a maximum when θ satisfies

$$\frac{\theta(2-\theta)}{(1-\theta)^{\frac{1}{2}}} = \frac{8}{3\sqrt{3}}\frac{\alpha_{00}}{\alpha_m}, \tag{504}$$

which is equivalent to the quartic equation

$$\theta^4 - 4\theta^3 + 4\theta^2 + \frac{64\alpha_{00}^2}{27\alpha_m^2}(\theta - 1) = 0. \tag{505}$$

If θ_m is the root of (505) which lies between zero and one, then the corresponding value of f_m is

$$f_m = \frac{\sqrt{3}\,\chi_p}{\pi\mu_1 g_1 t_1 \theta_m}\left[\frac{2-3\theta_m}{2-\theta_m}\right]^{\frac{1}{2}}. \tag{506}$$

We observe from either (503) or (506) that f_m is inversely proportional to t_1.

The values of θ_m and $\theta_m^{-1}[(2 - 3\theta_m)/(2 - \theta_m)]^{\frac{1}{2}}$ are plotted in Fig. 21 against α_m/α_{00}, which is just the ratio of the maximum attenuation constant to the minimum low-frequency attenuation constant which can be achieved with a Clogston cable of the same diameter. When α_m/α_{00} is unity, then $\theta_m = 2/3$ and f_m is zero to the present approximation (a better estimate of f_m would be the critical frequency f_1' defined by equation (467)). For values of α_m/α_{00} greater than about five, θ_m is given to a good approximation by

$$\theta_m \approx \frac{4\alpha_{00}}{3\sqrt{3}\,\alpha_m} \approx \frac{0.77\alpha_{00}}{\alpha_m}, \tag{507}$$

while

$$f_m \approx \frac{2.25\chi_p}{\pi\mu_1 g_1 t_1}\frac{\alpha_m}{\alpha_{00}}. \tag{508}$$

The low-frequency attenuation constant α_0 of a Clogston cable with $\theta = \theta_m$ will of course be greater than α_{00} if θ_m is not equal to 2/3. This is not really a disadvantage, however, since by assumption we only wish to insure that $\alpha \leqq \alpha_m$ over the operating band, and the nearer α approaches to α_m over the whole band the less serious will be the equalization problem. It may be shown that the ratio α_0/α_m decreases from unity toward one-half as α_m/α_{00} is increased indefinitely. Physically this means that the low-frequency attenuation constant of an optimum Clogston cable is always at least half as great as the attenuation constant at the upper end of the band, and the cable never contains more conducting material than would correspond to a total stack thickness of about two effective skin depths at the highest operating frequency.

We conclude with a few numerical formulas relating to the principal mode in a completely filled Clogston cable with copper conductors and no inner core. The low-frequency attenuation constant α_0 of such a

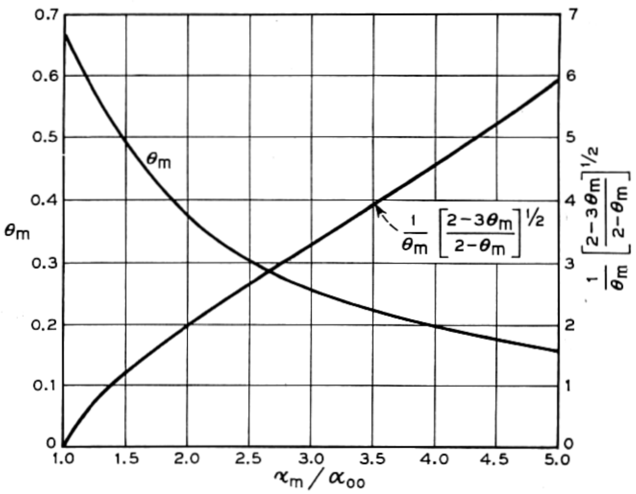

Fig. 21—Curves related to the optimum fraction θ_m of conducting material in Clogston cables with finite laminae, as a function of the attenuation ratio α_m/α_{00}.

cable is given by

$$\alpha_0 = \frac{0.521\sqrt{\epsilon_{2r}}}{\theta\sqrt{1-\theta}\, b_{\text{mils}}^2} \text{ nepers}\cdot\text{meter}^{-1} = \frac{0.728 \times 10^4\sqrt{\epsilon_{2r}}}{\theta\sqrt{1-\theta}\, b_{\text{mils}}^2} \text{ db}\cdot\text{mile}^{-1}, \tag{509}$$

for any value of θ, while if $\theta = 2/3$, we have

$$\alpha_{00} = \frac{1.353\sqrt{\epsilon_{2r}}}{b_{\text{mils}}^2} \text{ nepers}\cdot\text{meter}^{-1} = \frac{1.891 \times 10^4\sqrt{\epsilon_{2r}}}{b_{\text{mils}}^2} \text{ db}\cdot\text{mile}^{-1}. \tag{510}$$

The frequency f_m as a function of the ratio α_m/α_{00} is

$$(f_m)_{\text{Mc}} = \frac{44.93}{(t_1)_{\text{mils}} b_{\text{mils}}} \left[2.598\,\frac{(1-\theta)^{\frac{1}{2}}}{\theta}\,\frac{\alpha_m}{\alpha_{00}} - \frac{1}{\theta^2}\right]^{\frac{1}{2}}, \tag{511}$$

for any θ, and when $\theta = \theta_m$ the expression for f_m becomes

$$(f_m)_{\text{Mc}} = \frac{44.93}{(t_1)_{\text{mils}} b_{\text{mils}}}\,\frac{1}{\theta_m}\left[\frac{2 - 3\theta_m}{2 - \theta_m}\right]^{\frac{1}{2}}, \tag{512}$$

where the factor involving θ_m is plotted against α_m/α_{00} in Fig. 21.

If we consider a 3/8-inch Clogston cable with 0.1-mil copper conductors and polyethylene insulation ($\epsilon_{2r} = 2.26$), we find

$$\alpha_{00} = 0.809 \text{ db}\cdot\text{mile}^{-1}. \tag{513}$$

If we set

$$\alpha_m = 2\alpha_{00} = 1.618 \text{ db}\cdot\text{mile}^{-1}, \tag{514}$$

then it turns out that

$$\theta_m = 0.3745, \tag{515}$$

so that the insulating layers should be 0.167 mil thick. The low-frequency attenuation constant for θ_m is

$$\alpha_0 = 1.300\alpha_{00} = 1.051 \text{ db}\cdot\text{mile}^{-1}, \tag{516}$$

and α_m is reached at a frequency

$$f_m = 4.70 \text{ Mc}\cdot\text{sec}^{-1}. \tag{517}$$

If we had used $\theta = 2/3$, we should have reached α_m at a frequency of

3.59 $\text{Mc}\cdot\text{sec}^{-1}$, which is only 76.5 per cent of the frequency given by (517). An ordinary air-filled coaxial cable of the same size would have an attenuation constant equal to α_{00} at about 50 $\text{kc}\cdot\text{sec}^{-1}$ and equal to α_m ($= 2\alpha_{00}$) at about 200 $\text{kc}\cdot\text{sec}^{-1}$.

It should be borne in mind that in the preceding example we have neglected the effects of dielectric loss and of stack nonuniformity. Neither of these effects can be completely eliminated in a physical Clogston cable, and both will exert increasingly adverse influences on the attenuation constant as the frequency is raised.

XII. EFFECT OF NONUNIFORMITY OF LAMINATED MEDIUM

In the previous analysis of laminated transmission lines we have treated only perfectly uniform structures, in which every conducting layer is identical to every other conducting layer in thickness and in electrical properties, and all the insulating layers are similarly identical to each other. In practice, however, it will not be possible to lay down large numbers of absolutely identical thin layers, and we therefore need to know the effect on transmission of slight nonuniformities in the laminated stacks. Some indication that stack uniformity will be a very critical problem in laminated cables which are expected to give large improvements in attenuation over conventional coaxial cables of the same size may be obtained from the results of Section VI, which showed that in a Clogston 1 line, where the phase velocity is determined by the $\mu\epsilon$ product of the main dielectric, this product must be controlled very accurately to maintain the desired deep penetration of current into the laminated stacks. In a Clogston 2, where the main dielectric has been replaced by extensions of the stacks, one might expect similarly stringent requirements on the uniformity of the laminated material if the desired current distribution is to be maintained.

In this section we estimate the effects of stack nonuniformity by studying some particular idealized cases of nonuniformity in a parallel-plane Clogston 2 with infinitesimally thin layers, in which the average electrical properties of the stack vary only in the direction perpendicular to the layers. The principal conclusion is that if one attempts to realize with a Clogston line an attenuation constant which is a small fraction, say of the order of one-tenth, of the attenuation constant of a conventional line of the same dimensions at the same frequency, then long-range variations in the properties of the stack (as distinguished from short-range random fluctuations) must be controlled to within a few parts in 10,000. The price is less steep if the overall improvement sought is less, but in all practical cases it appears that the average properties of the stack must be held constant against slow variations to a fraction of a per cent. The requirement of extraordinarily high precision is in addition to the requirement that the individual layers must be extremely thin if a Clogston cable is to improve on a conventional coaxial cable at all in the megacycle frequency range.

For purposes of analysis, we consider a parallel-plane Clogston 2 transmission line bounded by infinite-impedance sheaths at $y = \pm\frac{1}{2}a$, as shown schematically in Fig. 10. The individual layers are supposed to be infinitesimally thin, so that near any given point the average electrical constants of the stack are

$$\begin{aligned} \bar{\epsilon} &= \epsilon_2/(1 - \theta), \\ \bar{\mu} &= \theta\mu_1 + (1 - \theta)\mu_2 , \\ \bar{g} &= \theta g_1 . \end{aligned} \tag{518}$$

The quantities $\bar{\epsilon}$, $\bar{\mu}$, and $\bar{g}$ may vary, continuously or with a finite number of finite discontinuities, as functions of the transverse coordinate y, owing to variations in any or all of μ_1, g_1, μ_2, ϵ_2, and θ; but they are not supposed to vary with x or z.

We shall be concerned with modes in which the fields are independent of x, and in which the only field components are H_x, $\bar{E}_y$, and E_z. Then Maxwell's equations are given by (269) of Section VIII, and reduce, if we write the field components in the form $H_x(y)e^{-\gamma z}$, $\bar{E}_y(y)e^{-\gamma z}$, and $E_z(y)e^{-\gamma z}$, to

$$\begin{aligned} -\gamma H_x &= i\omega\bar{\epsilon}\bar{E}_y , \\ dH_x/dy &= -\bar{g}E_z , \\ -\gamma\bar{E}_y - dE_z/dy &= i\omega\bar{\mu}H_x . \end{aligned} \tag{519}$$

If we eliminate $\bar{E}_y$ and E_z from these equations we obtain

$$\frac{d^2H_x}{dy^2} - \frac{1}{\bar{g}}\frac{d\bar{g}}{dy}\frac{dH_x}{dy} - i\omega\bar{\mu}\bar{g}\left[1 + \frac{\gamma^2}{\omega^2\bar{\mu}\bar{\epsilon}}\right]H_x = 0, \tag{520}$$

where H_x and E_z must be continuous at any points of discontinuity of $\bar{\epsilon}$, $\bar{\mu}$, or $\bar{g}$. The tangential magnetic field must vanish on the infinite-impedance surfaces at $y = \pm\frac{1}{2}a$; hence we have the boundary conditions

$$H_x(-\tfrac{1}{2}a) = H_x(\tfrac{1}{2}a) = 0. \tag{521}$$

These boundary conditions, taken in conjunction with the differential equation (520), define the values of γ which are the propagation constants of the various modes of the line.

While it is possible to find special forms of the functions $\bar{\epsilon}(y)$, $\bar{\mu}(y)$, and $\bar{g}(y)$ such that (520) can be solved exactly in terms of known functions, it is easier to make certain approximations in the beginning which retain only the important terms. For this purpose we shall write

$$\begin{aligned} \bar{\epsilon} &= \bar{\epsilon}_0 + \Delta\bar{\epsilon}, \\ \bar{\mu} &= \bar{\mu}_0 + \Delta\bar{\mu}, \\ \bar{g} &= \bar{g}_0 + \Delta\bar{g}, \end{aligned} \tag{522}$$

where $\bar{\epsilon}_0$, $\bar{\mu}_0$, and $\bar{g}_0$ are constants representing the average values of $\bar{\epsilon}$, $\bar{\mu}$, and $\bar{g}$ across the stack, so that the average values of $\Delta\bar{\epsilon}$, $\Delta\bar{\mu}$, and $\Delta\bar{g}$ across the stack are zero.* Furthermore the fractional variations in the stack parameters will be assumed small compared to unity; in practical cases they will never be larger than a few per cent and will usually be only a fraction of one per cent.

Referring now to equation (520), we see that the coefficient of H_x contains the large factor $\omega\bar{\mu}\bar{g}$, which is of the order of $1/\delta_1^2$, as compared with the term d^2H_x/dy^2, which is presumably of the order of $(1/a^2)H_x$. Hence small changes in $\bar{\epsilon}$ and $\bar{\mu}$ will make relatively large changes in the coefficient of H_x, since γ^2 is a constant. On the other hand, the coefficient of dH_x/dy will be small for any reasonable variations in the small quantity $\Delta\bar{g}/\bar{g}_0$. Hence we shall neglect this term entirely and deal with the approximate equation

$$\frac{d^2H_x}{dy^2} - i\omega\bar{\mu}\bar{g}\left[1 + \frac{\gamma^2}{\omega^2\bar{\mu}\bar{\epsilon}}\right]H_x = 0. \tag{523}$$

If we substitute (522) into (523) and drop second order terms in $\Delta\bar{\epsilon}/\bar{\epsilon}_0$, $\Delta\bar{\mu}/\bar{\mu}_0$, and $\Delta\bar{g}/\bar{g}_0$, we find that the coefficient of H_x becomes

$$\begin{aligned} &-\frac{i\bar{g}}{\omega\bar{\epsilon}}[\omega^2\bar{\mu}\bar{\epsilon} + \gamma^2] \\ &\approx -\frac{i\bar{g}_0}{\omega\bar{\epsilon}_0}\left[1 + \frac{\Delta\bar{g}}{\bar{g}_0} - \frac{\Delta\bar{\epsilon}}{\bar{\epsilon}_0}\right]\left[\gamma^2 + \omega^2\bar{\mu}_0\bar{\epsilon}_0 + \omega^2\bar{\mu}_0\bar{\epsilon}_0\left(\frac{\Delta\bar{\mu}}{\bar{\mu}_0} + \frac{\Delta\bar{\epsilon}}{\bar{\epsilon}_0}\right)\right]; \end{aligned} \tag{524}$$

and if

$$\Gamma_l^2 = \frac{i\bar{g}_0}{\omega\bar{\epsilon}_0}[\omega^2\bar{\mu}_0\bar{\epsilon}_0 + \gamma^2], \tag{525}$$

* The present use of zero subscripts on $\bar{\epsilon}_0$, $\bar{\mu}_0$, and $\bar{g}_0$ has of course nothing to do with the earlier convention that associated zero subscripts with the main dielectric in Clogston 1 lines.

so that

$$\gamma^2 = -\omega^2\bar{\mu}_0\bar{\epsilon}_0 - (i\omega\bar{\epsilon}_0/\bar{g}_0)\Gamma_\iota^2, \tag{526}$$

then (524) becomes, approximately,

$$\begin{aligned} -\left[1 + \frac{\Delta\bar{g}}{\bar{g}_0} - \frac{\Delta\bar{\epsilon}}{\bar{\epsilon}_0}\right]\left[\Gamma_\iota^2 + i\omega\bar{\mu}_0\bar{g}_0\left(\frac{\Delta\bar{\mu}}{\bar{\mu}_0} + \frac{\Delta\bar{\epsilon}}{\bar{\epsilon}_0}\right)\right] \\ \approx -\left[\Gamma_\iota^2 + i\omega\bar{\mu}_0\bar{g}_0\left(\frac{\Delta\bar{\mu}}{\bar{\mu}_0} + \frac{\Delta\bar{\epsilon}}{\bar{\epsilon}_0}\right)\right]. \end{aligned} \tag{527}$$

In all cases of interest we shall find that $(\Delta\bar{\mu}/\bar{\mu}_0 + \Delta\bar{\epsilon}/\bar{\epsilon}_0)$ is smaller than or at most of the same order of magnitude as $\Gamma_\iota^2/i\omega\bar{\mu}_0\bar{g}_0$. Hence the differential equation (523) takes the approximate form

$$\frac{d^2H_x}{dy^2} - \left[\Gamma_\iota^2 + i\omega\bar{\mu}_0\bar{g}_0\left(\frac{\Delta\bar{\mu}}{\bar{\mu}_0} + \frac{\Delta\bar{\epsilon}}{\bar{\epsilon}_0}\right)\right]H_x = 0, \tag{528}$$

where Γ_ι^2 is determined by the two-point boundary conditions (521).

The variations of the stack parameters appear in (528) only in the term $(\Delta\bar{\mu}/\bar{\mu}_0 + \Delta\bar{\epsilon}/\bar{\epsilon}_0)$, which is some as yet unspecified function of y. For convenience we shall write this term in the form

$$\frac{\Delta\bar{\mu}}{\bar{\mu}_0} + \frac{\Delta\bar{\epsilon}}{\bar{\epsilon}_0} = \frac{C}{\omega\bar{\mu}_0\bar{g}_0a^2}\varphi(y), \tag{529}$$

where C is a dimensionless parameter and $\varphi(y)$ is a function whose average value over the stack is zero, and whose maximum absolute value will usually be of the order of unity. It is worth noting that if the conducting and insulating layers all have equal permeabilities, then (529) becomes

$$\frac{\Delta\bar{\epsilon}}{\bar{\epsilon}_0} = \frac{C\delta_1^2}{2a^2\theta_0}\varphi(y), \tag{530}$$

where δ_1 is the skin depth in the average conducting layer and θ_0 is the average fraction of space filled with conducting material. If we solve the differential equation for different values of the scale factor C but the same $\varphi(y)$, we can calculate the effect of stack nonuniformities of the same type but different amplitudes, or the effect of nonuniformity in the same stack at different frequencies. In the latter case C is directly proportional to the frequency.

The final step in the transformation of the differential equation (528) will be to reduce it to dimensionless form by the substitutions

$$\begin{aligned} \xi &= y/a + \tfrac{1}{2}, \\ w(\xi) &= H_x(y), \\ f(\xi) &= \varphi(y), \\ \Lambda &= -\Gamma_\zeta^2 a^2. \end{aligned} \tag{531}$$

Then on making use of (529) we get

$$d^2w/d\xi^2 + [\Lambda - iCf(\xi)]w(\xi) = 0, \tag{532}$$

with the boundary conditions

$$w(0) = w(1) = 0. \tag{533}$$

Once Λ has been determined for a particular mode, the propagation constant γ is obtained from (526) and (531), namely

$$\gamma = i\omega\sqrt{\bar{\mu}_0\bar{\epsilon}_0}\,[1 + \Lambda/i\omega\bar{\mu}_0\bar{g}_0a^2]^{\frac{1}{2}}. \tag{534}$$

Assuming as usual that the attenuation per radian is small, we find that the attenuation and phase constants are given by

$$\alpha = \operatorname{Re}\gamma = \operatorname{Re}\frac{\Lambda}{2\sqrt{\bar{\mu}_0/\bar{\epsilon}_0}\;\bar{g}_0a^2}, \tag{535}$$

$$\beta = \operatorname{Im}\gamma = \omega\sqrt{\bar{\mu}_0\,\bar{\epsilon}_0} + \operatorname{Im}\frac{\Lambda}{2\sqrt{\bar{\mu}_0/\bar{\epsilon}_0}\;\bar{g}_0a^2}. \tag{536}$$

The eigenvalues Λ of the differential equation (532) with boundary conditions (533) may be found analytically for some simple forms of $f(\xi)$, or numerically using a differential analyzer for any given $f(\xi)$ which does not fluctuate too rapidly. When $C = 0$, as in the case of a perfectly uniform stack, the eigenvalues are obviously

$$\Lambda_1 = \pi^2, \qquad \Lambda_2 = 4\pi^2, \cdots, \tag{537}$$

corresponding to the eigenfunctions

$$w_1 = \sin \pi\xi, \qquad w_2 = \sin 2\pi\xi, \cdots. \tag{538}$$

As C varies continuously, we expect the eigenvalues and eigenfunctions to vary continuously in a manner depending on $f(\xi)$. In the following paragraphs we shall discuss the behavior of Λ_1, and sometimes also Λ_2, as a function of C for various simple types of nonuniformity.

(*i*) $f(\xi)$ *constant except at single discontinuity*. Let

$$f(\xi) = \begin{cases} -\dfrac{1}{2\xi_0}, & 0 \leqq \xi < \xi_0, \\ \\ \dfrac{1}{2(1 - \xi_0)}, & \xi_0 < \xi \leqq 1, \end{cases} \tag{539}$$

where ξ_0 is some fixed number between 0 and 1 but not, in the cases of interest, extremely close to either 0 or 1. Solutions of (532) satisfying the boundary conditions (533) are obviously

$$\begin{aligned} w(\xi) &= A \sin [\Lambda + iC/2\xi_0]^{\frac{1}{2}}\xi, & 0 \leqq \xi < \xi_0, \\ w(\xi) &= B \sin [\Lambda - iC/2(1 - \xi_0)]^{\frac{1}{2}}(1 - \xi), & \xi_0 < \xi \leqq 1, \end{aligned} \tag{540}$$

where A and B are arbitrary constants. The requirements that w and $dw/d\xi$ be continuous* at $\xi = \xi_0$ lead to the equations

$$\begin{aligned} &A \sin [\Lambda + iC/2\xi_0]^{\frac{1}{2}}\xi_0 = B \sin [\Lambda - iC/2(1 - \xi_0)]^{\frac{1}{2}}(1 - \xi_0), \\ &A[\Lambda + iC/2\xi_0]^{\frac{1}{2}} \cos [\Lambda + iC/2\xi_0]^{\frac{1}{2}}\xi_0 \\ &\qquad = -B[\Lambda - iC/2(1 - \xi_0)]^{\frac{1}{2}} \cos [\Lambda - iC/2(1 - \xi_0)]^{\frac{1}{2}}(1 - \xi_0), \end{aligned} \tag{541}$$

which will be consistent if this characteristic equation is satisfied:

$$\frac{\tan [\Lambda + iC/2\xi_0]^{\frac{1}{2}}\xi_0}{[\Lambda + iC/2\xi_0]^{\frac{1}{2}}} + \frac{\tan [\Lambda - iC/2(1 - \xi_0)]^{\frac{1}{2}}(1 - \xi_0)}{[\Lambda - iC/2(1 - \xi_0)]^{\frac{1}{2}}} = 0. \tag{542}$$

The roots in Λ of equation (542) are the eigenvalues of the problem; the eigenfunction corresponding to any given eigenvalue is given by equations (540) after the ratio B/A is determined from either of equations (541).

It is easy to show that when $C = 0$, the roots of (542) are $\Lambda_1 = \pi^2$, $\Lambda_2 = 4\pi^2, \cdots$. For large values of C, representing relatively great differences between the two parts of the stack, physical considerations lead us to expect that there will be pairs of modes, one member of each pair being essentially confined to each part of the stack and having a propagation constant determined approximately by the width of that part. It may in fact be shown that the asymptotic expression for the eigenvalue of the mode which is essentially confined to the region $0 \leqq \xi < \xi_0$ is

$$\Lambda \approx \frac{\pi^2}{\xi_0^2}\left[1 - 2\sqrt{\frac{(1 - \xi_0)}{\xi_0 C}}\right] - i\left[\frac{C}{2\xi_0} - \frac{2\pi^2}{\xi_0^2}\sqrt{\frac{(1 - \xi_0)}{\xi_0 C}}\right]; \tag{543}$$

* The continuity of $dw/d\xi$ is a consequence of the continuity of E_z, provided that we neglect any discontinuity in $\bar{g}$ at $\xi = \xi_0$.

and the asymptotic expression for the eigenvalue of the mode which is essentially confined to $\xi_0 < \xi \leqq 1$ is

$$\Lambda \approx \frac{\pi^2}{(1-\xi_0)^2}\left[1 - 2\sqrt{\frac{\xi_0}{(1-\xi_0)C}}\right] + i\left[\frac{C}{2(1-\xi_0)} - \frac{2\pi^2}{(1-\xi_0)^2}\sqrt{\frac{\xi_0}{(1-\xi_0)C}}\right]. \tag{544}$$

It is clear that if $\xi_0 < \frac{1}{2}$ the latter mode has the smaller attenuation constant, while if $\xi_0 > \frac{1}{2}$ the former mode has the smaller attenuation constant.

It is not difficult, although the details will be omitted here, to investigate the behavior of the eigenvalues for small C and to show that no matter whether $\xi_0 < \frac{1}{2}$ or $\xi_0 > \frac{1}{2}$, the eigenvalue which starts from π^2 at $C = 0$ tends to the asymptotic value which has the smaller real part, so that this eigenvalue, whether its asymptotic form be given by (543) or (544), may be called Λ_1. It appears that if $\xi_0 < \frac{1}{2}$, then Im Λ_1 is positive for positive C, while if $\xi_0 > \frac{1}{2}$, then Im Λ_1 is negative for positive C.

An interesting mathematical phenomenon appears when $\xi_0 = \frac{1}{2}$, so that the discontinuity in $f(\xi)$ is exactly at the center of the stack. In this case, when C is small Λ_1 and Λ_2 are both real, Λ_1 being somewhat greater than π^2 and Λ_2 somewhat less than $4\pi^2$. For a certain value of C the two eigenvalues coincide; this value is approximately

$$C = 17.9, \qquad \Lambda_1 = \Lambda_2 = 25.6. \tag{545}$$

For larger values of C, Λ_1 and Λ_2 are complex conjugates (it seems to be immaterial which is which) whose asymptotic forms are given by (543) and (544) with $\xi_0 = \frac{1}{2}$.

Approximate values of Λ_1 and Λ_2 were found for the symmetric case, $\xi_0 = 0.5$, and for one unsymmetric case, $\xi_0 = 0.6$, on the Laboratories' general purpose analog computer for $0 \leqq C \leqq 100$, and were refined afterward by desk computation, using a method of successive approximations to solve equation (542). The real and imaginary parts of Λ_1/π^2 and Λ_2/π^2 are plotted in Fig. 22 for the symmetric case, where it should be noted that different vertical scales are used for Re Λ/π^2 and Im Λ/π^2. The corresponding eigenfunctions $w_1(\xi)$ and $w_2(\xi)$ are shown in Fig. 23 for $C = 0$, $C = 17.9$, which corresponds to equal eigenvalues, and $C = 100$. It will be recalled that $w(\xi)$ is equal to $H_x(y)$, and the other field components can be derived from H_x by equations (519) if desired. Fig. 24 shows plots of Λ_1/π^2 and Λ_2/π^2 for the unsymmetric case $\xi_0 = 0.6$.

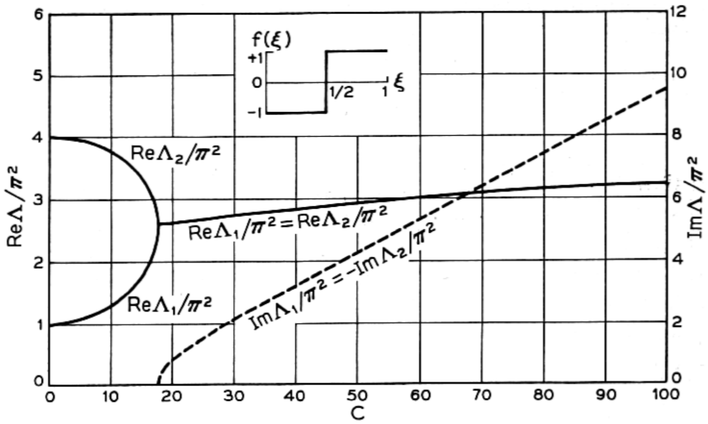

Fig. 22—Real and imaginary parts of Λ_1/π^2 and Λ_2/π^2 for a nonuniform stack whose average properties are constant except at a single, symmetric discontinuity.

(ii) $f(\xi)$ a symmetric rectangular step. Let

$$f(\xi) = \begin{cases} -\dfrac{1}{2\xi_0}, & 0 \leqq \xi < \tfrac{1}{2}\xi_0, \\ \dfrac{1}{2(1-\xi_0)}, & \tfrac{1}{2}\xi_0 < \xi < 1 - \tfrac{1}{2}\xi_0, \\ -\dfrac{1}{2\xi_0}, & 1 - \tfrac{1}{2}\xi_0 < \xi \leqq 1, \end{cases} \tag{546}$$

where ξ_0 is some fixed number between 0 and 1 but not, in the cases of interest, extremely close to either 0 or 1. Inasmuch as $f(\xi)$ has even symmetry about $\xi = \frac{1}{2}$, every mode will preserve the (even or odd) symmetry about $\xi = \frac{1}{2}$ which it has when $C = 0$. We shall consider the lowest even mode,* which has the eigenfunction $\sin \pi\xi$ when $C = 0$. Solutions of (532) having even symmetry about $\xi = \frac{1}{2}$ (we need consider only the region $0 \leqq \xi \leqq \frac{1}{2}$ on account of the symmetry) and satisfying the boundary conditions (533) are given by

---

* For large C the lowest even mode will be confined essentially to

$$\tfrac{1}{2}\xi_0 < \xi < 1 - \tfrac{1}{2}\xi_0,$$

while the lowest odd mode will be confined to the two regions

$$0 \leqq \xi < \tfrac{1}{2}\xi_0 \text{ and } 1 - \tfrac{1}{2}\xi_0 < \xi \leqq 1.$$

If $\xi_0 > 2/3$, the latter mode will ultimately have a lower attenuation constant than the former; but we shall not take space to investigate it here.

$$
\begin{aligned}
w(\xi) &= A \sin [\Lambda + iC/2\xi_0]^{\frac{1}{2}}\xi, & 0 \leqq \xi < \tfrac{1}{2}\xi_0 ,\\
w(\xi) &= B \cos [\Lambda - iC/2(1 - \xi_0)]^{\frac{1}{2}}(\tfrac{1}{2} - \xi), & \tfrac{1}{2}\xi_0 < \xi \leqq \tfrac{1}{2} .
\end{aligned} \tag{547}
$$

The requirements that w and $dw/d\xi$ must be continuous at $\xi = \frac{1}{2}\xi_0$ lead to the equations

$$
\begin{aligned}
&A \sin \tfrac{1}{2}[\Lambda + iC/2\xi_0]^{\frac{1}{2}}\xi_0 = B \cos \tfrac{1}{2}[\Lambda - iC/2(1 - \xi_0)]^{\frac{1}{2}}(1 - \xi_0),\\
&A[\Lambda + iC/2\xi_0]^{\frac{1}{2}} \cos \tfrac{1}{2}[\Lambda + iC/2\xi_0]^{\frac{1}{2}}\xi_0\\
&\qquad = B[\Lambda - iC/2(1 - \xi_0)]^{\frac{1}{2}} \sin \tfrac{1}{2}[\Lambda - iC/2(1 - \xi_0)]^{\frac{1}{2}}(1 - \xi_0),
\end{aligned} \tag{548}
$$

which will be consistent if the following characteristic equation is satisfied:

$$
\frac{\tan \frac{1}{2}[\Lambda + iC/2\xi_0]^{\frac{1}{2}}\xi_0}{[\Lambda + iC/2\xi_0]^{\frac{1}{2}}} = \frac{\cot \frac{1}{2}[\Lambda - iC/2(1 - \xi_0)]^{\frac{1}{2}}(1 - \xi_0)}{[\Lambda - iC/2(1 - \xi_0)]^{\frac{1}{2}}} . \tag{549}
$$

The roots in Λ of equation (549) are the eigenvalues corresponding to the even modes of the symmetrical structure.

When $C = 0$, the roots of (549) are $\Lambda = \pi^2, 9\pi^2, \cdots$. It appears that for $C > 0$ we have $\mathrm{Re}\,\Lambda_1 > \pi^2$ and $\mathrm{Im}\,\Lambda_1 > 0$. For large C the asymptotic expression for Λ_1 turns out to be

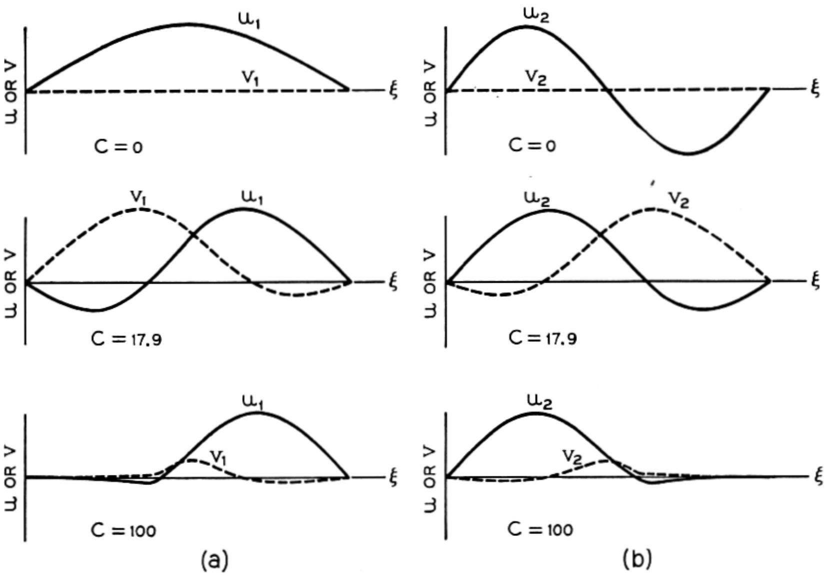

Fig. 23—Real and imaginary parts of the first two eigenfunctions, $w_1 = u_1 + iv_1$ and $w_2 = u_2 + iv_2$, for the nonuniform stack of Fig. 22.

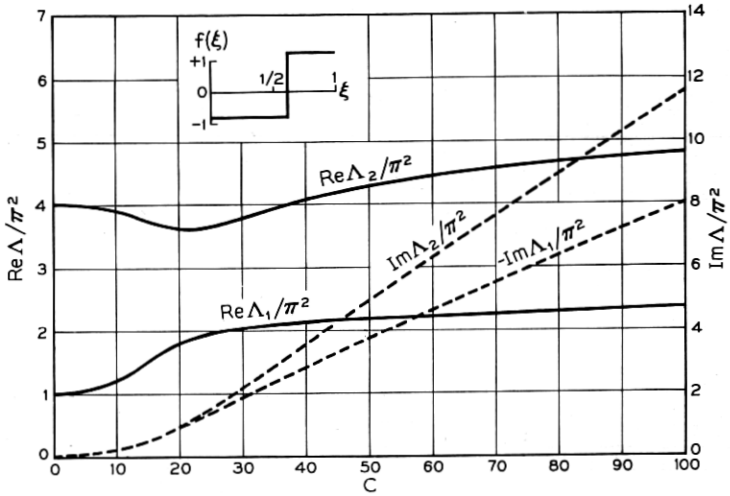

Fig. 24—Real and imaginary parts of Λ_1/π^2 and Λ_2/π^2 for a nonuniform stack whose average properties are constant except at a single, unsymmetric discontinuity.

$$\Lambda \approx \frac{\pi^2}{(1-\xi_0)^2}\left[1 - 4\sqrt{\frac{\xi_0}{(1-\xi_0)C}}\right] + i\left[\frac{C}{2(1-\xi_0)} - \frac{4\pi^2}{(1-\xi_0)^2}\sqrt{\frac{\xi_0}{(1-\xi_0)C}}\right]. \tag{550}$$

Numerical values of Λ_1 were found for the case $\xi_0 = \frac{1}{2}$ on the analog computer and refined afterward by desk computation. The real and imaginary parts of Λ_1/π^2 are plotted over the range $0 \leqq C \leqq 100$ in Fig. 25, and the corresponding eigenfunction $w_1(\xi) = u_1(\xi) + iv_1(\xi)$ is shown in Fig. 26 for $C = 0$, 20, and 100.

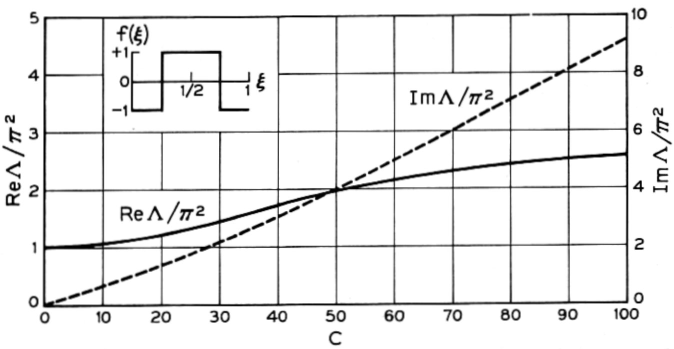

Fig. 25—Real and imaginary parts of Λ_1/π^2 for a nonuniform stack whose average properties vary as a symmetric rectangular step.

(iii) $f(\xi)$ a linear function. Let

$$f(\xi) = 2\xi - 1, \qquad 0 \leqq \xi \leqq 1, \tag{551}$$

so that $f(\xi)$ is a linear function varying from -1 at $\xi = 0$ to $+1$ at $\xi = 1$. Then equation (532) becomes

$$d^2w/d\xi^2 + [(\Lambda + iC) - 2iC\xi]w(\xi) = 0, \tag{552}$$

which, by the change of variable

$$\tau = \frac{2iC\xi - (\Lambda + iC)}{(2C)^{2/3}}, \tag{553}$$

is transformed into Stokes' equation,

$$d^2w/d\tau^2 + \tau w = 0. \tag{554}$$

The general solution of this equation may be written in the form

$$w = Ah_1(\tau) + Bh_2(\tau), \tag{555}$$

where h_1 and h_2 are the pair of independent solutions of Stokes' equation which have been tabulated for complex arguments by the Computation Laboratory of Harvard University.[27] (The solution may also be ex-

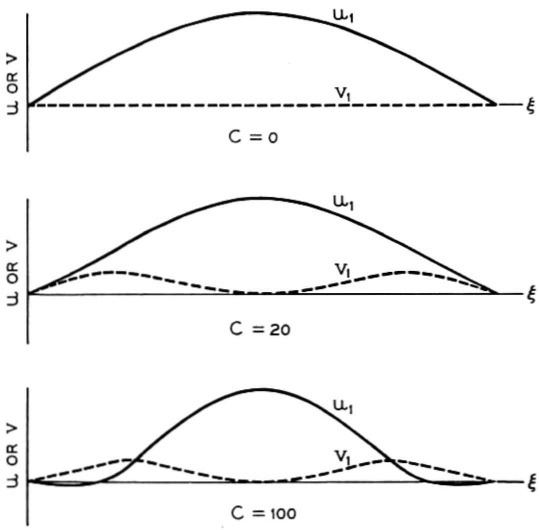

Fig. 26—Real and imaginary parts of the first eigenfunction, $w_1 = u_1 + iv_1$, for the nonuniform stack of Fig. 25.

[27] *Tables of the Modified Hankel Functions of Order One-Third and of Their Derivatives,* Harvard University Press, Cambridge, Mass., 1945.

pressed, though less conveniently, in terms of Bessel functions of order one-third.) It is easy to show that the boundary conditions (533) at $\xi = 0$ and $\xi = 1$ require

$$\begin{aligned} Ah_1(\tau_1) + Bh_2(\tau_1) &= 0, \\ Ah_1(\tau_2) + Bh_2(\tau_2) &= 0, \end{aligned} \tag{556}$$

where

$$\tau_1 = -\frac{(\Lambda + iC)}{(2C)^{\frac{2}{3}}}, \qquad \tau_2 = -\frac{(\Lambda - iC)}{(2C)^{\frac{2}{3}}}. \tag{557}$$

Equations (556) will be consistent if

$$h_1(\tau_1)h_2(\tau_2) - h_1(\tau_2)h_2(\tau_1) = 0; \tag{558}$$

and this is the relation which must be satisfied by the eigenvalues $\Lambda_1, \Lambda_2, \Lambda_3, \cdots$, for any given value of C.

Approximate values of Λ_1 and Λ_2 have been found using the analog computer for the range $0 \leqq C \leqq 100$, with spot checks by numerical solution of equation (558); and Λ_1/π^2 and Λ_2/π^2 are plotted in Fig. 27. The eigenfunctions are qualitatively similar to those shown in Fig. 23 for the stack with a symmetric discontinuity. As in the symmetric example in case (*i*) above, we find that for small positive C, Λ_1 is real and greater than π^2, while Λ_2 is real and less than $4\pi^2$. The two eigenvalues coincide at

$$C \approx 49, \qquad \Lambda_1 = \Lambda_2 \approx 29. \tag{559}$$

For larger values of C, Λ_1 and Λ_2 are complex conjugates. Their asymp-

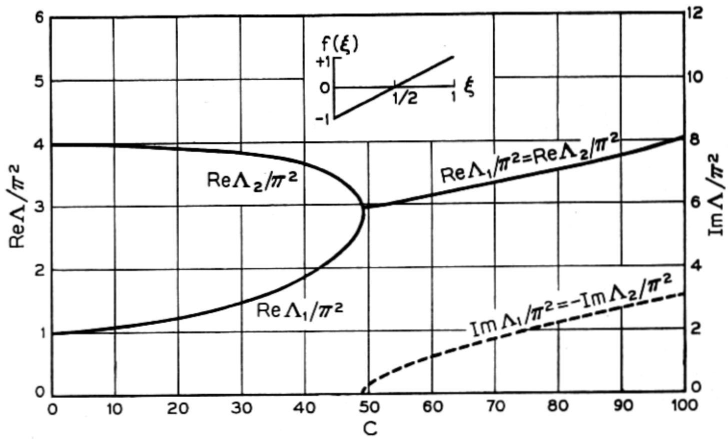

Fig. 27—Real and imaginary parts of Λ_1/π^2 and Λ_2/π^2 for a nonuniform stack whose average properties vary linearly across the stack.

totic forms as $C \to \infty$ may be deduced by considering the behavior of $h_1(\tau)$ and $h_2(\tau)$ for large arguments, and are

$$\Lambda_1 = \Lambda_2^* \approx 1.169(2C)^{\frac{2}{3}} + i[C - 2.025(2C)^{\frac{2}{3}}]. \tag{560}$$

The magnitudes of both the real and imaginary parts of Λ_1 and Λ_2 thus increase indefinitely with C.

(iv) $f(\xi)$ a sinusoidal function. Let

$$f(\xi) = -\cos 2\nu\pi\xi, \qquad 0 \leqq \xi \leqq 1, \tag{561}$$

where $\nu = \frac{1}{2}, 1, 2, 3, 4, \cdots$, so that $f(\xi)$ goes through ν complete cycles in $0 \leqq \xi \leqq 1$. Then equation (532) reads

$$d^2w/d\xi^2 + [\Lambda + iC \cos 2\nu\pi\xi]w(\xi) = 0. \tag{562}$$

If we make the transformations

$$\begin{aligned} \tau &= \nu\pi\xi, \\ W(\tau) &= w(\xi), \\ \lambda &= \Lambda/\nu^2\pi^2, \\ \vartheta &= -iC/2\nu^2\pi^2, \end{aligned} \tag{563}$$

we get

$$d^2W/d\tau^2 + [\lambda - 2\vartheta \cos 2\tau]W(\tau) = 0, \tag{564}$$

and the boundary conditions (533) become

$$W(0) = W(\nu\pi) = 0. \tag{565}$$

Equation (564) is one of the standard forms of Mathieu's equation. We are interested in solutions which are periodic with period 2 in ξ, and which approach the form $\sin m\pi\xi$ when $C \to 0$. In terms of τ and ϑ, the function corresponding to the mth mode in the Clogston line must reduce to the form

$$W(\tau) \underset{\vartheta \to 0}{\longrightarrow} \sin \frac{m}{\nu} \tau. \tag{566}$$

For any value of ϑ, this function may be denoted by[28]

$$W(\tau) = \mathrm{se}_{m/\nu}(\tau, \vartheta). \tag{567}$$

---

[28] See N. W. McLachlan, *Theory and Application of Mathieu Functions*, Oxford, 1947, pp. 10–25, especially p. 13 and p. 19. In this reference a or b corresponds to our λ, q to our ϑ, and ν to our m/ν.

In our problem ϑ is (negative) imaginary and m/ν may be an integer or a rational fraction. For any given ϑ and m/ν the conditions (565) together with the limiting form (566) determine an eigenvalue λ, and hence by (563) determine Λ; but only a small amount of work has been published on the eigenvalues of Mathieu functions with imaginary parameter or of fractional order. We shall look at some special cases.

$\nu = \frac{1}{2}$. The function $f(\xi)$ is one-half cycle of a cosine curve which varies from -1 to $+1$; we expect results similar to those found for the symmetric discontinuity of case (i) and the linear variation of case (iii). The eigenfunctions of the first two modes ($m = 1$ and $m = 2$) are $se_2(\tau, \vartheta)$ and $se_4(\tau, \vartheta)$. The eigenvalues of these two functions for purely imaginary ϑ have been computed by Mulholland and Goldstein[29] out to a point which corresponds to $C = 8\pi^2$, and an asymptotic formula is given for larger values of C. The values of Λ_1/π^2 and Λ_2/π^2 are plotted for $0 \leqq C \leqq 100$ in Fig. 28; the corresponding eigenfunctions resemble those shown in Fig. 23 for the stack with a symmetric discontinuity. Again we find that Λ_1 and Λ_2 are real for small positive C, equal for a particular value of C, and conjugate complex for larger C. The leading terms of the asymptotic formula are, in our notation,

$$\Lambda_1 = \Lambda_2^* \approx [4.7124C^{\frac{1}{2}} - 3.0842 - 1.0901C^{-\frac{1}{2}} - \cdots] + i[C - 4.7124C^{\frac{1}{2}} - 1.0901C^{-\frac{1}{2}} - \cdots]. \tag{568}$$

$\nu = 1$. Here $f(\xi)$ is one full cycle of a cosine function, varying from -1

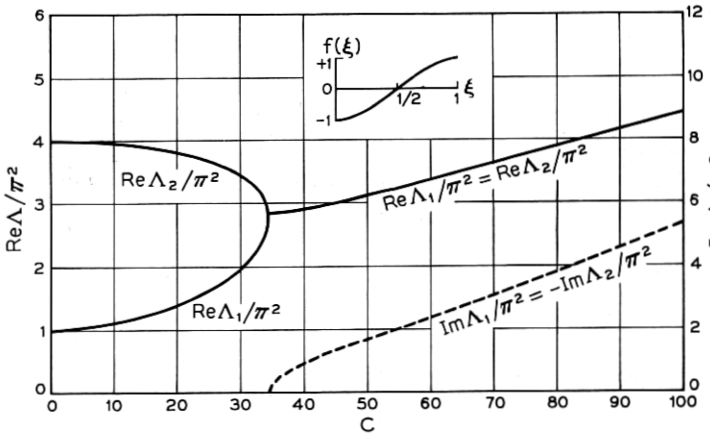

Fig. 28—Real and imaginary parts of Λ_1/π^2 and Λ_2/π^2 for a nonuniform stack whose average properties vary as one-half cycle of a cosine function across the stack.

[29] H. P. Mulholland and S. Goldstein, Phil. Mag. (7), **8**, 834 (1929). In this reference 4α or 4β corresponds to our λ and $8q$ to our ϑ.

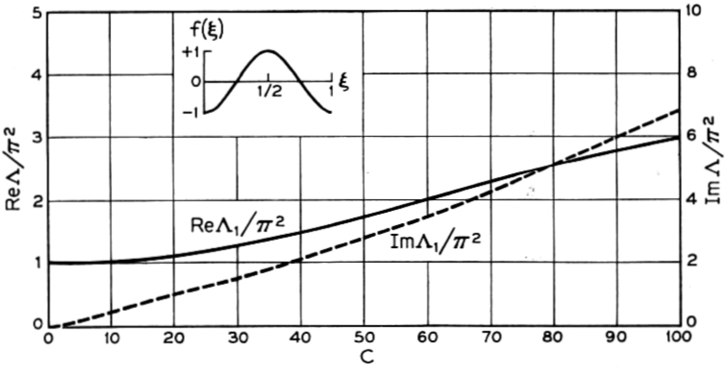

Fig. 29—Real and imaginary parts of Λ_1/π^2 for a nonuniform stack whose average properties vary as one cycle of a cosine function across the stack.

to $+1$ and back to -1. The eigenfunction of the lowest mode ($m = 1$) is $se_1(\tau, \vartheta)$, and the values of Λ_1 may be obtained from Reference 29 for ten equally spaced values of C out to $C = 32\pi^2$. Since our ϑ is negative imaginary, in the notation of this reference we have $\Lambda_1 = 4\pi^2\beta_1^*$. Approximate values of Λ_1/π^2 obtained on the analog computer for C at smaller intervals in the range $0 \leqq C \leqq 100$ are plotted in Fig. 29; and the eigenfunctions are similar to those shown in Fig. 26 for the symmetric rectangular step. The leading terms of the asymptotic formula for Λ_1 when C is large are as follows:

$$\Lambda_1 \approx [3.1416C^{\frac{1}{2}} - 2.4674 - 0.9689C^{-\frac{1}{2}} - \cdots] \\ + i[C - 3.1416C^{\frac{1}{2}} - 0.9689C^{-\frac{1}{2}} - \cdots]. \tag{569}$$

$\nu = 3$. Now $f(\xi)$ is a three-cycle cosine function and the lowest mode corresponds to $se_{\frac{1}{3}}(\tau, \vartheta)$. Approximate values of Λ_1/π^2 for $0 \leqq C \leqq 100$ were obtained on the analog computer and are plotted in Fig. 30; the eigenfunctions are shown in Fig. 31 for $C = 0$ and $C = 100$.

$\nu \gg 1$. For a ν-cycle cosine variation, the lowest eigenfunction is $se_{1/\nu}(\tau, \vartheta)$, and for the lowest eigenvalue there is an approximate formula given by McLachlan.[30] Incidentally this formula predicts no imaginary part for Λ_1 if ϑ is purely imaginary and $\nu > 1$, which agrees approximately with the results of our analog computations for $\nu = 3$; we found the imaginary part of Λ_1 to be only about 1 per cent of the real part even for $C = 100$. If C is fixed, one expects that as $\nu \to \infty$ the effects of the rapid fluctuations in $f(\xi)$ will average out, so that Λ_1 will ultimately approach

[30] Reference 28, p. 20, equation (6), where a corresponds to our λ_1, q to our ϑ, and ν to our $1/\nu$. McLachlan's formula was ostensibly derived for real q, but the derivation appears equally valid for complex q.

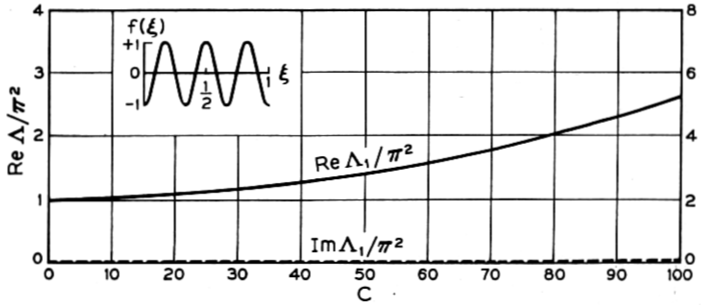

Fig. 30—Real and imaginary parts of Λ_1/π^2 for a nonuniform stack whose average properties vary as three cycles of a cosine function across the stack.

the value π^2 appropriate to a uniform stack. McLachlan's formula shows that this is indeed the case; in our notation, the leading terms give

$$\Lambda \approx \pi^2 + \frac{C^2}{8\nu^2\pi^2} = \pi^2 \left[1 + \frac{C^2}{8\nu^2\pi^4} \right], \tag{570}$$

assuming of course that the second term is reasonably small compared to the first.

This concludes our discussion of special types of nonuniformity. We shall now attempt to get an idea of what the numerical results mean in terms of the practical requirements on stack uniformity in a laminated transmission line which is expected to show a specified reduction in attenuation constant below a conventional line of the same dimensions. For this purpose we shall compare a plane Clogston 2 line having infinitesimally thin layers with a plane air-filled line of the same width a, bounded by electrically thick solid conductors.

At frequencies for which the conductor thickness of the "standard"

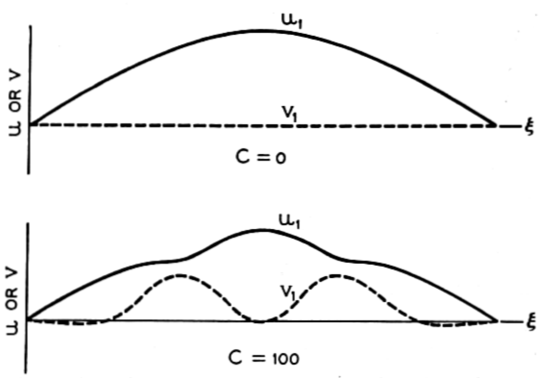

Fig. 31—Real and imaginary parts of the first eigenfunction, $w_1 = u_1 + iv_1$, for the nonuniform stack of Fig. 30.

air-filled line is great compared to the skin depth δ_1, its attenuation constant α_s is given by equation (25), namely

$$\alpha_s = 1/\eta_v g_1 \delta_1 a, \tag{571}$$

where η_v is the intrinsic impedance of free space. By equation (535), the attenuation constant α_c of the lowest mode in a plane Clogston 2 with infinitesimally thin layers is

$$a_c = \text{Re}\,\frac{\Lambda_1}{2\sqrt{\bar{\mu}_0/\bar{\epsilon}_0}\,\bar{g}_0 a^2}\,. \tag{572}$$

If we assume nonmagnetic materials and put in the optimum value of θ, namely $\theta = 2/3$, we obtain for a uniform stack with $\Lambda_1 = \pi^2$,

$$\alpha_{c0} = \frac{12.82\sqrt{\epsilon_{2r}}}{\eta_v g_1 a^2}, \tag{573}$$

where ϵ_{2r} is the relative dielectric constant of the insulating layers.

The attenuation constant of the conventional line is proportional to the square root of frequency, whereas the attenuation constant of the uniform Clogston 2 is independent of frequency up to some frequency at which the effect of finite lamina thickness begins to be appreciable. If we confine ourselves to the low-frequency, flat attenuation region, and denote the ratio of attenuation constants by r, then from (571) and (573),

$$r = a_{c0}/a_s = 12.82\sqrt{\epsilon_{2r}}\,\delta_1/a, \tag{574}$$

and the crossover frequency above which the uniform Clogston line is better than the conventional line occurs when

$$a/\delta_1 = 12.82\sqrt{\epsilon_{2r}}\,. \tag{575}$$

In the following numerical example we shall assume polyethylene insulating layers, with

$$\epsilon_{2r} = 2.26, \tag{576}$$

so that (574) becomes

$$r = 19.27\delta_1/a. \tag{577}$$

If the stack in a Clogston line is not uniform, then regardless of the thinness of the layers the attenuation constant will no longer be independent of frequency, but will increase with frequency at a rate depending on the nature and the magnitude of the nonuniformity. Since from equation (572) the attenuation constant is proportional to Re Λ_1, while from equation (529) or (530), C is proportional to frequency for a given stack, we see that our plots of Re Λ_1/π^2 versus C need only the introduction of appropriate scale factors to read directly the variation of attenuation with frequency due to nonuniformity in the stack. Although a nonuniform Clogston line may still be better under some conditions than a conventional line of the same size, the crossover frequency will be higher and the improvement at any given frequency will be less than if the stack were uniform.

Among the various interpretations which may be given to our numerical results, we shall consider here only the following: Suppose we have a plane Clogston 2 line which, if it were perfectly uniform, would have an attenuation constant smaller, at a certain frequency, than the attenuation constant of the corresponding conventional line by a given factor, say one-half, one-fifth, or one-tenth. For these particular attenuation reduction factors the ratio of a to δ_1 may be calculated from (574), or from (577) if the insulation is polyethylene. The question is: What variation in $\bar{\epsilon}$ across the stack is permissible if we are willing to have the actual attenuation constant of the Clogston line be double its ideal value; in other words, if we will settle for attenuation reduction factors of unity (no improvement), two-fifths, or one-fifth instead of the ideal values one-half, one-fifth, or one-tenth?

To answer this question for any particular type of nonuniformity, we have only to find, from the plot of Re Λ_1/π^2 versus C, the value of C for which Re $\Lambda_1/\pi^2 = 2$. Then the fractional difference between the maximum and minimum values of $\bar{\epsilon}$ corresponding to this value of C is given by equations (530) and (531) to be

$$\frac{\bar{\epsilon}_{\max} - \bar{\epsilon}_{\min}}{\bar{\epsilon}_0} = \frac{3C\delta_1^2}{4a^2}(f_{\max} - f_{\min}), \tag{578}$$

where we have taken $\theta_0 = 2/3$, and f_{max} and $f_{\min}$ are the extreme values of the function $f(\xi)$ which describes the type of nonuniformity being considered.

The special types of nonuniformity which have been studied above fall roughly into three different classes. In four of the cases, namely the symmetric and unsymmetric single discontinuities, the linear variation, and the half-cycle cosine variation, the function $f(\xi)$ varies monotonically from one side of the stack to the other. In the symmetric rectangular step and the one-cycle cosine variation, $f(\xi)$ oscillates from one extreme value to the other and back again, while in the three-cycle cosine variation, $f(\xi)$ exhibits three complete oscillations across the stack. The following table shows the permissible total variation in $\bar{\epsilon}$ for each of these types of nonuniformity.

Case	C	$\frac{\bar{\epsilon}_{max} - \bar{\epsilon}_{min}}{\bar{\epsilon}_0}$		
		$r = 1/2$	$r = 1/5$	$r = 1/10$
Symmetric discontinuity	16.5	0.0167	0.0027	0.0007
Unsymmetric discontinuity	28.0	0.0295	0.0047	0.0012
Linear	42.6	0.0430	0.0069	0.0017
Half-cycle cosine	29.5	0.0298	0.0048	0.0012
Rectangular step	53.0	0.0535	0.0086	0.0021
One-cycle cosine	59.8	0.0604	0.0097	0.0024
Three-cycle cosine	78.9	0.0797	0.0128	0.0032

It would be easy to construct a similar table for any other values of the attenuation ratio r, and for any specified degradation due to nonuniformity. It is, however, already obvious that the greater the improvement for which one strives, that is, the smaller the ratio r, the more stringent will be the requirement on $(\bar{\epsilon}_{max} - \bar{\epsilon}_{min})/\bar{\epsilon}_0$; in fact, the permissible value of this quantity is proportional to r^2. In any practical case the value of $\bar{\epsilon}$ will have to be controlled against long-range variations within a fraction of a per cent, and if attenuation reduction factors of the order of one-fifth or one-tenth are contemplated, the variations probably cannot exceed a few hundredths of a per cent. It also appears that a steady increase or decrease in the value of $\bar{\epsilon}$ across the stack will be the most serious type of nonuniformity, since the effects of very rapid fluctuations will tend to average out.

Clearly the nonuniform laminated transmission lines which we have been considering in this section are very highly idealized, even if we disregard the geometrical differences between plane and coaxial structures. Any real Clogston cable will be built up of layers of finite thickness with unavoidable random fluctuations from layer to layer, superimposed on slower variations in the average properties of the layers from one side of the stack to the other. The thickness of an individual layer will also vary more or less in both directions parallel to the layer, so that the properties of the stack will be functions of the coordinates ϕ and z as well as of ρ. A few qualitative remarks are in order concerning these neglected effects.

The effect of finite lamina thickness in a nonuniform stack can be calculated, by the method employed in Section XI for a uniform coaxial stack, if we make the plausible assumption that the macroscopic current distribution remains the same as for infinitesimally thin layers. The results will certainly be qualitatively the same for uniform and slightly nonuniform stacks, so long as the nonuniformity does not seriously distort the field pattern of the operating mode.

Some idea of how the effects of rapid random fluctuations in the average properties of the stack may be expected to average out is given by equation (570), which assumes for the function $f(\xi)$ a ν-cycle cosine variation across the stack. As a numerical example, suppose that with this variation of $\bar{\epsilon}$ we have

$$\frac{\bar{\epsilon}_{\max} - \bar{\epsilon}_{\min}}{\bar{\epsilon}_0} = 0.01 \tag{579}$$

in a line designed to give an attenuation reduction ratio of

$$r = 1/10. \tag{580}$$

Assuming polyethylene insulating layers, we have for this line

$$\delta_1/a = 1/192.7 = 0.00519, \tag{581}$$

and from (578) the corresponding value of C is

$$C = 247.6. \tag{582}$$

The value of ν for which the relative increase in Re Λ_1 due to the fluctuations is, say, one-quarter is given by

$$\frac{C^2}{8\nu^2\pi^4} = \frac{1}{4}, \qquad \nu = \frac{C}{\sqrt{2}\,\pi^2} = 17.7. \tag{583}$$

Thus a 1 per cent fluctuation in $\bar{\epsilon}$, repeated at intervals of about one-eighteenth of the stack width, will cause only a 25 per cent increase in attenuation, even for a Clogston line which is designed to have only one-tenth of the attenuation constant of a conventional line of the same size.

Finally there is the question of the effects of variations in the average properties of the stack in both directions parallel to the layers. Mathematical analysis of even a simple case of longitudinal variation would be much more difficult than what has been done here; yet on physical grounds it seems very likely that such variations will add an appreciable amount to the total attenuation of the line. If we consider two cross sections of a laminated cable separated by a certain distance and having different transverse nonuniformities, the field pattern of the lowest mode will be different at the two cross sections, and so in traversing the intervening distance the power will be partly reflected and partly converted to higher modes with higher attenuation constants. The reflected or mode converted power will be at least partly lost, with a consequent increase in the overall attenuation of the cable. Hence the estimate of the increase in attenuation which one gets from the present analysis, considering only the variations transverse to the layers at an average cross section, is certain to be optimistic in that it neglects completely the effects of variations in other directions.

XIII. DIELECTRIC AND MAGNETIC LOSSES IN CLOGSTON 2 LINES

To discuss dielectric and magnetic losses in Clogston 2 lines we may take the electrical constants of the conducting and insulating layers to be complex; thus

$$\begin{aligned} \mu_1 &= \mu_1' - i\mu_1'' = \mu_1'(1 - i \tan \zeta_1), \\ \mu_2 &= \mu_2' - i\mu_2'' = \mu_2'(1 - i \tan \zeta_2), \\ \epsilon_2 &= \epsilon_2' - i\epsilon_2'' = \epsilon_2'(1 - i \tan \phi_2). \end{aligned} \tag{584}$$

Almost all of the equations of the preceding sections, except of course those which involve explicit separation of real and imaginary parts, remain valid when we introduce complex values of μ_1, μ_2, and ϵ_2. In particular the propagation constant of the pth mode in a Clogston 2 with infinitesimally thin laminae and high-impedance walls is given, as in Sections VIII through X, by

$$\gamma^2 = -\omega^2\bar{\mu}\bar{\epsilon} + (i\omega\bar{\epsilon}/\bar{g})\chi_p^2, \tag{585}$$

where

$$\chi_p = p\pi/a \tag{586}$$

for a parallel-plane line, and χ_p is the pth root of

$$J_1(\chi a)N_1(\chi b) - J_1(\chi b)N_1(\chi a) = 0 \tag{587}$$

for a coaxial line. Taking the square root of the right side of (585) by the binomial theorem, we have

$$\gamma = i\omega\sqrt{\bar{\mu}\bar{\epsilon}} + \frac{\chi_p^2}{2\sqrt{\bar{\mu}/\bar{\epsilon}}\,\bar{g}}. \tag{588}$$

In the presence of dielectric and/or magnetic dissipation, we write, as in Section VII,

$$\begin{aligned} \bar{\epsilon} &= \bar{\epsilon}' - i\bar{\epsilon}'' = [\epsilon_2'/(1 - \theta)] - i[\epsilon_2''/(1 - \theta)], \\ \bar{\mu} &= \bar{\mu}' - i\bar{\mu}'' = [\theta\mu_1' + (1 - \theta)\mu_2'] - i[\theta\mu_1'' + (1 - \theta)\mu_2'']. \end{aligned} \tag{589}$$

Then the term $i\omega\sqrt{\bar{\mu}\bar{\epsilon}}$ in (588) has a small real part, namely

$$\alpha_d = \tfrac{1}{2}\omega\sqrt{\bar{\mu}'\bar{\epsilon}'}\,(\tan\phi_2 + \tan\bar{\zeta}), \tag{590}$$

where

$$\tan\bar{\zeta} = \frac{\bar{\mu}''}{\bar{\mu}'} = \frac{\theta\mu_1'' + (1-\theta)\mu_2''}{\theta\mu_1' + (1-\theta)\mu_2'}; \tag{591}$$

and α_d is the part of the attenuation constant which is due to dielectric and magnetic losses. If there were no dielectric or magnetic dissipation, the second term on the right side of (588) would be purely real and would represent the attenuation due to ohmic losses in the conducting layers. We neglect the small change in this term when $\bar{\mu}$ and $\bar{\epsilon}$ are complex, and thus as usual regard the metal losses, the dielectric losses, and the magnetic losses as additive.

We observe that α_d is the same for both plane and coaxial lines, and is also independent of the mode number p. Although derived here for the case of infinitesimally thin laminae, the same expression may be used for lines with finite laminae, so long as the conducting layers are moderately thin compared to the skin depth. The dielectric and magnetic losses do not depend on the overall dimensions of the transmission line, but are directly proportional to frequency provided that the loss tangents do not vary with frequency.

If it should be necessary to calculate the dielectric and magnetic losses in a partially filled Clogston line where the dissipation factor of the main dielectric is markedly different from the dissipation factor of the stacks, α_d may be obtained, using the method described in Section VII, as half the ratio of dissipated power per unit length to transmitted power. In this calculation we may use the field components given in Sections IX and X for the various modes in partially filled lines.

ACKNOWLEDGMENTS

Many people with whom I have discussed the theoretical and practical aspects of the laminated transmission line problem at various times have offered comments and suggestions which are reflected in this paper. I have especially to express my appreciation to A. M. Clogston, H. S. Black, and J. G. Kreer, Jr., for stimulating and helpful discussions.

My thanks are also extended to Mrs. M. F. Shearer, Mrs. D. R. Fursdon, and Miss R. A. Weiss for the extensive numerical computations which they carried out in connection with this study, and to Miss D. T. Angell for preparation of the curves and diagrams.

APPENDIX II

OPTIMUM PROPORTIONS FOR HEAVILY LOADED CLOGSTON CABLES

We wish to find the lowest root χ_1 of the equation

$$\frac{1}{\chi\rho_1}\frac{J_1(\chi a)N_0(\chi\rho_1) - N_1(\chi a)J_0(\chi\rho_1)}{J_1(\chi a)N_1(\chi\rho_1) - N_1(\chi a)J_1(\chi\rho_1)} + \frac{1}{\chi\rho_2}\frac{J_1(\chi b)N_0(\chi\rho_2) - N_1(\chi b)J_0(\chi\rho_2)}{J_1(\chi\rho_2)N_1(\chi b) - N_1(\chi\rho_2)J_1(\chi b)} = \frac{\mu_0}{\bar{\mu}}\log\frac{\rho_2}{\rho_1}, \tag{A9}$$

where b is fixed and $\mu_0/\bar{\mu} \gg 1$, and to minimize this root as a function of a, ρ_1, and ρ_2.

Since we expect χ_1 to approach zero as $\mu_0/\bar{\mu}$ approaches infinity, we shall replace the Bessel functions appearing in (A9) by their approximate values for small argument, namely

$$\begin{aligned} J_0(x) &\approx 1, \\ J_1(x) &\approx \tfrac{1}{2}x, \\ N_0(x) &\approx \frac{2}{\pi}\log 0.8905x, \\ N_1(x) &\approx -\frac{2}{\pi x}, \end{aligned} \tag{A10}$$

for $|x| \ll 1$. Then the equation becomes, approximately,

$$\frac{1}{\chi_1\rho_1}\frac{1/\chi_1 a}{\frac{1}{2}(-a/\rho_1 + \rho_1/a)} + \frac{1}{\chi_1\rho_2}\frac{1/\chi_1 b}{\frac{1}{2}(-\rho_2/b + b/\rho_2)} = \frac{\mu_0}{\bar{\mu}}\log\frac{\rho_2}{\rho_1}, \tag{A11}$$

which may be solved for χ_1^2 to yield

$$\chi_1^2 = \frac{2\bar{\mu}}{\mu_0 \log(\rho_2/\rho_1)}\left[\frac{1}{\rho_1^2 - a^2} + \frac{1}{b^2 - \rho_2^2}\right]. \tag{A12}$$

By inspection χ_1^2 will be a minimum, considered as a function of a, when $a = 0$. Setting $a = 0$ and then equating to zero the partial derivatives of χ_1^2 with respect to ρ_1 and ρ_2, we get the pair of equations

$$\begin{aligned} \frac{1}{\rho_1[\log(\rho_2/\rho_1)]^2}\left[\frac{1}{\rho_1^2} + \frac{1}{b^2 - \rho_2^2}\right] - \frac{2}{\rho_1^3\log(\rho_2/\rho_1)} &= 0, \\ -\frac{1}{\rho_2[\log(\rho_2/\rho_1)]^2}\left[\frac{1}{\rho_1^2} + \frac{1}{b^2 - \rho_2^2}\right] + \frac{2\rho_2}{(b^2 - \rho_2^2)^2\log(\rho_2/\rho_1)} &= 0, \end{aligned} \tag{A13}$$

which yield, on rearrangement,

$$\frac{1}{\log(\rho_2/\rho_1)}\left[\frac{1}{\rho_1^2}+\frac{1}{b^2-\rho_2^2}\right]=\frac{2]}{\rho_1^2},$$
$$\frac{1}{\log(\rho_2/\rho_1)}\left[\frac{1}{\rho_1^2}+\frac{1}{b^2-\rho_2^2}\right]=\frac{2\rho_2^2}{(b^2-\rho_2^2)^2}. \qquad \text{(A14)}$$

Subtracting the second of equations (A14) from the first and solving the resulting equation for ρ_1, we get

$$\rho_1=\frac{b^2-\rho_2^2}{\rho_2}=\frac{b^2}{\rho_2}-\rho_2, \qquad \text{(A15)}$$

whence, eliminating ρ_1 from the first of (A14),

$$\log\frac{\rho_2^2}{b^2-\rho_2^2}=\frac{b^2}{2\rho_2^2}. \qquad \text{(A16)}$$

Numerical solution of (A16) gives

$$\rho_2^2/b^2 = 0.67674; \qquad \text{(A17)}$$

and on making use of (A15) we obtain finally

$$\rho_1 = 0.39296b, \qquad \text{(A18)}$$
$$\rho_2 = 0.82264b.$$

Substituting these values, with $a = 0$, into (A12), we get for the minimum value of χ_1^2, when $\mu_0/\bar{\mu} \gg 1$,

$$\chi_1^2=\frac{25.905\bar{\mu}}{\mu_0 b^2}. \qquad \text{(A19)}$$

Appendix III

POWER DISSIPATION IN A HOLLOW CONDUCTING CYLINDER

Consider a hollow cylinder of inner radius ρ_1, outer radius ρ_2, and high conductivity g_1. Denote the total current flowing in the positive z-direction inside the radius ρ_1 by I_1 and the total current inside the radius ρ_2 by I_2; then the current carried by the conducting cylinder is just $I_2 - I_1$, and the net return current outside the cylinder is $-I_2$. We assume the current distribution to be independent of the coordinate angle ϕ, but the radial distribution of the currents inside and outside the given cylinder is of no importance.

General expressions for the field components in the conducting cylinder are given by equations (33) of Section II, which read

$$
\begin{aligned}
H_\phi &= AI_1(\sigma_1\rho) + BK_1(\sigma_1\rho), \\
E_\rho &= \frac{\gamma}{g_1}[AI_1(\sigma_1\rho) + BK_1(\sigma_1\rho)], \\
E_z &= \eta_1[AI_0(\sigma_1\rho) - BK_0(\sigma_1\rho)],
\end{aligned}
\tag{A20}
$$

provided that we drop the propagation factor $e^{-\gamma z}$ and make the usual approximations

$$
g_1/\omega\epsilon_1 \gg 1, \qquad \kappa_1 \approx \sigma_1\,, \qquad \kappa_1/g_1 \approx \eta_1\,, \tag{A21}
$$

for a good conductor. The constants A and B are determined by the boundary conditions

$$
H_\phi(\rho_1) = I_1/2\pi\rho_1\,, \qquad H_\phi(\rho_2) = I_2/2\pi\rho_2\,, \tag{A22}
$$

which follow directly from Ampere's circuital law. We find without difficulty

$$
\begin{aligned}
A &= \frac{(I_2/2\pi\rho_2)K_1(\sigma_1\rho_1) - (I_1/2\pi\rho_1)K_1(\sigma_1\rho_2)}{K_1(\sigma_1\rho_1)I_1(\sigma_1\rho_2) - K_1(\sigma_1\rho_2)I_1(\sigma_1\rho_1)}\,, \\
B &= \frac{(I_1/2\pi\rho_1)I_1(\sigma_1\rho_2) - (I_2/2\pi\rho_2)I_1(\sigma_1\rho_1)}{K_1(\sigma_1\rho_1)I_1(\sigma_1\rho_2) - K_1(\sigma_1\rho_2)I_1(\sigma_1\rho_1)}\,.
\end{aligned}
\tag{A23}
$$

The average power dissipated in the conducting cylinder is equal to one-half the real part of the inward normal flux of the complex Poynting vector $\mathbf{E} \times \mathbf{H}^*$. For the average power P dissipated per unit length we have

$$
\begin{aligned}
P &= \mathrm{Re}\,\tfrac{1}{2}[2\pi\rho_2 E_z(\rho_2)H_\phi^*(\rho_2) - 2\pi\rho_1 E_z(\rho_1)H_\phi^*(\rho_1)] \\
&= \mathrm{Re}\,\tfrac{1}{2}[E_z(\rho_2)I_2^* - E_z(\rho_1)I_1^*] \\
&= \mathrm{Re}\,\frac{\tfrac{1}{2}\eta_1}{(K_{11}I_{12} - K_{12}I_{11})}\left[\frac{I_2I_2^*}{2\pi\rho_2}(K_{11}I_{02} + K_{02}I_{11})\right. \\
&\qquad \left. - \frac{(I_1I_2^* + I_1^*I_2)}{2\pi\sigma_1\rho_1\rho_2} + \frac{I_1I_1^*}{2\pi\rho_2}(K_{01}I_{12} + K_{12}I_{01})\right],
\end{aligned}
\tag{A24}
$$

where

$$
I_{rs} = I_r(\sigma_1\rho_s), \qquad K_{rs} = K_r(\sigma_1\rho_s). \tag{A25}
$$

The combinations of Bessel functions appearing in (A24) are just those for which we gave approximate expressions in equations (A8) of Appendix I, assuming the thickness t_1 $(= \rho_2 - \rho_1)$ of the conducting cylinder to be small compared to ρ_1. Substituting these approximations into (A24) and rearranging, we get

$$P = \text{Re}\,\frac{1}{4\pi g_1 t_1}\left\{\frac{I_2 I_2^*}{\rho_2}\left[\sigma_1 t_1 \coth \sigma_1 t_1 + \frac{t_1}{2\rho_1}\right] - \frac{(I_1 I_2^* + I_1^* I_2)}{\rho_1}\left[1 - \frac{t_1}{2\rho_1}\right]\sigma_1 t_1 \,\text{csch}\, \sigma_1 t_1 + \frac{I_1 I_1^*}{\rho_1}\left[\sigma_1 t_1 \coth \sigma_1 t_1 - \frac{t_1}{2\rho_1}\right]\right\}, \tag{A26}$$

up to first order in t_1/ρ_1. If we set

$$\sigma_1 = (1 + i)/\delta_1, \tag{A27}$$

then on expanding the right side of (A26) in powers of t_1/δ_1 up to the fourth, we obtain

$$P = \frac{1}{4\pi g_1 t_1}\left\{\frac{| I_2 - I_1 |^2}{\sqrt{\rho_1 \rho_2}} + \frac{4t_1^4}{\delta_1^4}\left[\frac{I_2 I_2^*}{45\rho_2} + \frac{7(I_1 I_2^* + I_1^* I_2)}{360\sqrt{\rho_1\rho_2}} + \frac{I_1 I_1^*}{45\rho_1}\right]\right\}, \tag{A28}$$

where we have approximated $\rho_1(1 + t_1/2\rho_1)$ by $\sqrt{\rho_1\rho_2}$ in the interest of symmetry.

Now writing ΔP_j for P, ΔI_j for $I_2 - I_1$, ρ_{j-1} for ρ_1, and I_{j-1} for I_1, and neglecting curvature corrections of the order of t_1/ρ_1 entirely, we have, on setting I_1 and I_2 both equal to I_{j-1} in the coefficient of $(t_1/\delta_1)^4$, the approximate relation

$$\Delta P_j = \frac{1}{4\pi g_1 t_1 \rho_{j-1}}\left[| \Delta I_j |^2 + \frac{t_1^4}{3\delta_1^4} | I_{j-1} |^2\right], \tag{A29}$$

which is just equation (472) of Section XI.